

# Engine Simulation Model for a Formula SAE Race Car

*Applied Design, Development, Correlation and Optimization*



Ramin Gilani

Master of Science in Engineering Technology  
Mechanical Engineering

Luleå University of Technology  
Department of Engineering Sciences and Mathematics

This one year project with Monash University's Formula Society of Automotive Engineering team can be divided into two parts. The first part is to work as a mechanic and engineer, while the second part is to carry out my master thesis work. This report treats the thesis part of the project and can be subdivided into following six steps:

- **Learn** how to use Wavebuild and WavePost parts of the engine simulation software Ricardo Wave.
- **Build** Monash Motorsports new stock KTM SX-F engine in the software.
- **Compare** the simulations with the real stock engine on the dynamometer.
- **Rebuild** the simulation engine from corresponding to the stock engine to correspond to the upcoming changes which defines the race engine.
- **Optimise** the simulation models.
- **Provide** the team with recommendations on how to optimise the real engine.

## ABSTRACT

This report is the result of a one year project to provide Monash Motorsports FSAE team with vital predictions regarding how the 2011 450 CC KTM SX-F engine would respond to planned reconstructions and how to optimise different parts of the engine. The phases of operation have been: Learning the software, building the engine, confirming the trustworthiness of the results, rebuilding the engine to predict future results, optimising the simulation and finally providing Monash Motorsport with results and recommendations. The entire engine has been required to be fully defined to be able to run proper simulations. This includes: intake system, engine, exhaust system, physical and environmental properties and also combustion and other sub-models. There were three options to obtain the required data. Either by the engine manufacturer (KTM), manually measuring or using values from example engines included in the simulation software. All three options have been used depending on availability, the time it takes to get hold of topical data and the reliability of the source. By building the engine in the software and simulating the planned changes one step ahead of the team, the simulations have served part of their purpose to work as guidelines to shortening the time of optimisation.

Before approaching the real task the stock engine was created, tested and confirmed to work properly in the simulation. By doing so credibility was added to the simulation which are most important if the simulation predictions was to be accepted as guidelines. The stock engine worked as reference and the dynamometer results was used as benchmark together with results from KTM while building the engine. As a next step the simulation engine was upgraded to the geometry of the final design including components not yet created for the real engine. By doing so the simulation engine could take the role of reference and various simulation tests was performed to map out how each new component affect the engine individually and in conjunction with other related new components. The step of rebuilding the simulation engine to correspond to the future race engine was most crucial to be performed properly hence there was no reference to compare the outcome with but rather being the reference for the real engine.

The results from the final optimisation advocate that a spherical plenum chamber with the volume of 3.89 l should be added to the engine. By doing so a buffer of air is created after the restrictor decreasing the negative impact of the FSAE regulated restrictor. Plenum volume was selected with respect to power/torque, throttle response and packaging. Optimum runner length is 170 mm. This is with respect to the narrow engine speed of 7000 – 11000 rpm the car will be driven during competition. It is also necessary to limit the rpm range of maximum interest since different geometries are optimum within different rpm range. The simulation clearly states that a high discharge coefficient at the diffuser-plenum and plenum-runner ends is to prefer. To do so bell-mouths are beneficial and doe smoothen out the air flow. The components that have been delimited from this work are thous that will be limited affected by

the outcome of the simulations. This includes the air filter, throttle body and different shape of the diffuser including the restrictor. These components have already been carefully investigated and optimised by previous thesis students.

The FSAE regulation had made it extra challenging to optimise the car by allocating points on different criteria hence it is not only being the first car over the finish line that decide if you win or not. Optimum was therefore defined as the best compromise between all the criteria providing points. A total number of approximately 264 simulations were produced in the process which now lays the foundation for Monash Motorsport engine simulation database for future years to come. This report can serve new engine simulation users as a guideline through all steps to a solid foundation of how to design tests, interpret results and optimise an engine.

Ramin Gilani  
Sydney, February 1, 2012

## **ACKNOWLEDGEMENT**

I would like to extend my thanks to the following people for their effort and assistance to make it possible for me to carry out this thesis, for it would not have been possible without them: Pär Marklund, Sven Molin, Kim C. N, Sverker Fredriksson and fellow Monash FSAE team members and of course my supervisor Dr Scott Wordley for his insight and guidance.

© 2012 Ramin Gilani

Luleå 2012

Department of Engineering Sciences and Mathematics  
Division of Product and Production Development  
Luleå University of Technology  
SE-971 87 Luleå  
SWEDEN

[www.ltu.se](http://www.ltu.se)

Printed by Universitetstryckeriet 2012

# Contents

<b>1</b>	<b>INTRODUCTION</b>	<b>3</b>
1.1	FORMULA SOCIETY OF AUTOMOTIVE ENGINEERING . . . . .	3
1.2	PROJECT OBJECTIVES . . . . .	5
1.3	GOAL . . . . .	5
1.4	DELIMITATIONS . . . . .	5
<b>2</b>	<b>RESEARCH AND BACKGROUND INTO THEORIES OF ENGINE SIMULATION</b>	<b>7</b>
2.1	DISCHARGE COEFFICIENT . . . . .	8
2.2	FRICTION CORRELATION . . . . .	11
2.3	DISCRETIZATION . . . . .	15
2.4	HEAT TRANSFER MODEL Woschni VS Annand . . . . .	16
2.5	COMBUSTION MODEL . . . . .	19
2.6	COMPLEX Y-JUNCTION . . . . .	23
2.7	PRESSURE WAVE REFLECTION IN DUCTS . . . . .	24
	2.7.1 EXAMPLE CALCULATION . . . . .	25
<b>3</b>	<b>KTM STOCK ENGINE MEASUREMENTS AND SIMULATION SETUP</b>	<b>27</b>
3.1	DESIGN IN RICARDO WAVE . . . . .	29
3.2	INTAKE . . . . .	30
3.3	DUCTS . . . . .	31
3.4	INJECTOR . . . . .	34
3.5	CYLINDER . . . . .	35
3.6	VALVES . . . . .	36
<b>4</b>	<b>STOCK ENGINE SIMULATION</b>	<b>39</b>
4.1	KTM SX-F POWER AND TORQUE REFERENCE . . . . .	39
4.2	SIMULATION ARRANGEMENT . . . . .	42
4.3	DESIGN OF TESTS . . . . .	43
4.4	PREPARATION OF SIMULATION . . . . .	43
4.5	RUNNING SIMULATIONS . . . . .	44
<b>5</b>	<b>RECONSTRUCTION OF SIMULATION ENGINE TO PREDICT THE BEST RACE ENGINE CONFIGURATION</b>	<b>47</b>
5.1	RECONSTRUCTION OF THE INTAKE SYSTEM WITH CUSTOM MADE COMPONENTS . . . . .	48
5.2	SIMULATION ARRANGEMENT . . . . .	48

5.3	DESIGN OF TESTS . . . . .	49
5.4	PREPARATION . . . . .	49
5.5	RUNNING SIMULATIONS FOR INDIVIDUAL TESTING . . . . .	50
5.5.1	RUNNER LENGTH . . . . .	51
5.5.2	PLENUM VOLUME . . . . .	51
5.5.3	BELL-MOUTH . . . . .	53
<b>6</b>	<b>RESULTS FROM POST-PROCESSING</b>	<b>54</b>
6.1	STOCK ENGINE SIMULATION . . . . .	54
6.2	RACE ENGINE RUNNER LENGTH . . . . .	55
6.3	RACE ENGINE PLENUM VOLUME . . . . .	56
6.4	RACE ENGINE BELL-MOUTHS . . . . .	59
<b>7</b>	<b>FINAL OPTIMISATION</b>	<b>61</b>
<b>8</b>	<b>CONCLUSIONS AND RECOMMENDATIONS</b>	<b>63</b>
<b>9</b>	<b>REFERENCES</b>	<b>65</b>
<b>A</b>	<b>APPENDIX</b>	<b>67</b>
A.1	FSAE SCORE SYSTEM . . . . .	67
A.2	CHARGE MOTION IN CYLINDER & REFERENCE OF HEAT TRANSFER .	67
A.3	TECHNICAL DATA . . . . .	69
A.4	MATERIAL SURFACE ROUGHNESS . . . . .	70
A.5	ENGINE GENERAL PANEL . . . . .	70
A.6	SIMULATION OF THE CARBURETTOR . . . . .	71
A.7	MEASUREMENT TECHNIQS . . . . .	71
A.8	COMPLEX Y-JUNCTIONS . . . . .	73
A.9	RPM RELATED CONSTANTS . . . . .	75
A.10	RESULTS . . . . .	76
A.10.1	COMPARISON OF BHP AND TQ SIMULATION RESULTS VS REF- ERENCE . . . . .	76
A.10.2	TESTRUN SETTINGS FOR THE PROTOTYPE ENGINE . . . . .	79
A.10.3	INTAKE . . . . .	84
A.10.4	ALL SIMULATION RUNNER LENGTHS . . . . .	87
A.10.5	ALL SIMULATION PLENUM VOLUMES . . . . .	88



# NOMENCLATURE

$E$	-	Energy [J]
$m$	-	Mass [g]
$C_D$	-	Discharge coefficient
$D$	-	Cylinder bore [mm]
$P$	-	Cylinder pressure [bar]
$T$	-	Cylinder temperature [K]
$v_c$	-	Cylinder velocity [m/s]
$C_{enht}$	-	Multiplier
$v_m$	-	Mean piston speed [rpm]
$V_D$	-	Cylinder displacement [ $mm^3$ ]
$T_r$	-	Reference temperature [K]
$P_r$	-	Reference pressure [bar]
$V_r$	-	Reference volume [ $mm^3$ ]
$P_{mot}$	-	Motored cylinder pressure [bar]
$V_c$	-	Clearance volume [ $mm^3$ ]
$V$	-	Instantaneous cylinder volume [ $mm^3$ ]
$v_s$	-	Swirl ratio
$a$	-	Heat transfer multiplier
$\rho$	-	Density
$\mu$	-	Dynamic viscosity
$k$	-	Thermal conductivity [W/m/K]
$h_g$	-	Heat transfer coefficient

$TDC$	-	Top Dead Centre [deg]
$ATDC$	-	After Top Dead Centre [deg]
$BDC$	-	Bottom Dead Centre [deg]
$W_n$	-	Comulative burn rate
$W_n(\theta)$	-	Comulative burn rate at certain angle
$\theta_0$	-	Start of combustion [deg]
$\theta_i$	-	Given crank angle [deg]
$x_B$	-	Mass fraction burned [g]
$EOC$	-	End of combustion [deg]
$A$	-	Scaling factor, $A = -\ln(1 - x_{B,EOC})$
$B$	-	Combustion mode parameter
$\Delta\theta$	-	Total combustion duration ( $\theta_{EOC} - \theta_0$ ) [deg]
$DELX$	-	Characteristic length [mm]
$DIAB$	-	Expansion diameter [mm]
$FMEP$	-	Friction Mean Effective Pressure [Pa]
$IMEP$	-	Indicated Mean Effective Pressure [Pa]
$BMEP$	-	Brake Mean Effective Pressure [Pa]
$PMEP$	-	Pressure Mean Effective Pressure [Pa]

# 1 INTRODUCTION

Luleå University of Technology and Monash University have established collaboration since 1997. The cross-university collaboration has been growing steady since and will probably do so in the future based on new fundings. The collaboration bridges multiple departments and gives students and staff members at both universities the possibility to establish new international projects. For more information regarding the possibility to take part in the collaboration for e.g. thesis work please contact you're respective university. The Monash Motorsport FSAE team which this master thesis will be performed for is ranked 1st in Australia and the pacific-ocean and ranked third in the world 2010 and belong to the department of mechanical and aerospace engineering. The crew consist of 50 BSc, MSc and PHD students from multiple disciplines.

## 1.1 FORMULA SOCIETY OF AUTOMOTIVE ENGINEERING

Formula Society of Automotive Engineering (FSAE) is a student design competition that has been running since 1975 organized by SAE International. The concept behind FSAE is that a fictional company has hired an engineering team to design and build a formula-style race car from scratch, ready to race in one year.

FSAE promotes careers and excellence in engineering as it encompasses all aspects of the automotive industry such as research, design, manufacturing, testing, developing, marketing, management and finances. FSAE is a worldwide design competition in which university students are challenged out of the classroom and provided with the opportunity to apply textbook theories to real work experiences. The racing series are regulated by a 130 page rule book released and yearly revised by SAE International. Even though the series are strictly regulated there are relatively few performance restrictions compared to other formula style racing series. SAE navigate the focus of the series by adjusting the score system rather than limiting the series. This allow the engineers to more freely try to optimise their race car stimulating creativity and hence a large range of solutions to the same problem. Each event is allocated a maximum possible score, which when collated gives a total scoring maximum of 1000 points. In 2009 the fuel economy scores where increased from 50 to 100 points tweaking the teams to focus more towards energy efficiency. The competition ranks university teams on their ability to satisfy these conditions (FSAE Rules 2011) See Appendix A.1 for a breakdown of the scores. Figure 1 shows the final design of the 2011 Monash Motorsport FSAE race car.

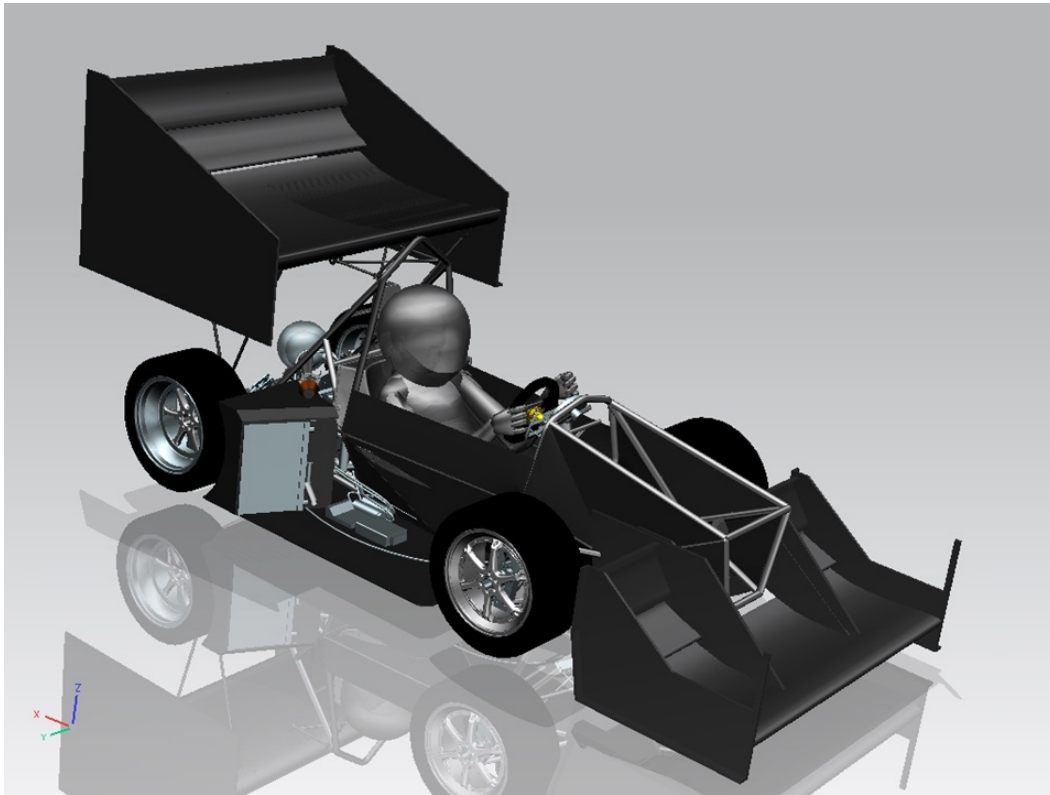


Figure 1 - CAD representation of the 2011 Monash Motorsport FSAE race car.

Two former engineering students and members of Monash Motorsport team (Sam Lister and Rick Grose) conducted an in-depth research of point scoring for the competition in response to the strong leaning towards fuel economy in 2009. This simulator was able to directly correlate changes in vehicle design to points scored at competition. As a result of this analysis a decision to change from a four cylinder  $600\text{ cm}^3$  Honda engine to a lighter and more fuel efficient single cylinder engine was made. In regard to the scoring system a  $450\text{ cm}^3$  Husqvarna engine was chosen as the best option in 2009. This was later adjusted to KTM due to sponsorship which will be implemented in the car for the first time in 2011.

## 1.2 PROJECT OBJECTIVES

Speed is the single most dangerous factor in motorsport. In order to limit the power capability from the engine, FSAE are limited in engine volume to  $610 \text{ cm}^3$  and the air intake system is limited by a single circular restrictor of 20 mm that must be placed between the throttle and the engine. The engine is originally not designed for intake restrictions and therefore suffers sufficient power loss. This introduces the challenge to optimise the engine to produce as much power as possible while working effectively during the new conditions. The purpose of this project is to expand the area of research within engine simulation with Monash Motorsport. Simulations will be employed to investigate means to most effective design and setup, hence optimise different areas of the engine. The purpose of engine simulation is to reduce the total experimental testing time required to investigate and find optimum. Areas in which to increase efficiencies of the engine will after thoroughly investigated in theory constitute the foundation of how to optimise the real engine.

## 1.3 GOAL

The goal of this project is to optimise Monash Motorsports new engine for race by creating a computer simulation model capable of determining the most effective design. Information obtained from KTM and manual measurement will be used in the design of the computer simulation. Results from the simulations will be given grounds for and handed over to the team as the results are obtained throughout the year. This will give more time to get the real engine optimised. The final goal of this project is to provide Monash Motorsport with a database of tests and results for the new 2011 engine and also hand in this report to help new engine simulation responsible to go from not knowing much about engine simulation in Ricardo Wave to a solid foundation of how to design tests, interpret results and optimise.

## 1.4 DELIMITATIONS

The components that will be excluded are those that will not be affected by the outcome of the simulations in this project. The air filter, throttle body and different shape of the restrictor have already been carefully investigated and optimised by previous thesis students and are therefore of lower priority to simulate. Monash Motorsport owns two KTM SX-F engines, which will be used for testing on the dynamometer and one which will be optimised with respect to the test results and will be located in the race car. The exhaust system on the engine located on the dynamometer is not identical to the one that will be designed for the car and will therefore not provide any data to be confirmed or dismissed. Optimisation of the exhaust system falls therefore also outside the scope of this project. These delimited components will on request by the team be simulated but it will be performed unofficially and will therefore not be treated

in this report.

Some parts of the software will undergo investigation to confirm that the algorithms provide correct results. It is however not possible to investigate more than just some random samples due to time limits, the wide range of built in algorithms and also due to some limitation in public algorithms.

## 2 RESEARCH AND BACKGROUND INTO THEORIES OF ENGINE SIMULATION

The simulation software that will be utilized is the market leading ISO approved, 1-D engine and gas dynamics simulation software from Ricardo. It is used worldwide with technical centres in China, Czech Republic, Germany, India, Italy, Japan, Korea, Russia, United Kingdom and United States. It is used in industry sectors including passenger car, motorcycle, truck, locomotive, motorsport and marine. Wave enable performance simulations to be carried out for steady-state as well as transient simulations applicable to virtually any intake, combustion and exhaust system configuration and includes a drivetrain model to allow complete vehicle simulation.

The software can be used throughout the entire engine design process, from early concept research to optimising a complete engine. Whether it concerns improving volumetric efficiency, designing complex boosting systems, improving transient response or extracting the maximum performance from a race engine, Wave is useful. The complicity of the software can be reduced for the user at the expense of quality. Default and tutorial values are available for basically every required input. This lowers the entry level for beginners and also makes it possible to run simulations even if some data is missing. The software includes an extended tutorial package split in basic, intermediate and advance levels.

To use the software for more than just education it is essential that the default values are kept to a minimum and each component are completely defined to eliminate source of errors. The quality and trustworthiness of the results gained from the post-processing part of the software (WavePost) are a direct consequence of the tolerance and quality of the inserted data and how well defined the engine is.

A combustion engine is a 3D-phenomenon in respect to combustion, ducts, valves etc. In order to investigate the concept of representing the KTM combustion engine in 1D in Wave, some additional information is required. The procedure is to split the three dimensions into multiple one dimension of data and keep track of how each dimension corresponds to one another. This is all done with equations pre-programmed in the software. For the software to be able to solve given tasks, coefficients and advanced sub-models are implemented. With user-provided data, pre-programmed equations and governing laws of physics like momentum, energy- and mass-conservation, different aspects of the particular engine can be solved. As can be seen in figure 2 the 1D solving for different aspects of the engine can be put together to sketch both 2D and 3D behaviour.

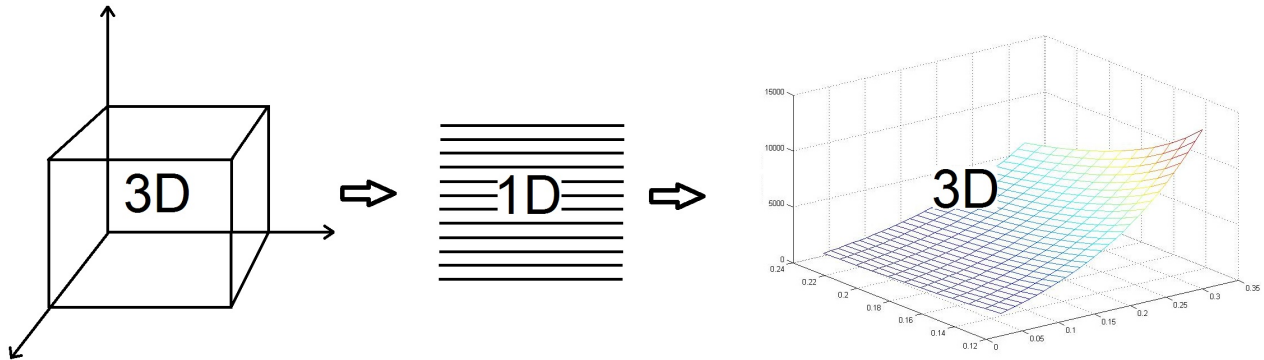


Figure 2 - The redefinition of dimensions in Wave.

Engine simulation software is developed to reduce cost of development by shortening testing time and effort required to reach desired results. Both Ricardo Wave and GT-Power to mention the two leading engine simulation software manufactures can provide valuable results on several hundred parameters for optimisation of components not yet created in reality. The plenum chamber for example which is one of the main components that will require extended research can easily be studied with simulation software. By dragging a complex Y-junction from the menu into the canvas attaching it properly to the engine and providing all geometries for the plenum, the simulation can provide results. No real dynamometer required and no need to rebuild the plenum to find optimum. Running tests on different parameters is with the new in real time controller easier than ever. By choosing one or more parameters to run tests on it is possible to view preferred output change in real time by moving regulators between different values.

## 2.1 DISCHARGE COEFFICIENT

Discharge coefficient treats the flow out of one end of a duct into the adjoining element. This is when set to "auto" automatically calculated with coefficient based on area ratios, smaller diameter divided by the bigger (usually in the range of 0.6 to 1.0). The coefficient decides the pressure drop ratio between the two connected elements.

An experiment will revile if the automatically calculated coefficient is calculated properly. The discharge coefficient has a great impact on the gas velocity from the ambient to the duct connected. It is therefore of great interest to confirm if it is done properly. The experiment arrangement to verify whether if the software properly calculates the discharge coefficient is done by comparing the simulated air velocity through the intake in a test engine. Observe that the test engine is not the KTM SX-F 2011 but only an engine built for experimentation. The



discharge coefficient  $C_D$  is in this particular case simulated for a round orifice calculated with the geometrical data shown in figure 3 [1].

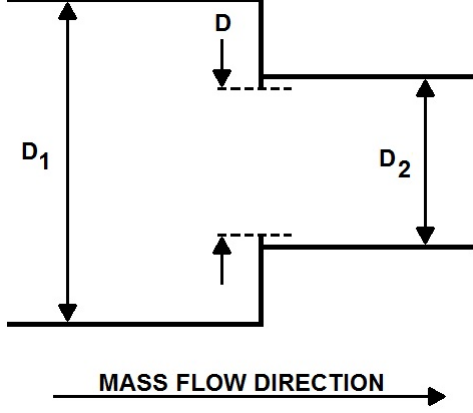


Figure 3 - Definition of  $D$ ,  $D_1$  and  $D_2$ .

$$C_D = 1 - \left(1 - \left(\frac{D}{D_1}\right)^4\right) * \left(0.2 + 0.2 \left(1 - \left(\frac{D}{D_2}\right)^4\right)\right), \quad (1)$$

where  $C_D$  is the discharge coefficient and  $D$ ,  $D_1$  and  $D_2$  as defined below:

$$D = \text{Orifice diameter} = 43.6\text{mm}$$

$$D_1 = \text{Upstream diameter} \rightarrow \infty$$

$$D_2 = \text{Downstream diameter} = 43.6\text{mm}$$

The air filter used on the physical engine is dimensioned for a much higher airflow rate than the KTM SX-F engine requires. Since the air filter is massively oversized the restriction is neglect-able small and can therefore be calculated as an open end.  $D_1$  contributes to the mathematical representation of the discharge coefficient by decreasing the discharge coefficient with larger upstream diameter. By letting the upstream diameter increase infinitely in the formula ( $D_1 \rightarrow \infty$ ) no increase in discharge coefficient due to restriction of intake will exist. This will simulate an open end in the software which is what the real engine experience.

In this case  $D = D_2$  since the orifice diameter is no smaller than the downstream diameter, leaving a 90 degree transition from the ambient to the intake ducts. See figure 3. Input of  $D$ ,  $D_1$  and  $D_2$  in  $C_D$  results in

$$C_D = 1 - \left( 1 - \left( \frac{43.6}{(D_1 \rightarrow \infty)} \right)^4 \right) * \left( 0.2 + 0.2 \left( 1 - \left( \frac{43.6}{43.6} \right)^4 \right) \right) \rightarrow$$

$$\rightarrow 1 - (1 - (0)^4) * (0.2 + 0.2 (1 - (1)^4)) \rightarrow 0.8.$$

The discharge coefficient is manually calculated to 0.8. Unfortunately Wave do not revile the discharge coefficient when set to "auto". It is therefore not possible to compare the manually and automatically calculated discharge coefficient. The automatic calculated value can however be reviled by experiments. By running an engine simulation and sampling air velocity which the discharge coefficient have an great impact on it is possible to evaluate and make sure that Wave discover the same discharge coefficient as is manually calculated. Two identical simulations will run where all values will be held constant, accept the discharge coefficient. The first simulation contained the discharge coefficient of 0.8 and the second with "auto". Air velocity through the intake should change distinctively if any differences between the discharge coefficients exist. Figure 4 shows the comparison between manually and automatically calculated discharge coefficients.

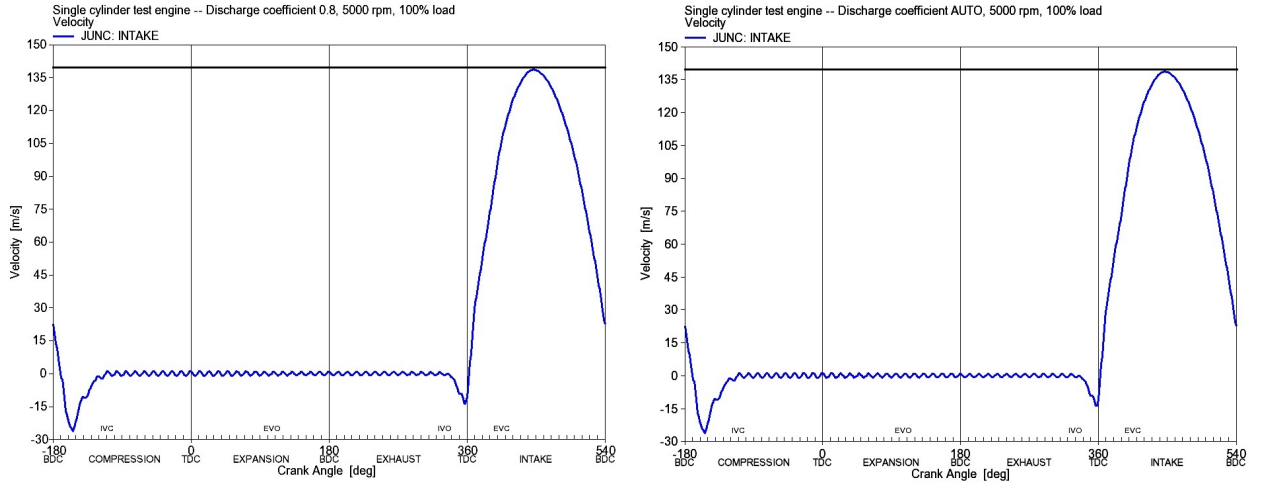


Figure 4 - Comparison between manually (left graph) and automatically (right graph) calculated discharge coefficient.

The left graph in figure 4 shows the air velocity through the intake with manually calculated discharge coefficient of 0.8 while the right graph represent the automatically calculated discharge coefficient by Wave. These two graphs are identical and suggest that the discharge coefficient is calculated properly by Wave when set to "auto".

To assure that the discharge coefficient contributes to the air velocity through the intake contributing to the algorithm one more test is required. To make sure that these two graphs are identical for the right reason and not due to an error eliminating the discharge contribution to the algorithm that is sketching the graph another discharge coefficient is tested and set to 0.7 instead of the previous value of 0.8 while all other parameters are kept constant. This resulted in a dramatic change in airflow velocity through the intake proving that the discharge coefficient indeed contribute and do so in proper manners. See graphs in figure 5

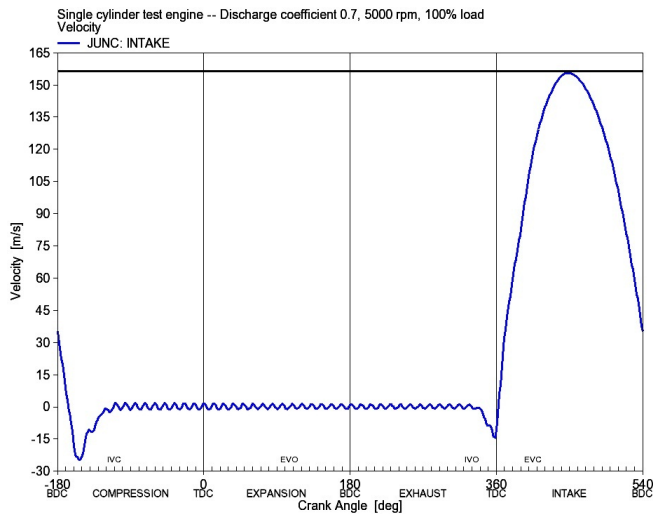


Figure 5 - Reference graph used to confirm the discharge coefficient contribution to the solution.

## 2.2 FRICTION CORRELATION

Friction caused by the piston motion inside the engine is modelled with a polynomial based modified version of the Chen-Flynn friction model, which is based on maximum cylinder pressure and piston speed [1], [2]. The Chen-Flynn model employs variables to represent the main sources of friction, referred to as Friction Mean Effective Pressure (FMEP). FMEP can be calculated with Eq 2. To do so  $A_{cf}$ ,  $B_{cf}$ ,  $C_{cf}$  and  $Q_{cf}$  (user inputs, see table 1) need to be known as they together with instantaneous simulated engine speed, pressure and stroke defines the friction.

Table 1 - Definition of terms for friction correlation

$A_{cf}$	=	<i>Constant portion of the equation</i>	(for accessory friction)
$B_{cf}$	=	<i>Peak cylinder pressure</i>	
$C_{cf}$	=	<i>Pistons peed</i>	
$Q_{cf}$	=	<i>Quadratically piston speed</i>	(for windage losses)
$RPM$	=	<i>Cycle – average engine speed</i>	
$Stroke$	=	<i>Cylinder stroke</i>	
$S_{fact}$	=	$RPM * \frac{stroke}{2}$	
$P_{cyl}$	=	<i>Cylinder pressure</i>	

There is three options to get hold of these engine related parameters. Either by extensive experiments on the dynamometer, use of recommended values from Ricardo Wave or get hold of the data from the engine manufacturer.

The equation that can be used to calculate friction is:

$$FM EP = A_{cf} + \frac{1}{ncyl} \sum_{i=1}^{ncyl} [B_{cf}(P_{cyl})_i + C_{cf} * (S_{fact})_i + Q_{cf} * (S_{fact})_i^2] \quad (2)$$

as can be seen in the equation for friction,  $A_{cf}$  stands alone and are therefore not depending on the engine running setup while the  $B_{cf}$ ,  $C_{cf}$  and  $Q_{cf}$  terms is to account for changes in maximum pressure and speed factor. Since the KTM SX-F only has one cylinder the engine friction equation can be simplified as shown in Eq 3.

$$FM EP = A_{cf} + B_{cf}(P_{MAX}) + C_{cf}(rpm * stroke/2) + Q_{cf}(rpm * stroke/2)^2 \quad (3)$$

Speed factor:

$$S_{fact} = rpm \left( \frac{stroke}{2} \right) \quad (4)$$

Wave will as the only given option automatically implement and calculate the friction when provided with required data. There is however one possible way to override and do the work manually. By entering the manually calculated total friction in the constant portion of the

equation ( $A_{cf}$ ) in the engine general panel for friction correlation and set  $B_{cf}$ ,  $C_{cf}$  and  $Q_{cf}$  to zero. The built in formula will be ignored and the provided input will be accepted as the FMEP. Overriding the software is however not recommended for other than steady state simulation since FMEP changes with speed and load. If there is an interest to use manual input for different speed and/or load changes, it is necessary to provide Wave with new FMEP data representing that change. Wave has recommended values that can be used for different type of engines. Values recommended by Wave will be used when constructing the KTM SX-F engine later on. If there is any interest in evaluating the FMEP it is optional to attach a sensor to the simulation model. If the sensor (sub-model) is connected to the cylinder, it will report the FMEP from the cylinder. If attached to the engine, it will report the FMEP for the complete engine.

Further test data is required to perform the correlation of the model. There are three other types of mean effective pressure necessary to provide and include in the model. These are Pumping-, Indicated- and Brake Mean Effective Pressure. The pumping losses (PMEP) are calculated separately with Eq 5 below. The engine indicated performance (IMEP) represents the software calculated performance and the BMEP is the sum of IMEP and FMEP.

$$PMEPPX = \frac{\oint_{lower}^{PDV}}{V_D} \quad (5)$$

where:

$$\begin{aligned} P &= \text{Cylinder pressure} \\ V &= \text{Cylinder volume} \\ V_d &= \text{Displacement volume of the cylinder} \end{aligned}$$

PX in equation 5 stands for the crossing point in the P-V curve (Pressure - Volume) which describes the three-dimensional relationship between pressure, volume and temperature. The curve is sketched by searching for the first crossing of the exhaust and compression strokes. There are built in backups in case no crossing point is to be found between the exhaust and compression stroke. PX can be predicted by the crossing point in the intake and expansion strokes as well. In case of multiple crossings, the one closest to BDC (Bottom Dead Centre) will be picked for maximum volume. The pressure to volume can be sketched in WavePost. To do so it is necessary to have the model running properly.

There is no sensor for PMEP to be used in Wave. If however there is interest in evaluat-

ing BMEP or IMEP it is optional to attach a sensor to the model. "If it is attached to a Cylinder element, it will report the work from that cylinder alone. If it is attached to the Engine, it will report the work from all cylinders and crankcases plus the work from gear driven superchargers and power turbines minus friction losses " -Ricardo Wave. Since the KTM SX-F is a one cylinder engine and do not have a supercharger it does not matter if the sensor is attached to the engine or directly to the cylinder.

## 2.3 DISCRETIZATION

Discretization can be explained as the equivalent to mesh net for FEM analysis. Restrictor, diffuser and runner are some of the engine ducts carrying fluids. These ducts will in the simulations provide the option of choosing discretization length. By discretization/dividing one single duct into more elements/sub-volumes a better resolution of results hence higher accuracy will be achieved, see figure 6. The discretization length has to be chosen with respect to the resolution required. This is due to the increased solving time that comes with increasing discretization. Maximum utility has to be balanced with solving time. Most of the work will be focusing on optimising the intake side of the engine encouraging high resolution on the ducts which will be carefully studied while a long exhaust pipe with few bends should be split into fewer elements per unit length saving computation time.

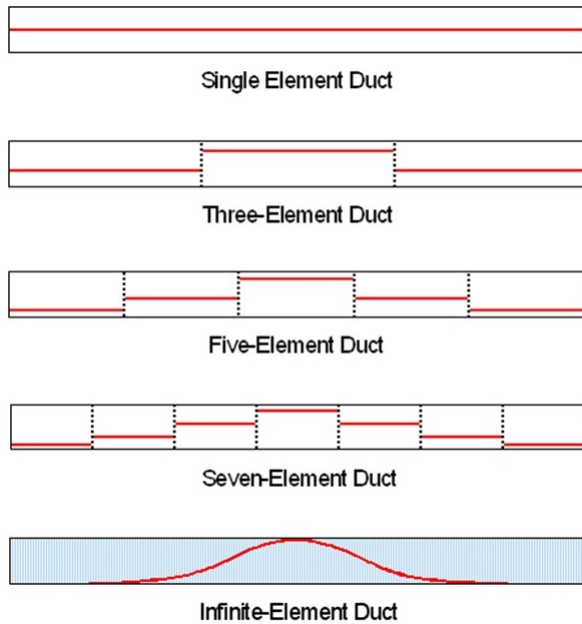


Figure 6 - Discretization length.

An experiment to see how the solving time are effected by the discretization showed that a 300 mm duct with a discretization length of 15 mm ( $\frac{300}{15} = 20 \text{ elements}$ ) took 2.5 seconds longer for the simulation to run compared to 150 mm ( $\frac{300}{150} = 2 \text{ elements}$ ).

## 2.4 HEAT TRANSFER MODEL Woschni VS Annand

An accurate estimate of the heat transfer between cylinder gases and cylinder wall of a combustion engine is necessary for a precise calculation of power, efficiency and emissions during engine development [3]. A great amount of the chemical energy is unfortunately lost and not transformed to the purposed kinetic energy. 30% of the fuel energy is carried away in the exhaust flow in form of heated exhaust gas and unburned fuel. 35% of the energy is dissipated to the surrounding through heat. This leaves only 35% of the total chemical energy available to be harvested as useful crankshaft work. Keeping the engine as close to optimum temperature as possible is highly desired since a low engine temperature increases wear and are inefficient due to thermal efficiency. On the other hand, it is important not to run the engine too hot to avoid increased wear and even epic failure.

The great amount of heat produced has a big impact on the engine efficiency, friction and wear. Several simulation models exist for evaluating the heat transfer coefficient, of which the most common correlation models in engine research are those from Annand [4] and Woschni [5]. The heat development in the simulation will be taken in consideration with Woschni correlative model for convective heat transfer. The original model for heat transfer Eq 4 assumes simple heat transfer from a confined volume surrounded on all sides by walls representing the cylinder head, cylinder liner and piston face areas exposed to the combustion chamber. Each area is calculated from the provided measurement for bore, stroke, connecting rod length, and clearance height. The original model does not compensate for varying levels of indicated mean effective pressure IMEP which is a compensation for the engine load. Wave are therefore equipped with the option of load compensation [6] Eq 5. Unfortunately Wave do not come with the option of entering the Woschni heat transfer coefficient manually and can therefore not be verified if the algorithm is neither correct nor properly implemented in the simulation. The only option is to provide the software with the input, choosing preferred options and having the program automatically calculating. Even though the simple original and more complex compensated Woschni equations cannot be manually used in the software it is still preferable to look into the composition of the Woschni and Annand equations for better understanding of how engine speed, heat, design, pressure and other parameters are related and contribute to the final output.

For the standard engine cylinder, there is only one type of heat transfer model available – the Woschni correlative model for convective heat transfer (1967). This model assumes simple heat transfer from a confined volume surrounded on all sides by walls representing the cylinder head, cylinder liner, and piston face areas exposed to the combustion chamber. The area of each is simply calculated from the provided geometry for bore, stroke, connecting rod length, and clearance height.



Woschni heat transfer coefficient is described as

$$h_g = 0.0128D^{-0.20}P^{0.80}T^{-0.53}v_c^{0.8}C_{enht} \quad (6)$$

were Woschni's original correlation is

$$v_c = c_1v_m + c_2\frac{V_D T_r}{P_r V_r}(P - P_{mot}) \quad (7)$$

and Woschni's modified correlation version with IMEP compensation is

$$v_c = \max \left[ \left( c_1v_m + c_2\frac{V_D T_r}{P_r V_r}(P - P_{mot}) \right) * \left( c_1v_m \left( 1 + 2 \left( \frac{V_c}{V} \right)^2 \right) IMEP^{-0.2} \right) \right] \quad (8)$$

$c_1$  in Eq 8 is used when the valves are scavenging. The constants  $c_1$  and  $c_2$  are necessary to consider changes in gas velocity over the engine cycle. The recommended values for  $c_1$  and  $c_2$  are as follows [7]:

$$c_1 = 6.18 + 0.417\frac{v_s}{v_m} \quad (9)$$

$c_1$  in Eq 9 is used when the valves are closed:

$$c_1 = 2.28 + 0.308\frac{v_s}{v_m} \quad (10)$$

To be able to calculate  $c_1$  in Eq 8 and 9 the swirl velocity ( $v_s$ ) is to be calculated with:

$$v_s = \pi * R_{swirl} * D * \frac{rpm}{60} \quad (11)$$

$c_2 = 0$  before combustion and during scavenging.  $c_2$  can be calculated as shown during combustion:

$$c_2 = 3.24 * 10^{-3} \left[ \frac{m}{s * K} \right] \quad (12)$$

The swirl can be set directly as a number of ratios or predicted by Wave which uses equations 6 - 12. If Wave is set to predict the swirl ratio the value specified is constant throughout

the duration of the simulation and is normally between 0 - 0.3 where 0 represent a non-swirl port design. For Wave to be able to predict the swirl ratio the entire piston bowl geometry is required. Piston bowl depth, diameter, rim diameter and volume. Adding swirl will increase the total heat transfer due to increased charge motion in the cylinder [17]. See appendix A.2 for more details. By observing the difference between Eq 7 and 8 the compensation term for load can be noticed. By substituting Eq 7 in Eq 6, the original Woschni heat transfer coefficient from 1967 will apply and substitution of Eq 8 in Eq 6 will provide the modified Woschni heat transfer coefficient from 1990 which include load. The Woschni's modified correlation will be used in this project and most likely set to be calculated automatically since the option of manually inserting the Woschni correlation is, as mentioned earlier, not provided by Wave but only the ratio.

Annand's heat transfer coefficient is given by [1]:

$$h_g = \left( a \left( \frac{\rho v_m D}{\mu} \right)^{0.7} \right) * \frac{K}{D} \quad (13)$$

The Annand heat transfer model from 1963 is mostly used to compare results with the Woschni model and is not an available option to use in Wave. The main difference between the woschni and Annand heat transfer models are that Annand can only be applied to an IRIS cylinder which is an advanced engine model. This does not mean that Annands model is more advanced, just more limited. Annand assumes a constant gas velocity equal to the mean piston velocity while Woschni takes the change in gas velocity inside the cylinder in consideration. Both the IRIS and the basic cylinder can provide with a stunning 64 different engine related standard time plots. Available time plot outputs from both Woschni and Annand is heat transfer rate, heat flux, Heat transfer coefficient and inner wall temperature. In addition both Woschni and Annand can provide three summary quantities regarding heat transfer rate which provides the user with seven different sensor options that can be added to the simulation cylinder and also seven actuators. The Woschni equation is the most widely used model for prediction of charge, heat flow coefficient and velocity on all surface of the cylinder<sup>1</sup> Explanation of abbreviation is listed at the beginning of the report.

---

<sup>1</sup>Ricardo Software, 2010. WAVE Knowledge Centre

## 2.5 COMBUSTION MODEL

The general engine cylinder in Wave models the heat release caused by combustion vs. time as a simplification of the real combustion. There are two combustion sub-models available to use – the SI Wiebe and profile sub-models. The profile sub-model is used when fuel mass burn vs. crank angle data is available for every speed and load that is set to run. The approach for this part of the project will be to define the combustion profile by the Wiebe function. Wiebe is most widely used, simply using an S-shaped curve to show the combustion duration. The curve simply represents the fuel mass burned in the cylinder. The Wiebe function is empirical constructed and are used to describes the heat release during combustion approximately but quite accurately. It is important to note how the combustion model handles the provided data in the simulation software.

The original Wiebe function from Steisch [7] is shown in Eq 14. While investigating the simple Wiebe function as showed in Wave and comparing with the original function from Steisch the difference of Wave not using division of duration can be noticed. Since the complete Wiebe function includes division of duration the use of the simple Wiebe can only be explained by Wave always using the same duration. Meaning that there is no need for the user to provide the software with the duration, this is however not likely. The other possible explanation is that Wave is receiving the input of duration from elsewhere. By screening through the input Wave asks for it is obvious that in practice the Wiebe function inputs are adopted for every case. This is a must since firstly; the parameters that appear in the function vary with operating conditions. Secondly a standard Wiebe function can only be made to adopt a limited range of combustion. To simulate an accurate Wiebe curve that correspond to the shape of the real combustion progress through all stages of combustion Eq 19 are being employed where external constants can be added and different provided values can be used for each case [8].

Steisch original Wiebe function:

$$W_n(\theta) = 1 - \exp \left[ -A \left( \frac{\theta - \theta_0}{\Delta\theta} \right)^{B+1} \right] \quad (14)$$

Simpel Wiebe function as shown in Wave:

$$W_n = 1 - \exp \left[ -A(\theta_i - \theta_0)^{B+1} \right] \quad (15)$$

The Wiebe function consists of two zones of mass fraction for the fuel. The two zones refer to burned and unburned fuel for each time step. The energy balance therefore moves fuel from the unburned zone to the burned zone over time of combustion. Each of the three cylinder areas: piston, cylinder head and cylinder linear may be exposed to burned or unburned fuel. The unburned fuel can be either in state if gas or liquid. The fraction of burned fuel is described as  $W_n$  for the duration or  $W_n(\theta)$  for a specific position of crank angle.  $\theta$  is the crank angle,  $\theta_0$  is the start of combustion and  $\Delta\theta$  refers to the total combustion duration. The symbol  $B$  is called the combustion mode parameter and defines the shape of the combustion profile with respect to time.

The time dependence of concentration of reaction ( $\rho$ ) is described by Eq 16 where  $k$  is a constant. Wiebe describe  $B$  to be in the range 2 - 4 for SI engines [8]:

$$\rho = kt^B \quad (16)$$

while  $A$  is a scaling factor defined as:

$$A = -\ln(1 - x_{B,EOC}) \quad (17)$$

It is necessary to provide Wave with location of crank angle for 50% burn point (ATDC), location of crank angle for combustion duration from 10 - 90% mass fraction burned points, exponent in Wiebe function (controlling the shape of the Wiebe curve) and the profile control terminate value for the SI Wiebe combustion model to be fully defined. The control terminate value refers to efficiency and will be set to 1. The absolute value of control terminate is between zero and one (0 - 1) scaling the efficiency from 0 - 100%. A quick experiment showed that Eq 17 cannot handle the mass fraction burned ( $x_{B,EOC}$ ) of 100% at the end of combustion ( $EOC$ ) since  $-\ln(0) \rightarrow \infty$  Wave have however solved this issue since a perfect combustion of 100% efficiency is an accepted value. How it is done is unfortunately not revealed but most likely with an “if” statement inserted and attached to the arithmetic of the combustion model to address this issue.

Observe that  $\frac{Q_{chem}(\theta)}{Q_{chem.tot}}$  is referred to as  $W_n(\theta)$  in Eq 14. Thereby  $\frac{dQ_{chem}}{d\theta}$  correspond to the instantaneous heat release by deriving eq 14 as showed in Eq 18.

$$\frac{dQ_{chem}}{d\theta} = a * Q_{chem,tot} * (m + 1) * \left(\frac{\theta - \theta_0}{\Delta\theta}\right)^B * exp \left[ -A \left(\frac{\theta - \theta_0}{\Delta\theta}\right)^{B+1} \right] \quad (18)$$

The burn profile as can be viewed in figure 7 to the left correspond to Eq 18 for the instantaneous heat release and integrated heat release as calculated in Eq 14 to the right. "M" represents the exponent in the Wiebe function.

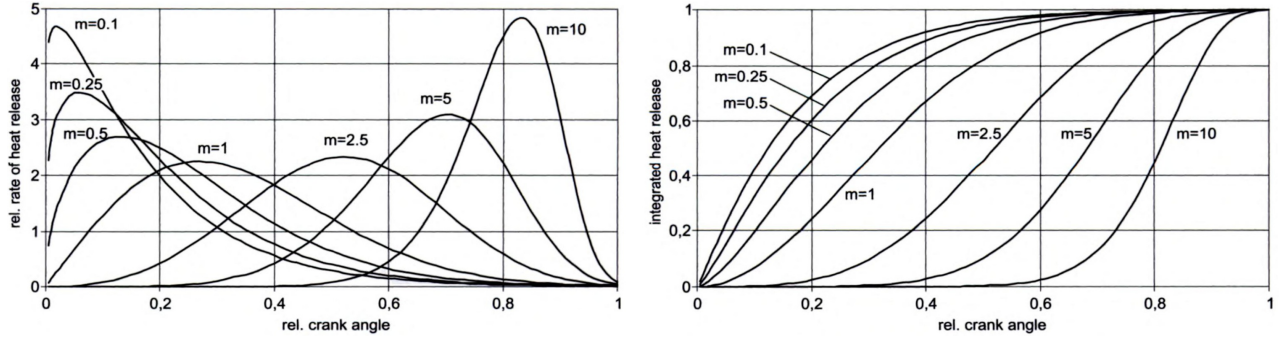


Figure 7 - Burn profile and the integrated burn profile.

To be able to transform maximum amount of chemical energy into kinetic energy it is crucial that the combustion starts, peaks and ends at the right position of the crankshaft. Since the compression ratio and air/fuel mixture is constant throughout the rpm range, the amount of time it takes to combust is constant. Therefore it is necessary to adjust the initiating of the combustion regarding to the crankshaft piston, earlier with higher rpm. The location of 50% burn point and the combustion duration will therefore not be set as constants but as a variable depending on rpm. The default value of 2.0 for the exponent in Wiebe Function and 1.0 for the profile control terminate is appropriate for most cases and will therefore be employed [1]. Csallner's [9] Wiebe combustion parameter correlations present a table of how Ignition delay, total combustion duration and combustion mode parameter  $B$  effect the Wiebe curve. The table can also be viewed in Fredrik Lindströms licentiate thesis [8]. The table is developed in part due to method used for fitting Wiebe functions to test data using a BMW 2 dm<sup>3</sup> four cylinder two valve engine and can be used to see that only air/fuel ratio and engine speed effects the combustion mode parameter.

AWI in the Wiebe function as used in Wave represent the internally calculated parameter to allow the user-entered combustion duration (BDUR) to cover the range of 10-90%. WEXP refers to the user-entered exponent.

$$W = 1 - \exp\left(-AWI \left(\frac{\theta}{BDUR}\right)^{WEXP+1}\right) \quad (19)$$

Values for 50% burn point has been set to 8.0 degrees ATDC as an experiment but will during the perform of the KTM SX-F engine be set to {CA50} which provide the software with a new burn point for each case by a user provided constant table. Varying the 50% burn point simply shifts the entire curve forward or backward. AWI represent the internally calculated parameter to allow the combustion duration of 31 degrees to cover the range of 10-90% which also will be provided with a case depending variable named {BDUR}. Varying the 10-90% duration will extend the total combustion duration, making the profile extend longer or compress shorter. Varying the Wiebe exponent will shift the curve to burn mass earlier or later. WEXP refers to the user-entered exponent [1]. Figure 8 shows the SI Wiebe combustion model in Wave and the reference heat release rate [10]. The values used for now is based on tutorial values from Wave for research purpose.

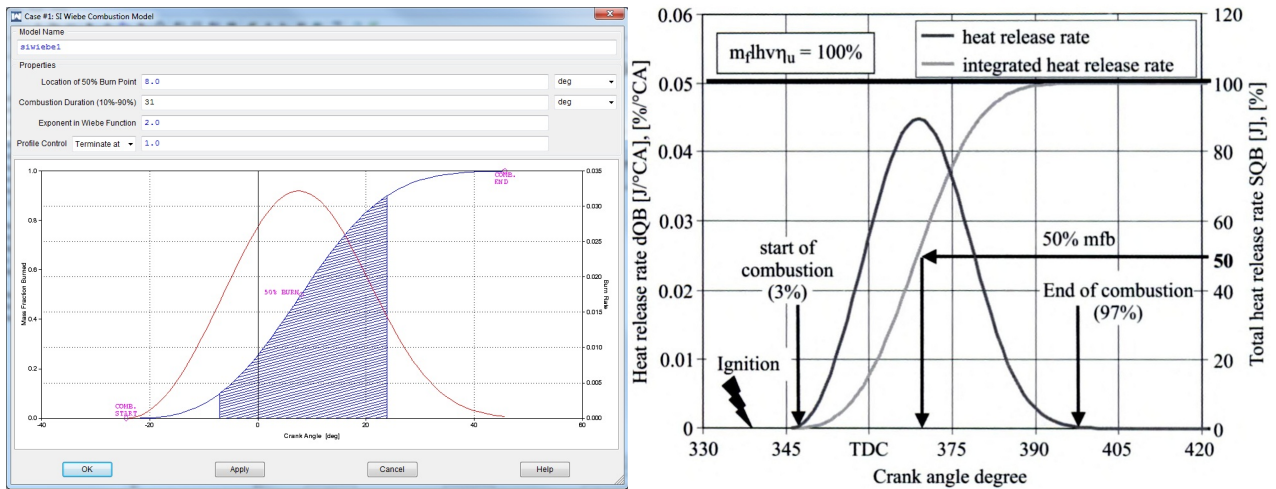


Figure 8 - SI Wiebe combustion model in Wave to the left and the reference heat release rate to the right.

There are no sensors available for the SI Wiebe combustion sub-model but there are still available outputs such as average unburned and burned-zone temperatures, combustion fuel burn, heat release rate and instantaneous combustion equivalence ratio. The available summaries are timing of start of combustion, timing of any desired percentage and/or duration between any

two levels of fuel mass burned.

## 2.6 COMPLEX Y-JUNCTION

The complex Y-junction (collector) is a more flexible option to the simple Y-junction with more possibility to control and adjust. The junction is a one cell massless representation in the flow network and can be utilized to describe any type of merge or split of ducts. In this particular case, port canals. The complex Y-junction shape is not required to be provided, this enable to construct all shapes of junctions but is a rather complicated input to measure hence there is some specific distances required for Wave to be able to approximately represent the junction. By providing the number of ducts connected to the junction together with DELX, DIAB, pressure, flow direction, duct shape, diameter and angle in between the ducts the matrix for the system can be solved. The Y-junction diameter is required to be able to find local flow velocity which effect the friction and heat transfer. E.g. a decrease in Y-junction diameter gives an increase in heat transfer out of the Y-junction doe to increase in velocity for a given mass flow. The characteristic length (DELX) values for the runner connections is the distance across the sub volume in the direction of flow into the runner are internally calculated by Wave. DELX is used to calculate the total distance travelled by the substance through the volume and are calculated similar to the discretization length for ducts. By calculating the distance between the two closest nodes which is the total flow length in figure 9 from opening A to opening B through the volume the equation for discretization length Eq 20 can be used.

$$Total\ flow\ length = \frac{1}{2} * DELX\_A + \frac{1}{2} DELX\_B \quad (20)$$

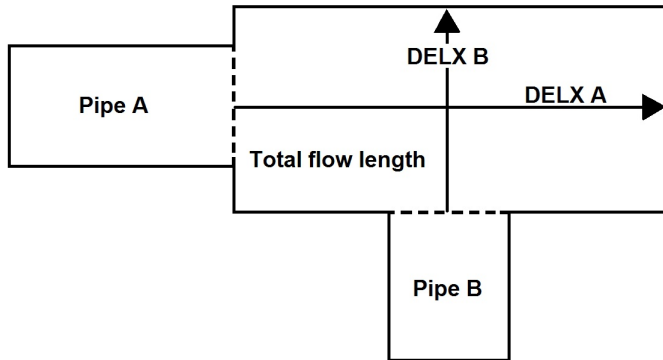


Figure 9 - A simple representation of Y-junction as defined<sup>2</sup>.

<sup>2</sup>Ricardo Software, 2010. WAVE Knowledge Centre

In a simple Y-junction the expansion diameter (DIAB) used to determine area ratios for flow losses entering and leaving the Y-junction is internally set equal to the Y-junction diameter divided by 1.1 for each connected duct. The recommendation from Wave is to use simple Y-junction when the junction geometry is spherical. The junctions in the KTM engine are spherical but complex Y-junctions will still be used for increase in design options. Using the complex Y-junction increase however the possibility of error and should therefore be used with caution. It is possible to use the simple Y-junction value for DIAB by manually calculate it as Wave does or optionally, enter the value "auto". By entering DIAB values equal to the duct diameters, no expansion or contraction occurs. DIAB will be set to "auto" in all simulations in this project.

## 2.7 PRESSURE WAVE REFLECTION IN DUCTS

Internal combustion engines can be equalised to a wave generator when it comes to pressure waves [11], [12]. The downward motion of the piston (intake stroke) accelerates air through the intake system of the engine. The air and/or air-fuel mixture gain kinetic energy during this process. When the intake valve closes rapidly pressure are created due to the compressibility of air. The pressure wave locked outside the plenum chamber due to the rapid closer of the intake valve will result in a resonance occurring bouncing back and forth in the intake runner. This ramming phenomenon can be used to fill up the cylinder. If this phenomenon is utilized properly the return of the pressure wave towards the intake valve can be timed to arrive when the intake valve is open. In that case a filling degree of more than 100% will accrue. In other words, the cylinder chamber will be filled with air and the air pressure will be higher than the atmospheric pressure effectively acting like a turbocharger. This phenomenon is always strived towards, hence the amount of fuel possible to burn is a direct consequence of the number of air molecules available in the cylinder at time for combustion.

The magnitude of the filling degree is depending of the diameter and length of the intake runner, hence a bigger runner contain more air available to be set in motion. The filling degree occurs due to inertia of the air, requiring energy to brake the air in motion towards the cylinder. Keep in mind that the pressure wave is not lost when reached the plenum side of the runner. Pressure waves reflected from open ends are just as strong as from closed ends, except that the sign are alternating between positive and negative. The ramming phenomenon can be timed by the intake runner length which has a large influence on the engine performance. Changing the intake runner length not only impact on power and torque but also at what rpm it peaks. As the runner lengths are increased the tuning peak occurs at lower rpm. The intake runner length can therefore be adjusted so that power and torque peaks at desired rpm. This can be contemplated as the limitation of this technique since it only provides a benefit in a fairly narrow range of rpm.



Another parameter that affects this phenomenon is the diameter of the intake runner. By decreasing the diameter of the intake runner the air speed is increased and as a consequence more air can be forced into the combustion chamber. When deciding intake runner diameter it is important to keep in mind that a smooth transition between the runner and intake port is essential to eliminate the risk of having undesired turbulence between the components increases the discharge coefficient. Since the same amount of air is set in motion depending only by the cylinder volume and the downwards motion of the piston unregarded by the intake runner geometry, a more narrow diameter will increase the friction between the air and the inside wall of the intake runner. The extra energy required to set the same amount of air in motion but with higher speed through the runner is taken from the energy source which is the downward motion of the piston generating the low pressure. This is not to be neglected. Even though the extra energy required to increase the speed of approximately one litre of air slightly is not much, this has to be balanced with the benefits of increasing the air speed.

To optimum benefit from this phenomenon in practice it is essential to time the arrival of the pressure wave by the so called "80-90" rule. The term "80-90" is to do with the camshaft timing starting the process and where the piston is when the reflected pulse arrives (between 80 - 90 degrees after TDC during the intake stroke). To maximise the filling degree the pressure wave have to be timed to arrive as the inlet flow is falling off, but the intake valve is still open, to get that extra addition of air before the valve closes. To be able to tune the intake runner length to time the arrival of the pressure wave the rpm for which the ramming phenomenon is to be optimised for have to be decided and the duration of the intake valve and speed of sound in air are required. An example calculation to understand the speed and location of the pressure wave for later use can be seen in chapter 2.7.1.

### 2.7.1 EXAMPLE CALCULATION

\*The engine speed for which the 2011 KTM 450 SX-F power peaks is 9500 rpm.

\* The intake valve is open 220 degrees out of 720 degrees in total.

\*Speed of sound in air at 30 degrees Celsius is  $349.08 \text{ m} * \text{s}^{-1}$

The engine speed is required to be described in rps (revolution per second) as SI units is preferred:  $9500 \text{ rpm} = \frac{475}{3} \text{ rps}$ . This means that one revolution takes  $\frac{1}{(\frac{475}{3})} \text{ s} = 0.0063\text{s}$  and the intake valve will remain closed for  $720 - 220 = 500 \text{ degrees}$ . Which is  $\frac{500}{360} = 1.38$  revolutions.

The time it takes between when the valve closes and when it opens again is:  $0.0063 * 1.38 = 0.0088\text{s}$ . The wave moving at the speed of sound during that time will cover the distance of:  $0.0088 * 349.08 \approx 3.075\text{m}$  before the intake valve opens again. Since the pressure wave has to

travel back and forth, the optimum length for the intake runner when it comes to using the ramming phenomenon at 9500 rpm is half of the calculated length ( $\approx 1.538m$ ). A runner length of approximately  $1.5m$  would be very difficult to fit in the car.

To address the ungainly size of the intake runner length required to utilize the ramming phenomenon a solution is to shorten the runner length to exactly one fourth of the calculated length. That will provide a runner length of  $\frac{1.5375}{4} = 0.3844m$  which is conveniently short enough to incorporate the component within the envelope regulation for an FSAE car. If the runner length is shorten to one forth, making it  $0.3844m$ , the pressure wave will travel up and down the pipe four times before the intake valve opens again. But it still arrives at the valve at the same time. This is a way to shorten the intake runner and still get some benefit from the pressure wave, preferred to as quarter wave resonator.

### 3 KTM STOCK ENGINE MEASUREMENTS AND SIMULATION SETUP

The majority of data have been manually measured or provided by technical manuals from KTM. These values are considered as known and was therefore set as constants. See appendix A.10.2. Figure 10 shows the engine in the dynamometer room during test run which the simulation measurements were taken from. The unknown values have undergone investigation and appropriately determined.



Figure 10 - The KTM SX-F stock engine in the dynamometer room at Monash University.

Figure 11 and 12 describe the process of manually measuring components in the workshop at Monash University hence there is no reference to refer to. A list of engine data that Wave required to completely define the engine can be seen in table 2. This includes the cylinder head, inlet and exhaust ports and all dimensions and characteristics associated with the actual engine itself. The given dimensions are given in table 2.

Table 2 - Important engine dimensions

- *Bore*
- *Stroke*
- *Connecting rod length*
- *Wrist pin offset*
- *Compression ratio*
- *Mechanical friction details*
- *Port flow coefficients*
- *Valve diameters*
- *Valve event timings*
- *Cam profiles*
- *Piston ring and cylinder liner friction*
- *Orientation and size of piston top shapes*
- *Wall temperature characteristics and transfer coefficients*
- *Shape of the cylinder head, ports and combustion chamber*
- *Position of valves in the combustion chamber and position of spark plug*

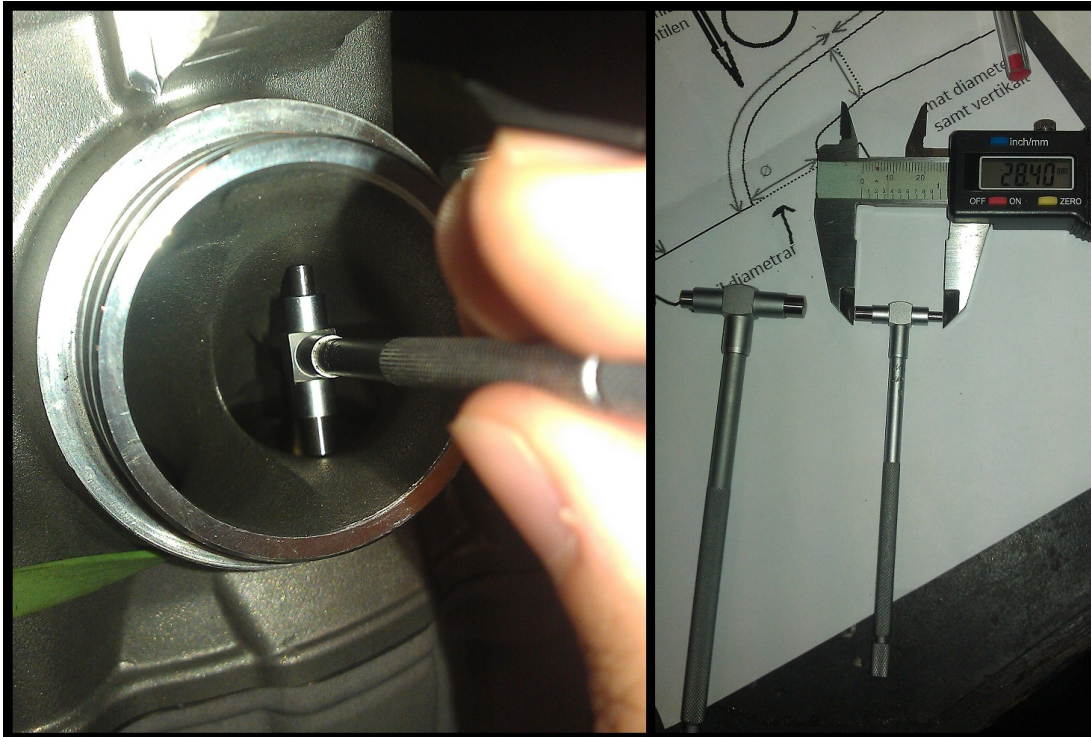


Figure 11 - Example of port measurement.

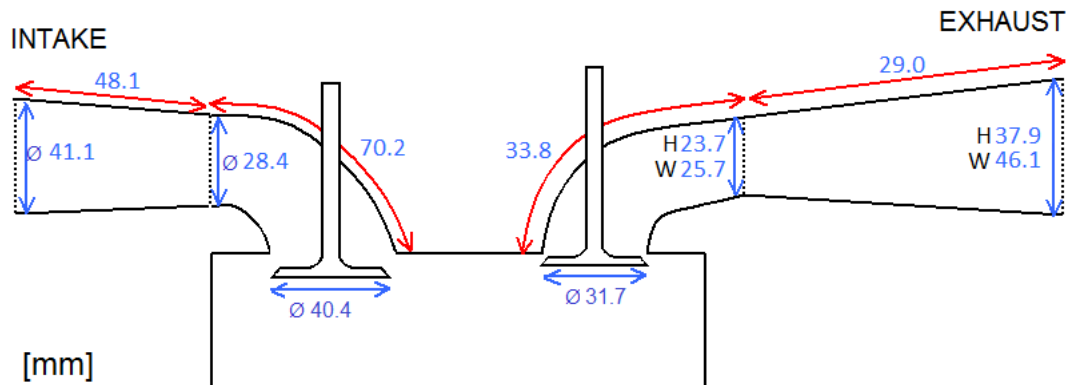


Figure 12 - Schematic picture to illustrate some of the geometrical measurements.

### 3.1 DESIGN IN RICARDO WAVE

Before attempting to construct the KTM SX-F engine in Wave by adding components it was required to provide the software with some general information. All units in the simulation control were defined in the SI system with [mm] as the basic unit for length. The basic fuel available in the FSAE Series is unleaded gasoline with octane rating of  $93 (R+M)/2$  (approximately 98 RON)<sup>3</sup>. Fuel in reality can vary in quality. The simulation was therefore operating on a special laboratory fuel called indolene. The fuel has an equal amount of energy value as 98 RON unleaded which is a liquid test fuel and should therefore correspond well to reality. Some other preconstruction settings were the surrounding air composition which was set to 21% oxygen and 79% nitrogen<sup>4</sup>,<sup>5</sup>[13]. As the general parameters were defined the next step was to feed in geometric characteristics data as well as specify the initial and boundary conditions. Figure 13 shows the stock engine as it looked on the canvas in Wave.

<sup>3</sup>Society of Automotive Engineers, 2011 FSAE rules

<sup>4</sup><http://www.engineeringtoolbox.com>

<sup>5</sup><http://www.grc.nasa.gov>

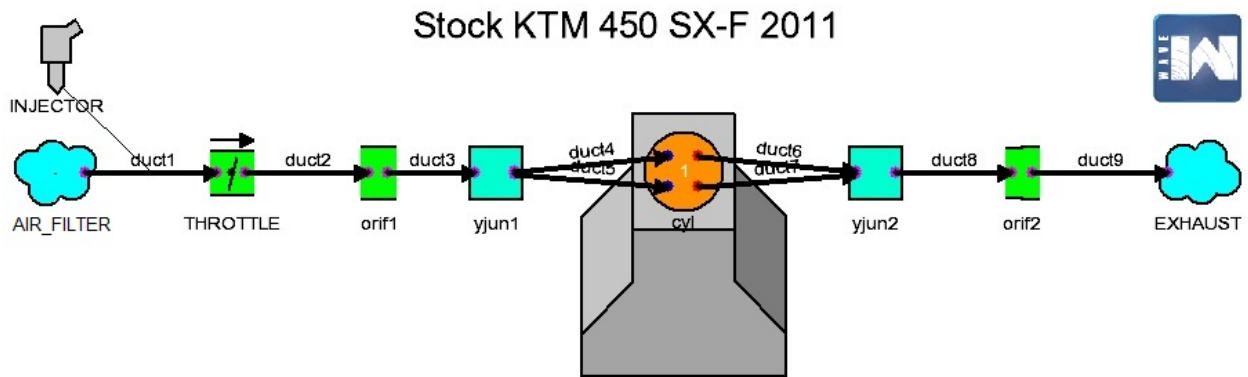


Figure 13 - The stock engine design on the canvas in Wave.

The connection from duct 4-5 and duct 6-7 in figure 13 to the cylinder junction was directly connected to the valves. The two dots on the left side of the cylinder which duct 4-5 are attached to are connected to the intake valves while the two dots on the right side of the cylinder which duct 6-7 are attached to are connected to the exhaust valves

### 3.2 INTAKE

The ambient providing the engine with air via the air filter was as mentioned represented with the composition of 21% oxygen and 79% nitrogen. Figure 14 shows the input for the air intake. The "auto" diameter adjust automatically to the connected duct. Value of 1.0 [bar] and 300 [K] and a composition of 100% fresh air represent the environment well. The discharge coefficient [ $C_d$ ] was set to "auto". This was as the experiment in 3.1 showed providing the matrix with the proper discharge coefficient.

Ambient		Initial Fluid Composition	
Diameter	AUTO	mm	
Pressure	1.0	bar	
Temperature	300.0	K	
Discharge Coefficient	AUTO		
Additional Acoustic End Correction	0.0	mm	
Solution Type <input type="radio"/> Fixed <input checked="" type="radio"/> Floating			

Ambient		Initial Fluid Composition		Passive Scalars			
Fresh Air	1.0			Name	Molecular Weight	Concentration	Units
Vaporized Fuel	0.0						
Burned Air	0.0						
Burned Fuel	0.0						
Liquid Fuel	0.0						

Figure 14 - Air intake settings.

### 3.3 DUCTS

As mentioned in chapter 2.3 (discretization), lower discretization length has the advantage of higher accuracy and the disadvantage of longer solving time. The discretization length for duct1 was set to 20 mm. This is a low discretization length. Since this is a one cylinder engine instead of four the solving time was not an issue and it was affordable with a higher accuracy. The total length of duct1 is 41.7 mm which is 2.85 times the discretization length. Wave automatically divides the duct into 2 equal length of 20.85mm since  $2 * 20.85$  correspond to the total length. View figure 6 for further details.

The entire engine head is made of aluminium, therefor the roughness height for duct1 was set to  $1.5 \mu m$ , which is an average value for new aluminum<sup>6</sup> [1]. Please see table in appendix A.4 for roughness height of other metals. The discharge coefficient for the left and right end of duct1 was set to "auto" and also for all other orifice and ducts since automatic calculation of the discharge coefficient has been proven trustworthy in chapter 2.1. Table 3 shows a brief list of settings.

Table 3 - Settings for duct1

{	<i>Shape</i>	<i>circular</i>	}
	<i>Wall friction</i>	1	
	<i>Wall heat transfer</i>	1	
	<i>Atmospheric pressure</i>	1atm	
	<i>Temperature</i>	300K	
	<i>Wall temperature</i>	300K	
	<i>Fresh air</i>	1	
}			

Wall friction and wall heat transfer input is only multiplier of the standard calculation and was set to one (1) since normal conditions applied. The atmospheric pressure and the surrounding temperature have a great impact on the outcome and needed to be very accurate. Wave default value for the atmospheric pressure is 0.986atm. The value of 1 atm was however used instead. The atmospheric pressure chosen was an average from physics handbook and physical geography<sup>7</sup> [14]. The temperature of the inhaled air was more complex to set. The air intake is located only centimetres away from the combustion chamber; it was most likely that the intake air temperature flux several degrees during a single test run. For the simulation to correspond accurately to the real engine it was set to  $300K = 26.86C$  which is slightly above

---

<sup>6</sup>www.engineeringtoolbox.com

<sup>7</sup>www.physicalgeography.net

the initial air temperature in the dynamometer room. Strong ventilation in the dynamometer helped to keep the intake air at room temperature.

Wave as can be seen in figure 15 is equipped with the options of circular and rectangular shape for ducts. Duct 1 - 5 and 9 was set to circular and was provided with the diameter measured from the KTM engine. Duct 6 - 8 however is elliptical. Since elliptical shape is not optional in Wave this has to be compensated for. In the case when circular ducts have been used the provided diameter was used to calculate the effective area. It is important to keep in mind that Wave used the provided data to run the engine in one dimension. The shape of the ducts chosen and the diameter was therefore only used to calculate the effective area. The challenge of not being able to choose the correct shape of the ducts was choosing "circular" and manually calculating the circular diameter that provided the same effective area as the ellipse. Duct and the duct measurements can be viewed in chapter 3.



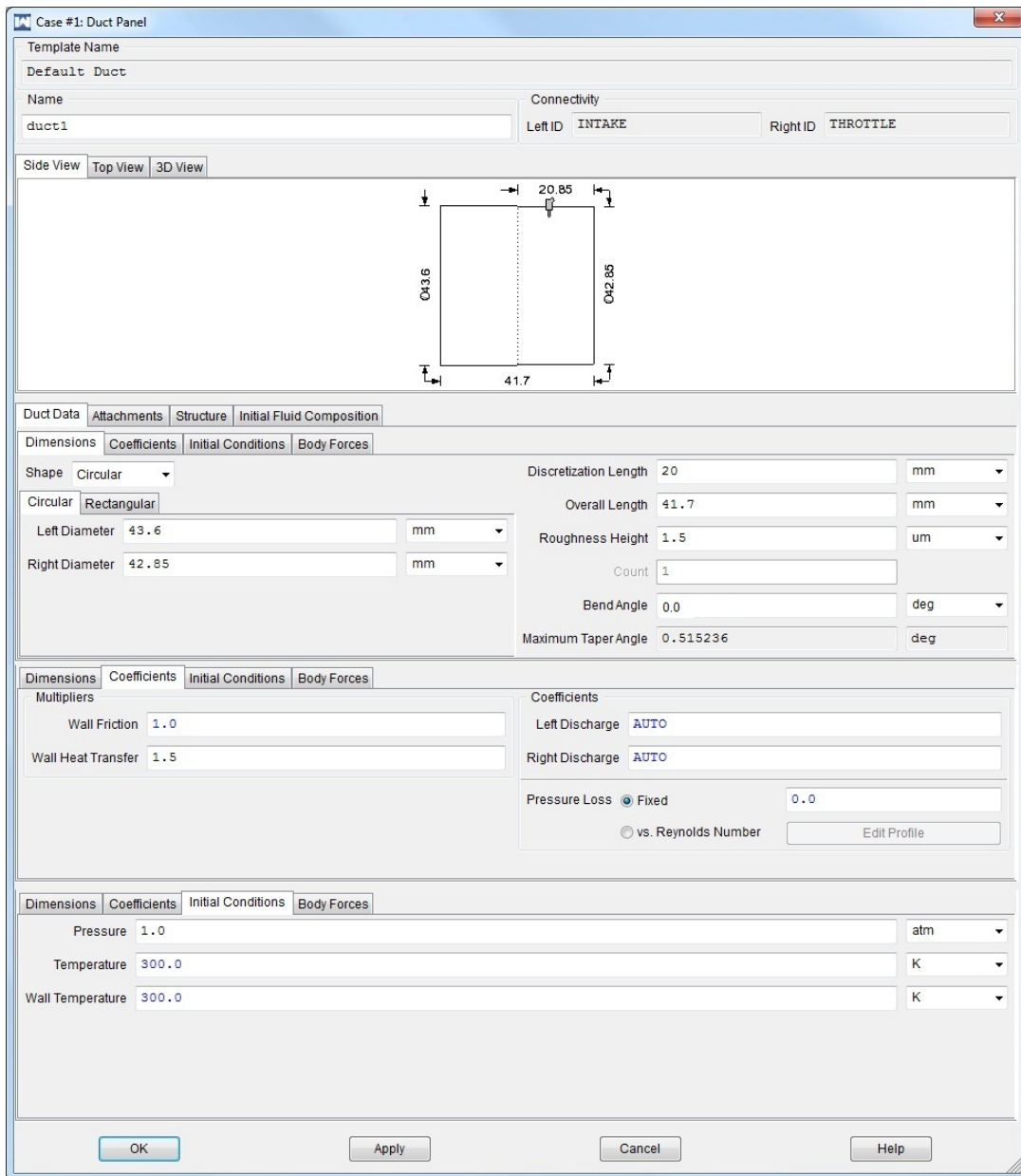


Figure 15 - General input for duct1.

### 3.4 INJECTOR

Since there is an injector on duct1 to simulate a carburettor a brief analysis on the options for injector was required. Wave has many injector types which may be used to model port fuel injection. Each has a different method of specifying what values to use as inputs and what values to calculate as outputs. The injector that was used, preferred to as a proportional type injector. This injector has the option "carb" built in which can help to simulate a carburettor, see appendix A.6. The initial injection velocity was when set to "carb" representing the fuel supply from a carburettor setting the instantaneous injection velocity equal to the local gas flow velocity.

The carburettor type on the KTM SX-F engine is KEIHIN FCR-MX 41 which is a modern 41 mm flat slide carburettor. The recommended air/fuel ratio of 1/14.7 was set for the test fuel indolene which as mentioned represents 98 RON well. Figure 16 shows a view through the carburettor.

"The proportional type injector can connect to a duct or Y-junction flow element, but not cylinder elements. A Proportional injector always inject enough fuel to the fluid stream to match a targeted air-fuel ratio. This is the simplest type of injector and is very commonly used." [1].

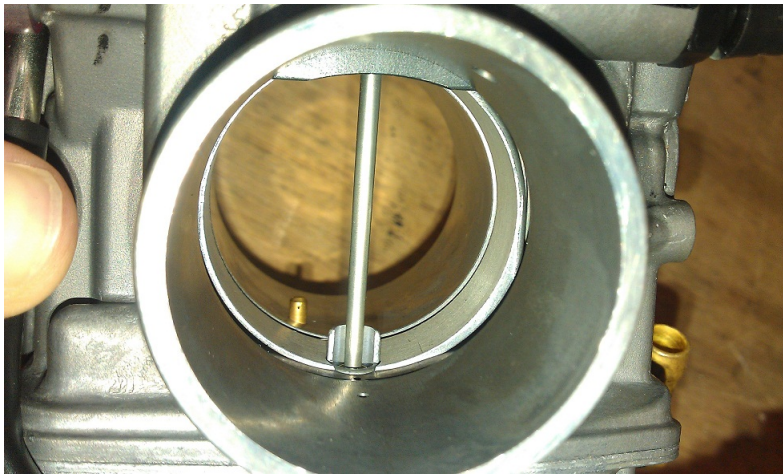


Figure 16 - Picture of Duct1, throttle (which is almost completely open) and duct 2 . The picture is taken from the engine side (duct 2).

### 3.5 CYLINDER

As outlined in theories of Chen-Flynn earlier in the report there was three options to get hold of engine related constants for the purpose of friction correlation. Either by manual measurement, use of recommended values from Wave or acquiring necessary data from the engine manufacturer. Since the necessary data could not be obtained from the engine manufacturer due to limited collaboration with KTM nor be manually measured due to limited equipment. Recommended values from Wave was employed. The available database in Wave has a wide range of engines. Recommended values for friction correlation from the most similar engine, a 400cc single cylinder four stroke SI engine was used which gives  $A_{cf} = 0.3 \text{ bar}$ ,  $BCF = 0.005$ ,  $C_{cf} = 400 \text{ Pa} * \text{min}/\text{m}$  and  $Q_{cf} = 0.2 \text{ Pa} * \text{min}^2/\text{m}^2$ .

The piston bowl depth and diameter, rim diameter and volume was set to zero since the cylinder head is almost completely flat as can be seen in the cross-section view in figure 17 together with the engine configuration and be read in the KTM engine specification manual. Data-sheet as shown in KTM SX-F specification manual is provided in appendix A.3.

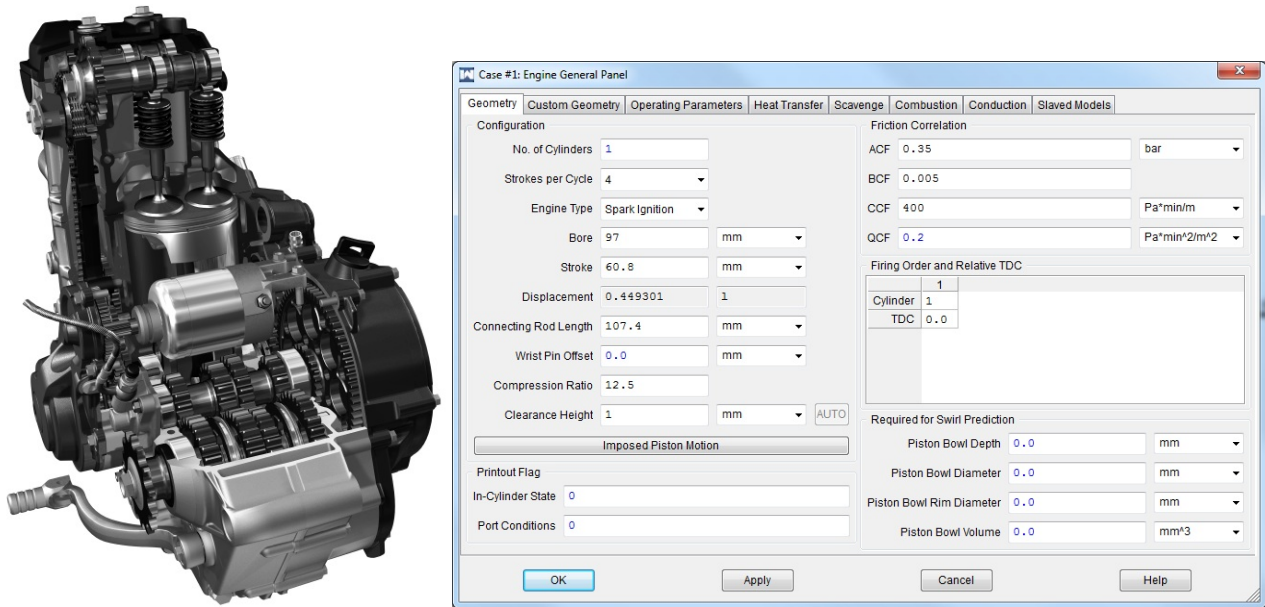


Figure 17 - Cross-section view of the KTM SX-F engine and the engine configuration setting panel as shown in Wave.

### 3.6 VALVES

The reference diameter and the heat transfer diameter for the intake valves was set to 40.4 mm and the exhaust valve to 31.7 mm as shown in figure 12. This value is typically the inner-seat diameter  $D$  (view figure in appendix A.7). The valve lift profile describes the lift of the valve vs. time. Time was in this case entered with respect to crank angle degrees.

The valve profile data has been manually gathered from the KTM SX-F as can be seen in figure 18. The data was gathered while the engine was cold, therefore it was necessary to add "hot lash". The hot lash moves the entire valve lift curve down to simulate the thermal expansion of the camshaft and valve when the engine was simulated to run hot. Wave automatically take the user provided hot lash value in account when the engine is hot. Measuring the lash can be done with a thickness gauge (see figure in appendix A.7). Recommended camshaft clearance for this particular engine is between 0.07 - 0.13 mm for the intake valve when cold [15]. Through experiment with different hot lash values in Wave 0.14 mm showed to be the minimum value to close the valve completely, over a wider range when the engine was running hot. Therefore the maximum recommended value from KTM of 0.13 mm clearance was used. This does not mean that the intake valve was leaking by ignoring the last 0.01 mm since as can be viewed in the table in figure 19 the intake valve was still completely closed during 150 degrees of the total duration.



Figure 18 - The valve profiles were manually measured at Monash University.

Recommended camshaft clearance for the exhaust valve is between 0.12 - 0.18 mm when cold [15]. Through experiment with different hot lash values in Wave a hot lash value of 0.19 mm showed to be the minimum value to close the valve completely over a wider range when the engine was running hot. Therefore the maximum recommended value from KTM of 0.18 mm clearance was exceeded with 0.01 mm since otherwise the exhaust valves would be leaking during 150 degrees of duration. The leakage from the exhaust valves would occur during the intake stroke. Therefore unlike the intake valves a hot lash value of 0.19 mm was used to prevent the undesired leakage. See figure 19.

Whether it was most wisely to fully follow recommendations from KTM or not, required use of common sense. In this case it was most likely that the valve lift was shifted by 0.01 mm when measured. If this source of error was not compensated for, the error would multiply and most likely prevent the simulated engine to fully correspond to the real engine. Exceeding the tolerance with 0.01 mm for the hot lash for the exhaust valves was therefore a better option than having the exhaust valves slightly open during part of the intake stroke. This compensation was most likely to bring the simulation closer to reality since it was most unlikely that the real engine was leaking. If the brand new 2011 KTM SX-F engine would have leaking valves the dynamometer testing would have showed a decrease in power since the slightest valve leakage have a great impact on the performance. The engine has been running on the dynamometer several times so far and there was no sign of power loss comparing to the specification from KTM.

A	B	C	D	E	F	G
	Angle	EV dial gauge reading	EV Disp	IV dial gauge reading	IV Disp	
	0	28	0	32	0	
	15.00	28	0	32	0	
	30.00	28	0	32	0	
	45.00	27.99	0.01	32	0	
	60.00	27.76	0.24	32	0	
	75.00	25.83	2.17	32	0	
	90.00	22.13	5.87	32	0	
	105.00	19.22	8.78	32	0	
	120.00	17.77	10.23	32	0	
	135.00	17.64	10.36	32	0	
	150.00	19.06	8.94	32	0	
	165.00	21.77	6.23	31.66	0.34	
	180.00	25.2	2.8	30.69	1.31	
	195.00	27.48	0.52	26.76	5.24	
	210.00	27.81	0.19	22.48	9.52	
	225.00	27.81	0.19	20.64	11.36	
	240.00	27.81	0.19	20.32	11.68	
	255.00	27.81	0.19	21.34	10.66	
	270.00	27.81	0.19	24.52	7.48	
	285.00	27.81	0.19	28.31	3.69	
	300.00	27.81	0.19	31.19	0.81	
	315.00	27.81	0.19	31.62	0.38	
	330.00	27.81	0.19	31.73	0.27	
	345.00	27.81	0.19	31.76	0.24	
	360.00	27.81	0.19	31.78	0.22	

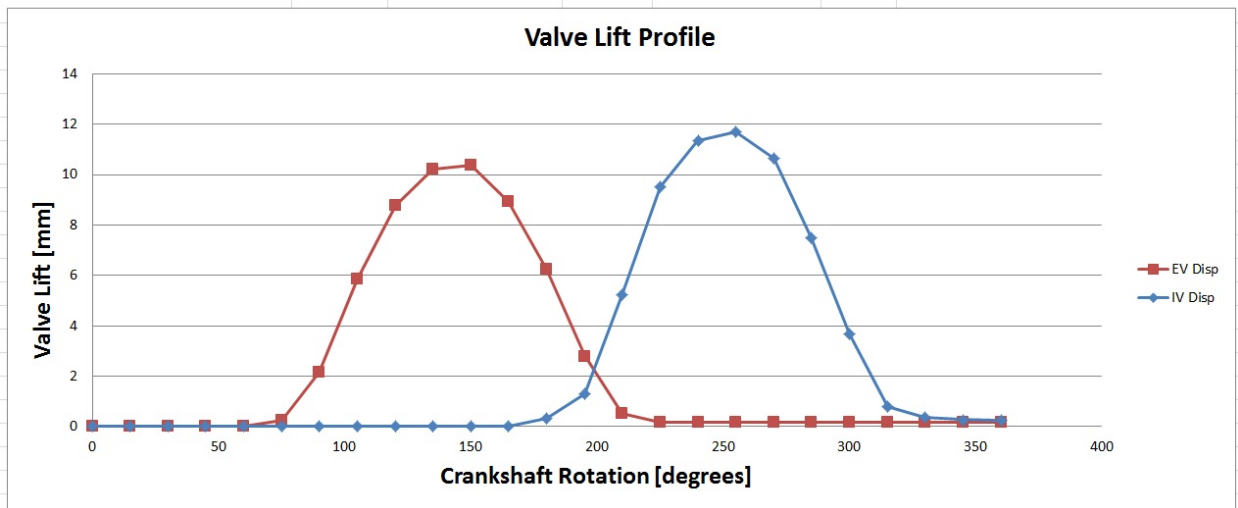


Figure 19 - Excel representation of the intake and exhaust valve lift profiles. The small overlap between the intake and the exhaust valves enables a compression of 12.5:1 to be achieved.

## 4 STOCK ENGINE SIMULATION

The purpose of these first series of simulations was to verify that the gathered data produce a simulation with comparable results to the real stock KTM SX-F engine by comparing simulation output to dynamometer results. The comprehension of the simulations tested should generically be relative to the number of unknown parameters in need of being defined. The number of parameters defining the engine in the simulation was depending on the number and type of components. The number of parameters defining the KTM SX-F engine is 629 parameters in total parameters where a vast majority was geometrical, environmental and material but also details which specify how the software should gather data and the accuracy. Most of the focus was on 154 of these values either due to their conditional nature in need of extra observation or for research purpose required for later optimisation. 32 of these parameters was unknown and therefore object for the first series of simulation.

The unknown parameters cannot be defined individually. Observation of one specific parameters impact on the output until the best value was boxed in does not mean that the current value have the same impact if changes was made to another value due to parameters depending on each other. Only a small number of sub equations are public for the user of the simulation program and available for display. These few sub equations shows which parameters are depending on each other and how. The limited knowledge of how the software utilise the provided data eliminate the possibility to solve the matrix with tools like MatLab. The mathematical but yet not optional solution would have required the matrix of 32 unknown parameters to be solved in one go or in several steps depending on how the parameters interact.

The majority of the 32 unknown parameters are not abstract which makes it possible to get a good understanding of their contribution, what other parameters they depend on and also group them into different experiments. Another tool in the quest to minimize the unknowns was the software provided default values. The default values give a good hint of where optimum can be expected. It was however necessary to critically dispute the default values due to the great difference between the topical engine and the average car engine the default values refers to.

### 4.1 KTM SX-F POWER AND TORQUE REFERENCE

The simulation of the KTM SX-F engine was compared and questioned with respect to the real engine. The trustworthiness was determined as a direct result of how well the power and torque curve from the simulation fitted the recognized output, see figure 20. The power and torque graphs available from the dynamometer was unfortunately limited in several considerations and

new data cannot be gathered due to extended reconstruction of the engine available. An effort to maximize the usage of the provided dynamometer results was instead carried out. The reference graphs was based on two dynamometer runs in second gear, third gear and also graphs provided by KTM them self. The KTM provided power and torque graphs represented output by the wheel and therefore only served as a reference of behaviour in case of any irregularity between the two runs on the dynamometer done by Monash Motorsport could be spotted. Unfortunately result from the two runs on the dynamometer was only sampled between 4000 - 11000 rpm in 500 rpm steps. There was however an desire to run the simulations throughout the entire rpm range from 1000 - 12000 rpm in steps of 250 rpm for increased resolution of behaviour. The missing data at speeds below 4000 rpm was extrapolated. Speeds between 11000 - 12000 rpm was too uncertain to extrapolate and was therefore not extrapolated but rather set to distinctly change pattern to easy be spotted as uninteresting reference. The gaps in between known rpm steps was set to average of known values. This was performed so the dynamometer results with the resolution of 500 rpm steps have the same number of reference points as the simulation.

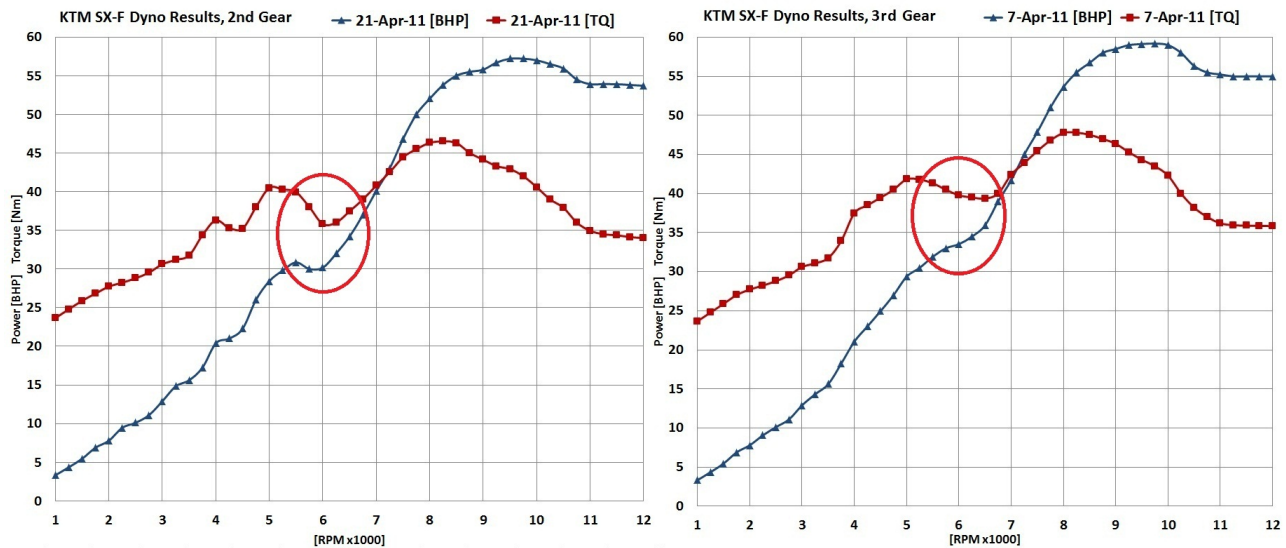


Figure 20 - Dynamometer power and torque graphs with 2nd and 3rd gear.

The two runs on the dynamometer on second and third gear follows the same pattern throughout the rpm range except at 6000 rpm with the second gear where an unexpected instant drop in power and torque can be noticed by comparing the two graphs. The sudden irregularity of behaviour does not exist in the third gear run nor in the graphs provided by KTM figure 21 and was therefore compensated for. Note that the reference points right before and after 6000



rpm are the result of average from known values and therefore gives the illusion of the value at 6000 rpm being possible. By erasing the faulty value att 6000 rpm and replace it with the average value from 5500 rpm and 6500 rpm an more likely reference point was created. The gap between the known values was too big but the behaviour approximated by calculating the average was supported by the third gear dynamometer run and the engine manufacturer.

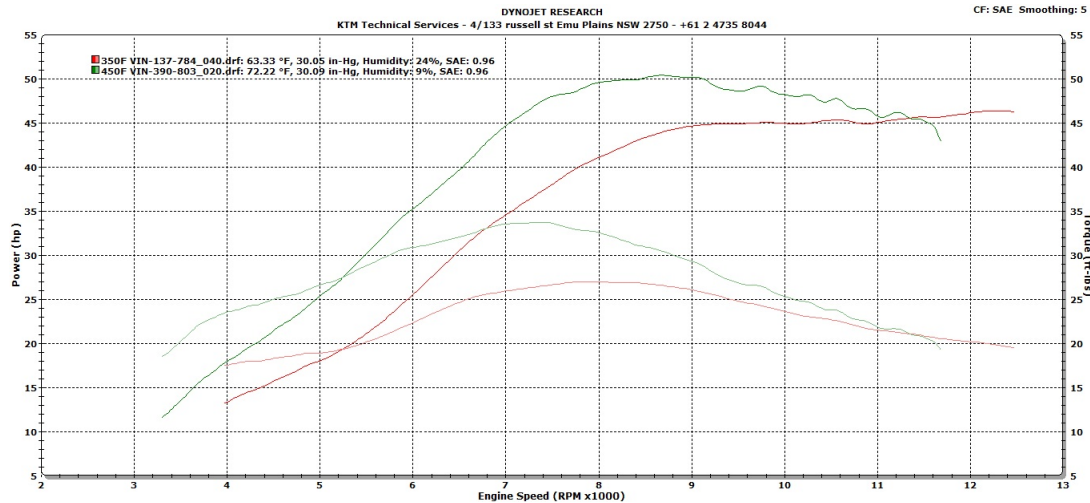


Figure 21 - Dynamometer power and torque graph from KTM. The more powerful engine is the topical KTM 450 SX-F. The less powerful engine can be disregarded.

The graph in figure 22 served as the reference power and torque output. Extrapolated below 4000 rpm, average values to increase the reference point to cover every 250 rpm step and a straight line after 11000 rpm to note the last confirmed reference point was the 11000 rpm point.

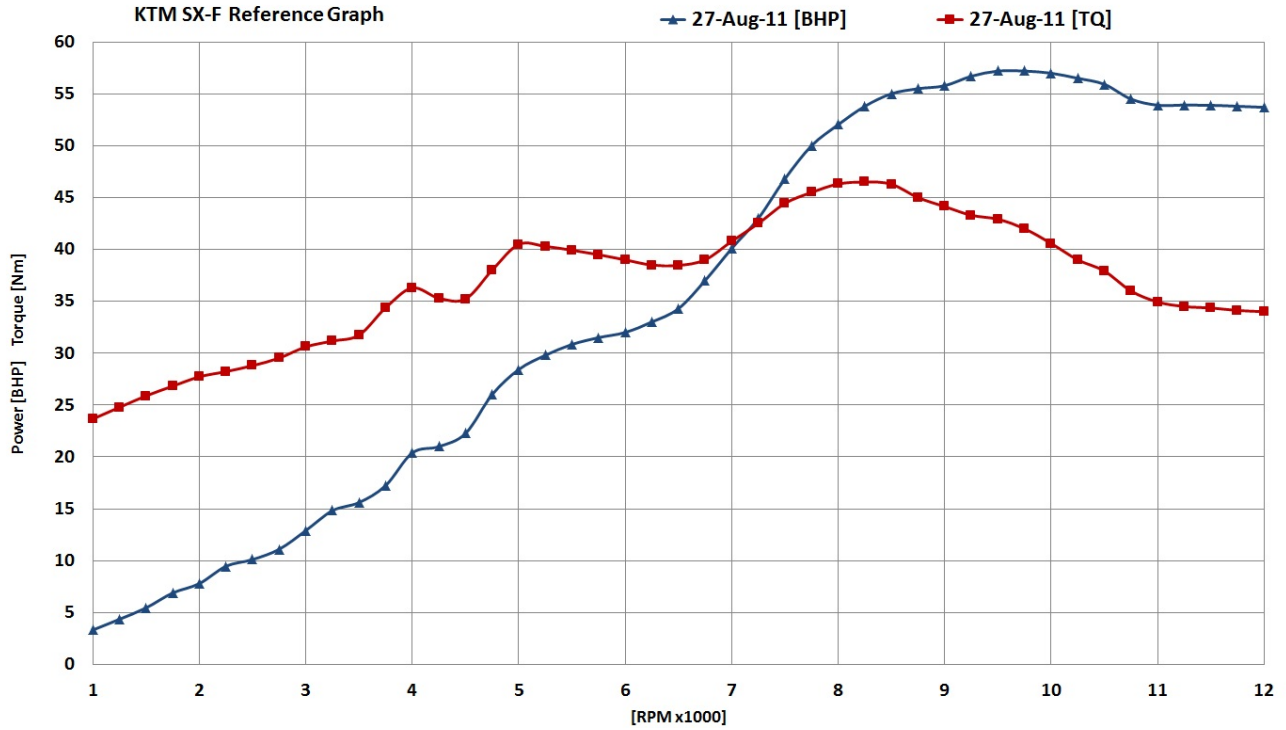


Figure 22 - The custom made reference power and torque graphs.

## 4.2 SIMULATION ARRANGEMENT

To manually find the missing values which fully define the KTM simulation engine a database with judgment samples was required. Since half of the sought values are temperature, pressure and wall heat transfer multipliers of different components all test engines run in three different conditions named Hot, Cold and Exp. Hot and Cold consider the two steady-state temperatures of the engine which was operating and room temperature. Note that steady-state operating temperature are the most interesting one while the cold runs are more used as reference to observe the impact of operating temperature hence risk and possibility of improved cooling. The primarily purpose of the runs named "Exp" was to investigate wall heat transfer multipliers and was set to be 50% higher than the "Hot" and "Cold" runs which was running on default wall heat transfer multipliers on all components. The secondary purpose of the Exp runs are to extend the range each parameter are tested. For consistency all engines with the same mark Hot, Cold and Exp was running with the same temperature, pressure and wall heat transfer multiplier.

The experimental "Exp" version can however differ from simulation to simulation and con-

tributes to the database by showing what can be gained or lost if particular condition that in the present condition was less likely to occur and are designed to give a wider picture, new ideas and warnings.

### **4.3 DESIGN OF TESTS**

As earlier mentioned, most of the unknown parameters are figurative. There was therefore no need to cover the entire absolute range of each parameter in search of value comporting with reality. All known parameters was considered as constants throughout all tests. The test groups was named Engine1 - 9 where each group covered experiments of variables that are most likely to depend on each other. The number of subgroups and number of tests of each subgroup depending on the number of unknown parameters in the group and the range each value had to be tested for to cover the most likely correct value. The Exp tests will increase the probability of covering correct value in the experiments. Even though this only can be considered as sample tests, increasing the number of tests and keeping them in area where to most likely correct values might be hidden was with available time and resources the best option.

The implementation of the sample tests was operated systematically rather than randomly. By pre-studying default values and example engines provided by the software manufacture, each parameter was at first be set most likely to correspond to the KTM engine and compared to runs with a couple of slightly and significantly higher and lower values. This was done for parameters individually and in their specific groups which make it possible to notice if the output was moving towards or further away from optimum by comparison with the dynamometer results as preference.

### **4.4 PREPARATION OF SIMULATION**

Before running the simulation in Wave and exceeding to WavePost for analysis, it was necessary to setup how the engine was supposed to run in terms of speed, load and what data we which Wave to sample and how to sample. The objective was to have the simulated and real engine performing identical runs with identical output before trying to improve the simulated engine and use it as a reference for the real engine. The simulation therefore correspond to how the real engine was being tested on the dynamometer.

The engine speed was sweeping through from 1000 to 12000 rpm in 250 rpm incline steps to simulate multiple steady-state test points in one speed sweep. Wave recommends the opposite since decreasing instead of increasing benefits by increasing the possibility of finding any problems with the general setup earlier when running the simulation. This is due to the higher

number of cycles run per seconds at higher rpm [1]. The advantage of running the simulations in increasing rpm order was however more in this particular case since the results when exported to excel was not requiring transposing. One simulation takes approximately 20 seconds to run with all 45 cases hence the time loss if a simulation fails are neglect able in this case. To be able to run more than one rpm case in a single run it was necessary to replace the steady state engine speed with a variable. The variable {SPEED} was implemented and specified to run 45 different cases, one case for each rpm step. Each case also contains rpm related values such as combustion duration and position of 50% burn point in respect to position of piston and also temperatures for different components. For complete details about rpm related parameters utilized please see appendix A.9 and the theory behind them in chapter 2.5. Wave does not put any difference between if the engine inclines or decline in rpm. The system was solved as 45 individual steady-state cases.

The simulation duration was set to 30 cycles. This relative high number was preferred since auto-convergence stopped the simulation as soon as the engine converge and was specified in order to assure that each output value tested reached a converged steady-state input value. The convergence boundary was set to abort the simulation if it converges within 1% for one cycle within the tolerance of  $\pm 1.0 * 10^{-7}\%$ . If the number of engine cycles to run was set to low there was an immediate risk of the simulation being aborted before all valuable behaviour of the engine was gathered.

## 4.5 RUNNING SIMULATIONS

It was of interest to compare the pressure and temperature in the exhaust port and compare it to the conditions in the intake port. Therefore data for intake and exhaust ports was connected on the same plot in Wave. Pressure and temperature plots was being requested to be plotted and connected for duct 3, 9 and 6, 7. This enables comparison between the same distance before and after the cylinder. Se appendix A.7 (connected data) Time plots can be created which represent the engine cylinder, crankshaft and general overall engine behaviour.

To be able to do some more advanced post-processing analysis and find any deviation from preferred/normal behaviour, velocity and volumetric flow through the entire network of engine components was requested to be sampled. This is beyond earlier mentioned sampling of data. Also since the tolerance of hot lash for the exhaust valves was trespassed with 0.01 mm in regards to recommendation from KTM (appendix A.3) there was a great interest in requesting datasets that can revile leakage or timing problem from the valves. This was done by adding discharge coefficient (chapter 2.1), flow coefficient and lift over diameter (appendix A.7) to the requested datasets.

Wave automatically creates requested plots at the end of each simulation. Pressure and temperature was being sampled from all cells of duct 3, 6, 8 and 9. The other available ducts was either identical with one of the sampled ones or of no interest to be sampled. Please see delimitations in chapter 1.4. Visually it might seem like the data was gathered from the mid point of the ducts but this is not the case. It is possible to enter custom locations which are specific locations in the selected duct where plots gather their data from. Locations are defined by a normalized value from zero to one (left end of duct is 0, middle of duct is 0.5, right end of duct is 1). The number of locations for which data can be collected from is controlled by the number of cells which was set with the discretization length decided when the particular duct was created. Duct 6 for example has an overall length of 70.2 mm and the discretization length of 20 mm (chapter 2.3). Meaning that there was four different location on the duct that Wave solved for e.g. data was collected from. The accuracy of number of cells should be utilised, otherwise there was no point in increasing the solving time by splitting the cells. The position from which data was requested from one of the intake ducts (duct6) is the midpoint if each one of the four cells, position 0.125, 0.375, 0.625 and 0.875.

The model was at this stage ready to run through an input check and was set to create the requested data for post-processing. Figure 23 shows the end of the engine run log on the right hand side of the engine. The log was printed in real-time to examine and a output file was also printed with the fully detailed log. The log was an important source of information for troubleshooting the simulation. Simple informational messages starts with I\*\*\*, warning messages with W\*\* and finally, failure message which cause Wave to abort the simulation are marked with F\*\*\*.

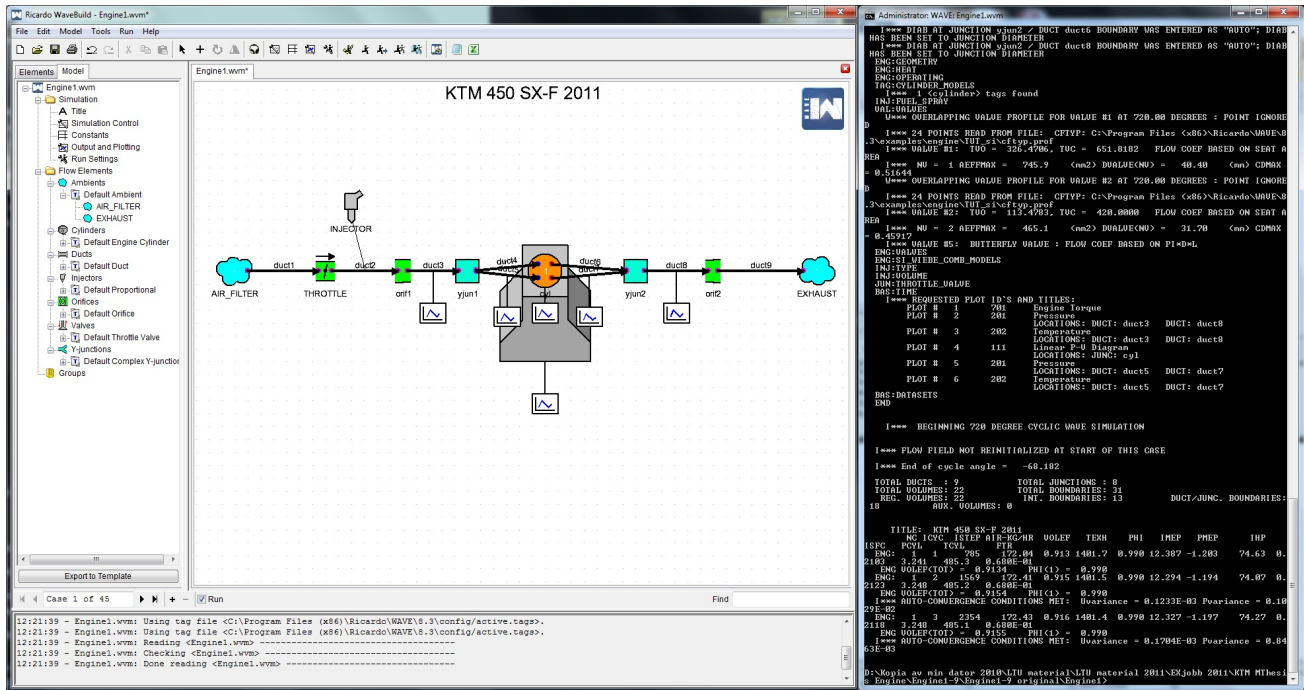


Figure 23 - A screen shot of Wave work environment to the left and the engine run log on the right hand side of the engine which is printed in real-time.

## 5 RECONSTRUCTION OF SIMULATION ENGINE TO PREDICT THE BEST RACE ENGINE CONFIGURATION

The simulation engine was completed and verified to correspond well to the stock KTM SX-F engine. The theoretical engine can at this stage be put under experiments to utilize how the real engine can be improved when restricted to follow the FSAE regulation. This part of the project was most crucial to be operated with caution. The adjustments that was performed changing the simulation engine from stock to correspond to the future race engine for improvement studies was harder to confirm if it was done properly or not due to usage of research geometry specific for Monash Motorsport. The stock engine was at this stage of the project undergoing massive changes where the purpose of this and the next chapter was to provide Monash Motorsport with vital predictions regarding upcoming results. Consequently the simulation did not have any real results as reference compared to the dynamometer output in previous chapter.

The new components added to the engine was partly custom-made and partly sponsored, which includes air filter, throttle body, restrictor, runner, plenum chamber, injector, bell-mouths and the entire exhaust system. The geometry and configurations of the new components are already established by different team members within their area of responsibility. It is highly complex to compile and configure components in respect to the rest of the system due to the need to map out the behaviour of depending components. The uncertainly are countered with experiments and the component are made adjustable for increased option of settings.

To translate these conditions and approach the task from an engineering and engine simulation point of view. The new components geometry and optimum configuration can be considered as unknown while the geometry and configuration chosen by the team can be utilised as benchmark while running the simulations. By choosing this approach, knowledge and experience gained in previous chapter can be implemented in respect of execution. The unknown in previous chapter are at this stage determined and can be considered as constants which makes it possible to run new experiments to find optimum for the new conditions.

This part of the project can be considered as the ultimate qualitative test of the simulation. The results from this chapter provided vital information to the team and most likely influence the scope of engine simulation in Monash Motorsport in future years to come. It is most crucial for the team to get access to the results from the simulations during an early stage of development for the simulation to have maximum utility value. It is an urbane concept of success to at an early stage obtain simulation results. It is most common that these types of project get very

stressful at the end due to unexpected time consuming hinder. Simulation results which shorten the development stage can be crucial for meeting the deadline. The quality and utility value of the simulation results was at the final stage of this project confirmed with dynamometer results by the real engine. The real engine versus the simulation model can be seen in figure 24.

## 5.1 RECONSTRUCTION OF THE INTAKE SYSTEM WITH CUSTOM MADE COMPONENTS

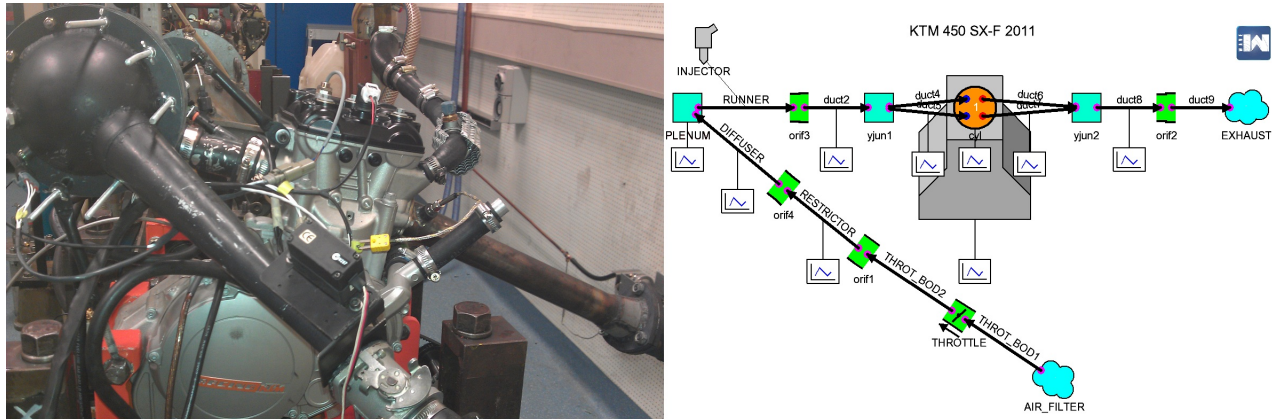


Figure 24 - To the left, the real KTM SX-F with the new custom made intake system and to the right the corresponding simulation model.

The restrictor was determined in both shape and geometry and was based on Stephen Leach FYP Report from 2009 [16]. The Plenum was designed by the Monash Motorsport team member George Kariotakis for this year and is completely round and adjustable in volume from 1.8 - 4.9 l with 0.3 l increments, see appendix A.10.3. A runner was placed between the plenum and the engine head. The runner length was another geometry relevant for testing. It was however not adjustable but can easily be remade. The geometries on the provisional custom made components was considered as benchmark.

For more details regarding the custom made components please see appendix A.10.2.

## 5.2 SIMULATION ARRANGEMENT

The new components relevant for simulation are the plenum, bell-mouths and runner. The components was at the first stage added with benchmark geometry in place on all components and individually be tested over a range of different geometry to map out the behaviour affected by each particular part. This helped to narrow the range of possible optimum for each com-



ponent. To complete the map, all new components was running experiments at a later stage simultaneously within a more narrow range to determine how the new components contribute to the complete system hence find global optimums.

### 5.3 DESIGN OF TESTS

To fully investigate the contribution of each new part, one engine was made for every component making it easier to perform individual research and creating a database for future use. All was based on Engine1 Hot which represent the KTM SX-F engine best, see chapter 4.2 and appendix A.11.1 for details regarding Engine1 Hot. The individual tests can be seen in table 4.

Table 4 - Test plan for individual components

<i>Component</i>	<i>Benchmark geometry</i>	<i>Min</i>	<i>Max</i>	<i>Increment</i>
<i>Runner length [mm]</i>	150	100	240	10
<i>plenum size [l]</i>	2.562	1.767	4.948	0.265
<i>bellmouths [mm]</i>	0.75	0	1	0.1

During the individual testing when all custom made components was added simultaneously Engine1 Hot represented how the first Monash Motorsport race engine for 2011 was presented.

### 5.4 PREPARATION

Before running the simulation in Wave and exceeding to WavePost for analysis, it was necessary to setup how the engine was supposed to run in terms of speed, load and what data was topical for Wave to sample and how to sample. The information of interest was those who can be verified by the real race engine at a later stage in the project. From the new intake system as stated earlier, runner length, bell-mouths and plenum volume was particularly interesting to simulate since there was no previous tests for these while air filter, throttle, restrictor and diffuser have been widely investigated previous years and the geometry for thous are overall determined and therefore of low priority in this project.

The engine speed was sweeping from 1000 - 12000 rpm in 250 rpm increments to simulate multiple steady-state test points in one speed sweep just like in previous tests. Each steady-state test point has its own case which implies 45 cases in total. For more details regarding what data each case contains please see appendix A.9 and the theory behind them in chapter 2.

## 5.5 RUNNING SIMULATIONS FOR INDIVIDUAL TESTING

Maximum power and torque within the range of 7000 - 11000 rpm was the criteria for which the different components was judged. The limited rpm range of interest was due to the interval of rpm when driving. It was also necessary to limit the rpm range of maximum interest since different geometries are optimum within different rpm range.

Before proceeding to run geometrical experiments on relevant components it was of interest to observe how the components behave with benchmark values in place. The purpose of the plenum chamber was to create a buffer of air to consequently decrease the negative impact of the restrictor required to compete in FSAE. During the individual testing when the custom made components where added one at the time the restrictor where tested without the plenum and vice versa, the plenum where added while the restrictor where removed and eventually both added simultaneously. It was expected and confirmed that the plenum chamber decreased the negative flow through the restrictor and provided a more even power and torque curve. An interesting unexpected behaviour was however noticed, the plenum chamber only in affiliation with the restrictor was only beneficial. The power and torque behaviour over the rpm range showed a better behaviour than when the plenum was added without the restrictor.

As can be seen in graph 25, the restrictor really unstable the power and torque if added without the plenum. This behaviour adds credibility to the simulation hence this behaviour was expected. It is impressive how good results are produced when the restrictor and plenum was added to the engine simultaneously. The plenum erases the negative impact of the restrictor effectively. Some power and torque are lost on average over the entire rpm range but not as much as expected. Testing the components in this matters and forming an understanding of how the components affect the engine was valuable to later on interpret the results for further tests. There was no purpose in optimising the simulation and offering recommendations if there was something wrong with the simulation at this stage.

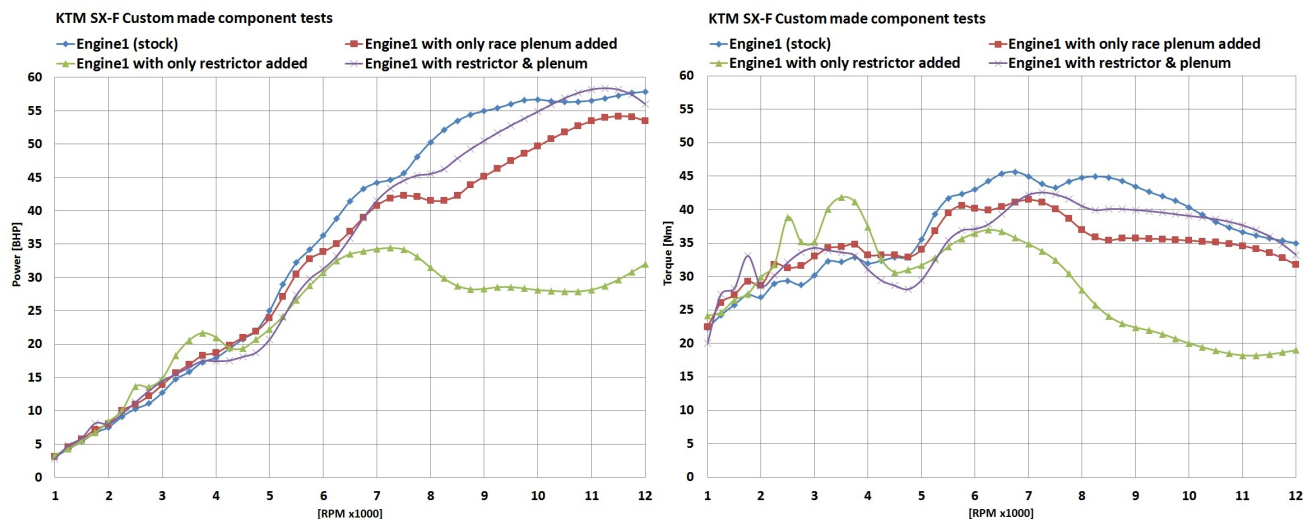


Figure 25 - Simulation test results for custom made components.

Note how the simulation reacts with only the plenum or restrictor added and also that the configuration, plenum & restrictor produce more power and torque than the stock unrestricted engine at 11000 rpm.

### 5.5.1 RUNNER LENGTH

A benchmark length for the runner of 150 mm was in place on the real engine. The limits for runner length simulated was due to possibility to install that particular runner on the real engine. The runner was equipped with an injector with the angle of 20 degrees. The injector and the connection makes it difficult to shorten the runner much more than it already was. The length of the runner was however simulated for every 10 mm between 100 - 240 mm as can be seen in table 4.

### 5.5.2 PLENUM VOLUME

The plenum chamber affects the engine in many ways. To run simulations and obtain results which recommendations regarding the plenum volume can be based on requires that significant amount parameters are deliberated. The power and torque are two significant parameters that are affected by the plenum volume, especially in this case where the air intake are restricted. The three investigated options which can be seen in figure 26 are the horizontal, vertical and spherical plenum chambers. The chosen shape was the spherical plenum chamber and as phrased by George: "This concept is more complex and is limited to the materials to be made out of. It does however have the advantages of being smooth with no sharp edges to

hinder flow and possess the ability to change the runner and restrictor angles making it easy to package in the car. It also has the advantage of being spherical shaped which provides excellent strength, this was crucial when the final intake was to be manufactured as light as possible.”

Briefly the chosen plenum was based on two half of a sphere where middle sections can be added to increase the volume. With no middle sections the plenum has the smallest possible volume of 1.767 l and each additional middle section increase the volume by 0.265 l. The total number of volume increasing middle sections is 12, giving the adjustability of 0 to 12, totally 13 different volumes which when all in place gives a volume of 4.948 l. The spherical shape of the plenum, adjustability and range has been chosen by team member George Kariotakis to be the best option based on research. The simulations of plenum volume aim to investigate what number of middle sections provides the best results based on criteria of power/torque, throttle response and volumetric flow through the restrictor. By studying all 13 possible volumes for all criteria the best compromised results was searched for.

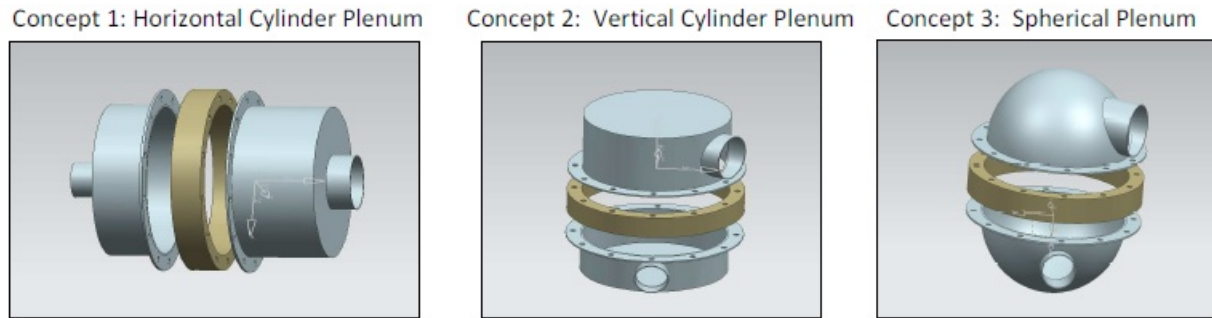


Figure 26 - Different shape-options for plenum chamber.

The throttle response was affected by the plenum volume and therefore tested by switching from closed to full throttle for all plenum volumes at 1000 and 5000 rpm. The criteria looked at was the time it takes for the engine to react and speed up to 12000 rpm.

Since the restrictor heavily limit the airflow to the engine the criteria was also to map out how the plenum volume effect the flow through the restrictor. The aim was to optimum utilize the small passage for air through the restrictor hence a high flow is preferable. When the intake valve closes a pulse of compressed air bounces back through the runner, plenum and eventually through the restrictor creating a low pressure in the intake system. By increasing the plenum volume this can be prevented. The buffer of air created in the plenum can help to prevent the negative flow. Wave is equipped with a highly useful and pedagogic feature to study this behaviour by running animations.

### 5.5.3 BELL-MOUTH

Different shape of the bell-mouths was simulated with help of the discharge coefficient. These features are built in the software and was therefore very straight forward to use. As can be seen in picture 27 and be read about in chapter 2.1 the discharge coefficient is a number between 0 – 1 representing the smoothness in flow, hence square/bell-mouth transition. Unsymmetrical shapes was also addressed. Meaning that the discharge coefficient between diffuser-plenum and plenum-runner was set to different values. The purpose was to investigate more closely how the two transitions affect the engine individually. When changing two parameters at once it was not possible to know for sure the contribution of each parameter. Therefore each transition was changed individually.

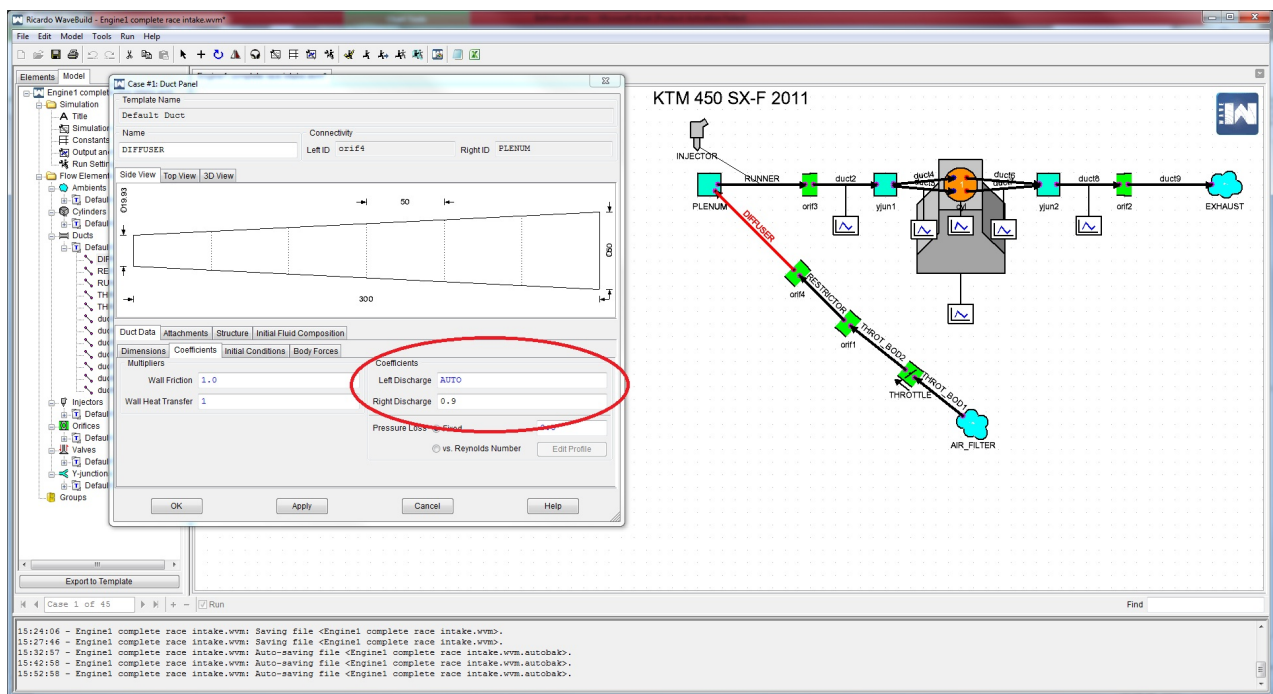


Figure 27 - The duct panel for the diffuser as shown in Wave.

## 6 RESULTS FROM POST-PROCESSING

The quality and utility value of the simulation results in this chapter will at the final stage of this project be confirmed by the real engine by comparison with the produced results from the dynamometer.

### 6.1 STOCK ENGINE SIMULATION

The total number of tests could not be predicted due to unawareness if the parameters tested individually and in group follow a certain pattern or not. Each setup could not be recorded in detail but rather noted due to the high number of simulations of 264. Detailed notes were only taken for the particular interesting simulations limiting the data gathered from the experimental simulations to the area of interest. When the pattern of the individual and grouped parameters was estimated a new subgroup was created to confirm the behaviour and observed optimum. The number of graphs saved with log of setup varies from 3 to 60. Each line represents one engine setup and each engine has been sampled three times Hot, Cold and Exp. The 65 best results in respect to different parameters and parameter groups can be viewed in appendix A.10.1. In table 5 a short summary of the settings can be viewed and in figure 27 the best engine (Engine1) can be seen. Engine1 is the result of the substantial research of all the earlier mentioned parameters individually and in group implemented in one engine.

Table 5 - Short summary of the engine simulation settings

<i>Intake Temperature [K]</i>	300	<i>Intake and Exhaust Valve Lift Multiplier</i>	1
<i>Fluid pressure duct1 – 5 [bar]</i>	0.986923	<i>Intake Angle Type</i>	<i>Cam</i>
<i>Duct1 – 9 Wall Heat transfer Multiplier</i>	1	<i>Intake and Exhaust Valve Flow Coefficient Profile</i>	<i>CFTYP</i>
<i>Duct3 Temperature [K]</i>	300	<i>Exhaust Valve Anchors Cycle [deg]</i>	0
<i>Duct3 Wall Temperature [K]</i>	300	<i>Exhaust Valve Duration Multiplier</i>	1
<i>Y – Junction1 Initial Fluid Temperature</i>	320	<i>Exhaust Angle Type</i>	<i>Cam</i>
<i>Y – Junction1 Wall Temperature [K]</i>	350	<i>Duct6 – 7 Fluid pressure [bar]</i>	1.03627
<i>Duct4 – 5 Temperature [K]</i>	330	<i>Duct6 – 7 Temperature [K]</i>	1000
<i>Duct4 – 5 Wall Temperature [K]</i>	400	<i>Duct6 – 7 Wall Temperature [K]</i>	500
<i>Engine Friction Correlation ACF [μ]</i>	0.35	<i>Y – Junction2 Initial Fluid Temperature</i>	900
<i>Engine Friction Correlation BCF [μ]</i>	0.005	<i>Duct8 – 9 Fluidpressure [bar]</i>	1.03627
<i>Engine Friction Correlation CCF [μ]</i>	400	<i>Duct8 Temperature [K]</i>	950
<i>Engine Friction Correlation QCF [μ]</i>	0.2	<i>Duct8 Wall Temperature [K]</i>	550
<i>Intake Valve Anchors Cycle [deg]</i>	0	<i>Duct9 Temperature [K]</i>	900
<i>Intake Valve Duration Multiplier</i>	1	<i>Duct9 Wall Temperature [K]</i>	700
<i>Intake Valve Lash [mm]</i>	0.3	<i>Exhaust Temperature [K]</i>	600

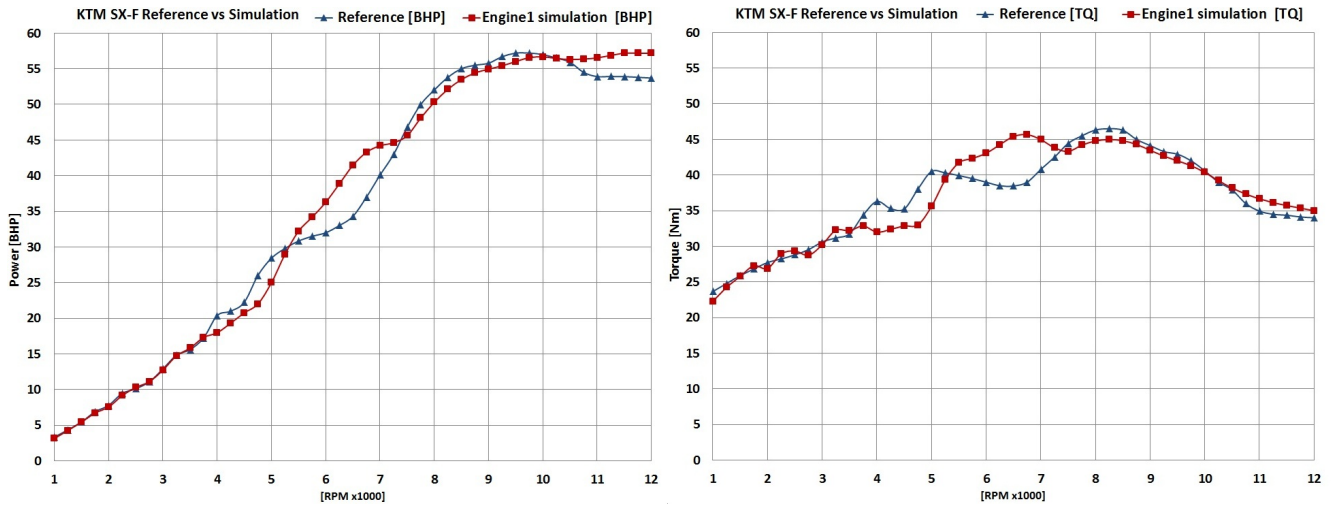


Figure 27 - Comparison between the developed reference and simulation graphs.

As earlier mentioned 11000 rpm is the last reference point hence the simulation output between 11000 - 12000 rpm was taken in respect but not compared to and put effort to fit the reference graph.

## 6.2 RACE ENGINE RUNNER LENGTH

The optimum runner length is not univocal but depending on what rpm range is valued. As can be seen in Figure 28 and in appendix A.10.4 where all different runner length tested are presented, the characteristics of the power and torque over the rpm range changes. A swing point at 9000 rpm has been noticed were longer runner rotates the graph clockwise and shorter runners anticlockwise. Unfortunately our driving range covers the swing point, forcing the optimum chosen runner length to be a compromise of more power below or over 9000 rpm.

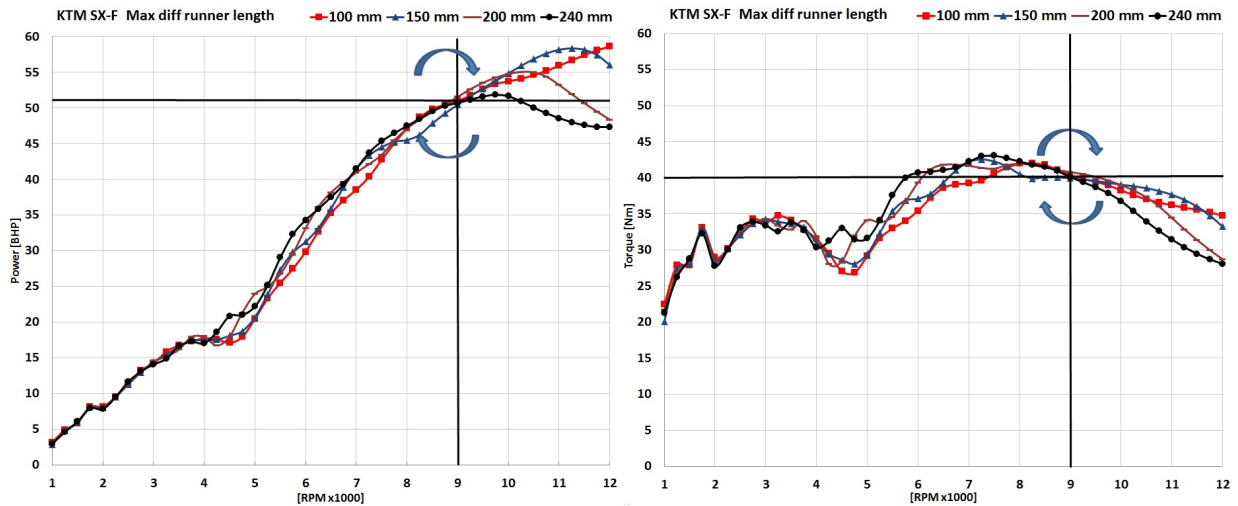


Figure 28 - Simulation results for 100, 150, 200 and 240mm runner length.

### 6.3 RACE ENGINE PLENUM VOLUME

The more number of middle sections the more power the engine produces between 5000 - 11000 rpm. The reason this statement does not cover engine speed below 5000 or over 11000 rpm has to do with the behaviour below 5000 rpm are not linear. Please see graphs in figure 29 and appendix A.10.5. The more number of middle sections the less impacts each additional middle section have. The graphs almost overlap when the numbers of middle sections surpass 3. This means that 4 - 12 middle sections increase the power marginally while 0 - 3 middle sections makes more difference. Another impact the increased plenum volume has is that the peak power are reached at a lower rpm and are decreasing. To best grasp what the change in plenum volume does to the power and torque please view the Max-Min graphs in figure 29 and appendix A.10.5. Even though the power are minimal affected by the plenum volume the torque at 7000 rpm differs with 8 Nm. The engine produces 38 Nm without any middle sections and increases the torque with each additional middle section up to 46 Nm, all at 7000 rpm which gives the biggest difference. The conclusion is that maximum plenum volume is to prefer if only maximum power and torque are parameters of interest while packaging and throttle response are ignored.



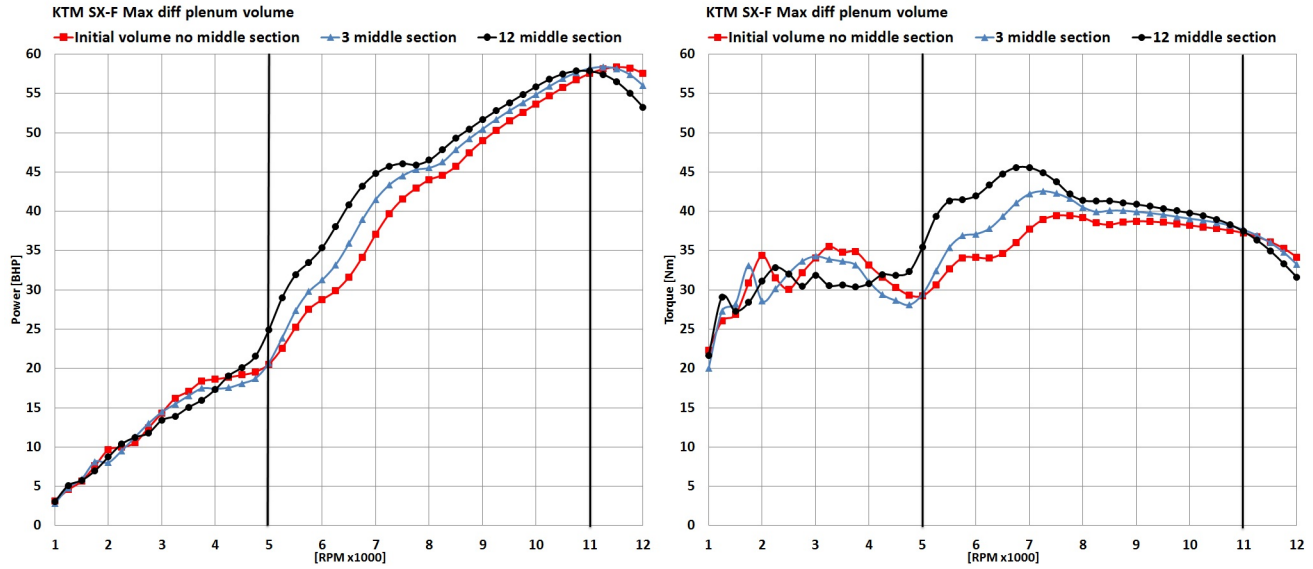


Figure 29 - Simulation results for 0, 3 and 12 middle sections which represent 1.77, 2.56 and 4.95 l plenum volume.

Since smaller plenum is preferred when it comes to packaging the power and torque gained for each additional middle section should be taken in respect to the possibility to fit the plenum.

These results confirm that bigger plenum improve performance when the restrictor are added and also help to define the power/torque to plenum volume ratio.

The throttle response was tested for all plenum volumes at 1000 and 5000 rpm. The results from these tests can be seen in appendix A.10.5 and are unfortunately contradictory. The throttle response tests are designed to go from closed to full throttle at specific rpm and measures the time it takes for the engine speed to rush up to 12000 rpm. The maximum spool up time differed by 0.5 s at the 1000 rpm throttle test. The simulations however fail to show a certain univocal pattern. The number of spacer used for altering the plenum volume is as mentioned 12 in total. The number of middle sections in order from faster to slower throttle response is 0, 9, 11, 10, 1, 3, 8, 7, 12, 6, 5, 4 and 2 middle sections. The throttle response pattern when going full throttle at 5000 rpm listing the number of middle sections in the order from faster to slower response is 7, 5, 6, 0, 2, 1, 8, 11, 3, 10, 9, 4 and 12. At the 5000 rpm throttle test, the maximum spool up time differed by 1.4 s.

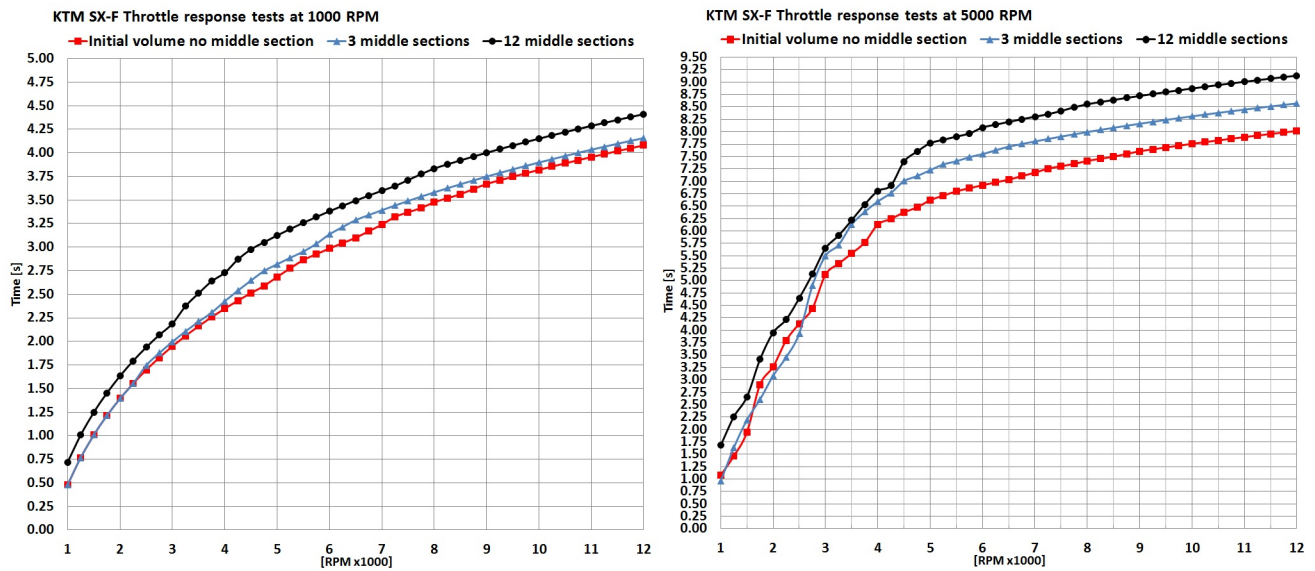


Figure 30 - Simulation results for throttle response test at 1000 rpm.

The throttle response graphs in figure 30 represent 0, 3 and 12 middle sections. 0 and 12 represent the extremes and 3 middle sections represent the benchmark value as this is the number of middle sections mounted on the plenum on the real engine on the dynamometer. The obvious pattern of faster throttle response with smaller plenum is the reasonable outcome and is clearly shown in figure 30. This distinct pattern are however vague when all plenum volume throttle responses are plotted simultaneously. The knowledge gained with this outcome from which recommendations will be based on is that the smaller plenum chamber will improve throttle response but some of the volumes gives an unexpected fast/slow throttle response this motivates that not only the volume effects the response but also the resonance. For throttle response of all plenum volumes at 1000 and 5000 rpm please see appendix A.10.5.

The bigger the plenum volume is made, less negative flow through the restrictor there is and the flow as a direct consequence are also transported more evenly through the restrictor which is preferable. Below you can see a screen shot from the real time animation.

All topical plenum volumes have been animated where each animation contain one of total 13 different plenum volumes. Each animation show volumetric flow vs distance as a real time operation showing how fast all fluids move through the entire system hence direction and magnitude of airflow. By observing animation of different plenum volume it can be noticed that a greater buffer of air created by a bigger plenum chamber decrease the tendance of negative flow through the restrictor. Figure 31 is a screen shot of the animation representing a plenum

volume of 3.89 l which is the smallest plenum with only positive flow through the restrictor at all time.

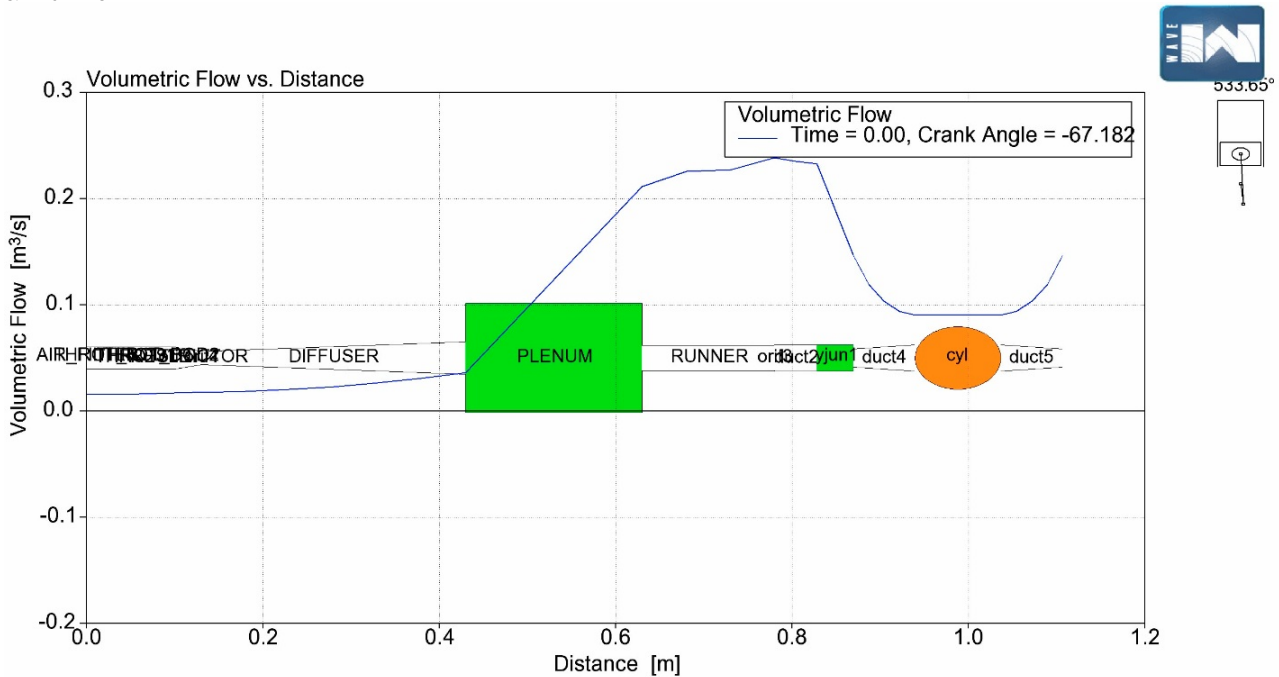


Figure 31 - Screen shot of the volumetric flow animation representing a plenum volume of 3.89 l.

## 6.4 RACE ENGINE BELL-MOUTHS

The results clearly states that the smoother the bell-mouth is the more power and torque are gained due to less disruption to airflow. The discharge coefficient in Wave represents the smoothness, hence 0.1 represent an almost perfect square mouth while 0.9 represent an almost perfect bell-mouth. While looking at the power graph, it can be noticed that even if the bell-mouth are far away from perfect it still make a great difference. The power increases by 10 hp when the discharge coefficient is changed from 0.1 to 0.2 but only increase by 3.5 hp when the discharge is increased from 0.2 to 0.3. The same pattern continues all the way to an almost perfect bell-mouth at 0.9. The extremes (0.0 and 1.0) are excluded due to the unrealistic nature. By experimenting with different discharge coefficients at the restrictor side and runner side it was discovered that it is more important with a high discharge coefficient (bell-mouth) on the restrictor side of the plenum than the runner side. This behaviour can be explained with the great majority of positive flow from the ambient through the intake system towards the combustion chamber. The results for this are included in the same graphs as the symmetrical

tests in figure 32 and are named "Restrictor discharge 0.1 runner discharge 0.9" and "Restrictor discharge 0.9 runner discharge 0.1".

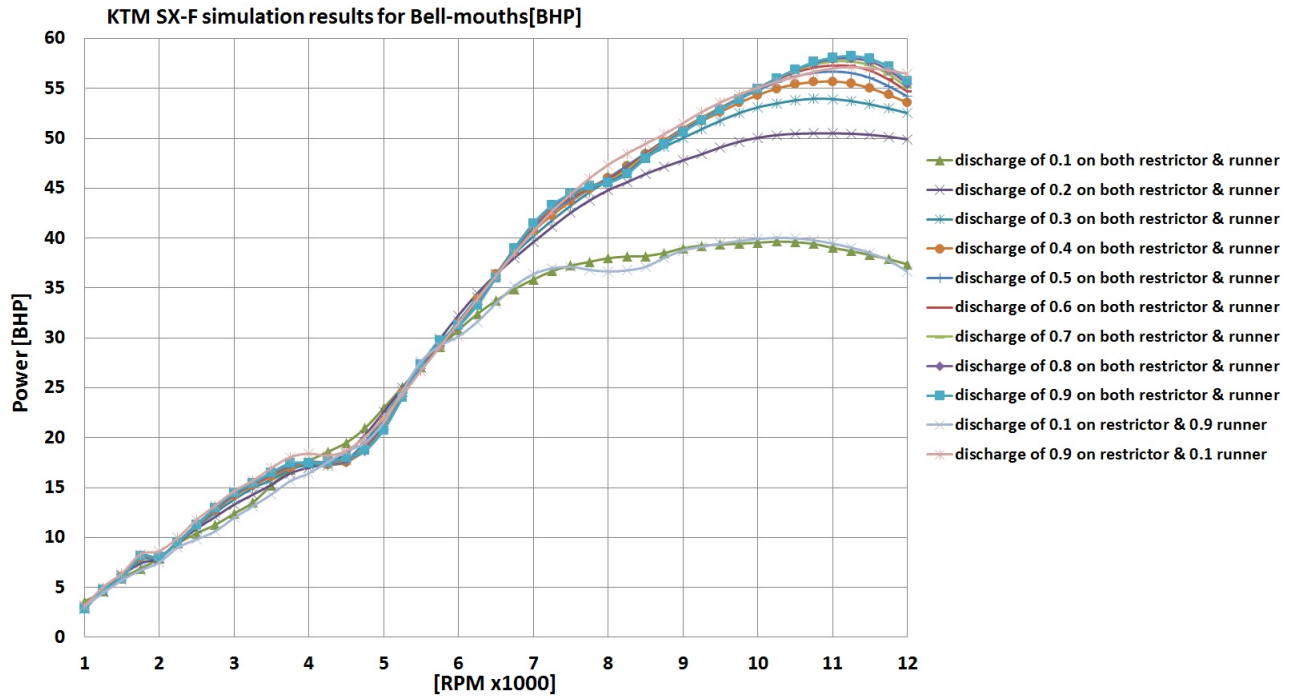


Figure 32 - Simulation results for bell-mouths.

## 7 FINAL OPTIMISATION

All new components was added simultaneously in this chapter, the components previous individually optimised have to perform well together. The reconstruction of a simulation engine for race and the tests to find optimum runner length, plenum volume and the impact of high discharge coefficient for the bell-mouths provided a good fundamental understanding of how the engine is affected by individual geometry. At this stage the different geometries can be tested versus each other to find the global optimum. By doing so the aim is to answer the question of what plenum volume and runner length are optimum for this engine and these driving conditions.

Since longer runner are prefer able if the engine speed range of peak power are below 9000 rpm and shorter runner length are prefer able if the rpm range for peak power are for higher rpm the optimum runner length for this particular engine that during competition are mostly driven between 7000 - 11000 rpm is 170 mm. The benchmark length of 150 mm runner length is an acceptable compromise between high powers over the driving rpm range. Since this is 20 mm shorter than the optimum runner length for the racing engine speed range this will benefit if the engine speed drops below 7000 rpm and disadvantageous if the engine are over revving.

Plenum volume is most complex to optimise. If the plenum is too small it will not be able to buffer enough air hence not preventing the starvation of air optimally. On the other hand a big plenum volume will cause slow throttle response due to the large volume of air available for the engine to burn on the engine side of the throttle. As two revolutions will consume 450cc of air assuming 100 % volumetric efficiency it may take some amount of time before the engine actually start starving on air and drops in rpm. This can result in a significant loss in throttle response and hence driveability. Unfortunately the reverse applies for open throttle as well. During race condition it is essential that the power is there immediately.

Optimum plenum volume is depending on elements of flow through the restrictor, packaging, throttle response and power/torque. The non-linear pattern between plenum volume and throttle response motivates research of wave resonance of the intake system. Since no data regarding wave resonance for this particular intake system is available at the moment the recommendation to the team is not to assume that a bigger plenum volume for sure decreases the throttle response. The non-linear relation between plenum volume and throttle response can be contemplated as experimental results of what number of middle sections that will synchronise and provide a better resonance at a particular range of rpm. 7 middle sections is most likely to be the best compromise, creating a plenum volume of 3.89 l. It provides a relative big plenum volume, decreasing the negative flow through the restrictor and do provide a large buffer of air after the restrictor. The graphs of all throttle response shows that this particular number of

middle sections gives a good throttle response, (most likely due to resonance). When it comes to packaging, 7 middle sections are an in between size and should therefore be able to fit within the envelope regulation for the car. The power and torque results for all number of middle sections clearly advise a big plenum chamber. The power and torque gained of choosing 12 middle sections instead of 7 are however neglect able ( $< 5\%$ ) (See results in appendix)

## 8 CONCLUSIONS AND RECOMMENDATIONS

A recurring scenario throughout the project has been regarding the three options to get hold of data as input. Either using recommended values from Wave, measuring manually or receiving data from the engine manufacture. Some of the measurement is extremely hard to measure without proper equipment. Smallest error in measurement can have a great impact on the output lowering the standard of the simulation and therefore in need to be verified. Which of the three options to get hold of required data have to be picked should be with respect of area of use. Since this model will be used as foundation for optimising the Monash Motorsport FSAE engine it is necessary to take safety and quality measure. The most complicated data have therefore been determined as too unsafe to collect manually. Recommended value from Wave have as the best available option been applied If the measurements were not provided by the engine manufacture (KTM). In-cylinder temperatures are for example rarely measured but typical values are listed in Wave together with a range of typical operating temperatures for various parts of the engine.

The runner length should either be kept as 150 mm or be lengthen to 170 mm to even more benefit power between 7000 - 11000 rpm which is the most used rpm range<sup>8</sup>. There are benefits with keeping the runner length as it is since this save time from building a new runner and also benefits if the rpm at any time during race surpass 11000 rpm hence shorter runner benefits higher engine speed. If the chance of revving the engine over 11000 rpm exist, it is up to the team to base on criteria and possibility to build a new runner decide to either keep the runner as it is or build a longer one. Runner length is not recommended to be shortening for neither stock nor race configuration of the engine since the current 150 mm runner length is short enough to benefit engine speeds up to 11250 rpm. This is 250 rpm higher than usage rpm range.

When it comes to plenum volume, smaller plenum chamber will improve throttle response but some of the volumes gives an unexpected fast/slow throttle response hence not only the volume effects the response but also the resonance. The plenum should be built with 7 middle sections, creating a volume of 3.623 l. This particular volume has experimentally with simulation proven to perform well. This is a good compromise with respect to throttle response, packaging and performance. Each additional middle section increase the power and torque less than the previous added one and do so nonlinearly which further motivates not adding more than 7 middle sections.

Results for bell-mouth advice that a high discharge coefficient is preferable meaning the smoother the bell-mouth are the more power and torque is gained due to less disruption to airflow. The

---

<sup>8</sup>Monash Motorsport

recommendation is therefore to include bell-mouths in both the transition between the diffuser to plenum and also from plenum to the runner. Even small changes to go from an edge to a bell-mouth will make great difference hence the relationship between discharge coefficient and power proven by the simulations is not linear. The power increases by 10 hp when the discharge coefficient is changed from 0.1 to 0.2 but only increase by 3.5 hp when the discharge is increased from 0.2 to 0.3. The same pattern continues all the way to an almost perfect bell-mouth at 0.9. The extremes (0.0 and 1.0) as mentioned in the results are excluded due to the unrealistic nature. The experimenting with different discharge coefficients at the restrictor side and runner side proved that the impact differs from these two locations. It is beneficial to have a high discharge coefficient on both side of the plenum. It makes however more of a difference on the restrictor side of the plenum smoothening the flow through the engine than the runner side. This behaviour is expected due to the direction of airflow.



## 9 REFERENCES

- [1] Ricardo Software, WAVE Knowledge Centre, 2010.
- [2] Rohde, S. M. "A Mixed Friction Model for Dynamically Loaded Contacts with Application to Piston Ring Lubrication". Proceedings of the 7th Leeds-Lyon Symposium on Tribology 1980
- [3] Heywood, J.B.: Internal Combustion Engine Fundamentals. McGraw Hill, 1988
- [4] Annand, W. J. D. "Heat Transfer in the Cylinders of Reciprocating Internal Combustion Engines". Proc. Inst. Mech. Eng. Vol. 177, 1963
- [5] Woschni, "A universally applicable equation for the instantaneous heat transfer coefficient in the internal combustion engine", SAE Paper 670931, 1967.
- [6] Huber K., G. Woschni, and K. Zeilinger. "Investigations on Heat Transfer in Internal Combustion Engines under Low Load and Motoring Conditions". Proceedings of the 23rd FIS-ITA Congress, Paper 905018, Turin 1990
- [7] Stiesch G. "Modeling engine spray and combustion processes", 2003.
- [8] Fredrik Lindström, Empirical combustion modeling in SI engines, Department of Machine Design, Royal Institute of Technology, 2005
- [9] Csallner, Peter; Eine Methode zur Vorausberechnung der Änderung des Brennverlaufes von Ottomotoren bei Geänderten Betriebsbedingungen; München Techn. Univ., Diss., 1981.
- [10] Hires, S. D., R. J. Tabaczynski, and J. M. Novak. "The Prediction of Ignition Delay and Combustion Intervals for a Homogeneous Charge, Spark Ignition Engine", SAE Paper 780232, 1978
- [11] Selamet, A., N. S. Dickey, P. M. Radavich, and Jim M. Novak. "Theoretical, Computational and Experimental Investigation of Helmholtz Resonators: One-Dimensional versus Multi-Dimensional Approach," SAE paper 940612, 1994

- [12] Silva, F., Ph. Guillemain, J. Kergourmard, and B. Mallaroni. "Approximation formulae for the acoustic radiation impedance of a cylindrical pipe," "Journal of Sound and Vibration 322, 1-2 255-263", 2009.
- [13] Poling, Bruce E., John M. Prausnitz, and John P. O'Connell. The Properties of Gases and Liquids, 5th Edition. New York: McGraw-Hill Publishing Company, 2000
- [14] Nordling, Carl & Östman, Jonny, Physics Handbook. Lund ISBN 978-91-972860-2-2, 2006
- [15] KTM engine specification, 2011
- [16] Stephen Leach, Design and Optimisation of a FSAE Race Car Air Intake, Monash University, 2005
- [17] Uzkan, Teoman, Claus Borgnakke, and Thomas Morel. "Characterization of Flow Produced by a High-Swirl Inlet Port", SAE Paper 830266, 1983
- [18] Assistant Professor K. Wattanavichien, Ph.D. Department of Mechanical Engineering Chulalongkorn University, 2007

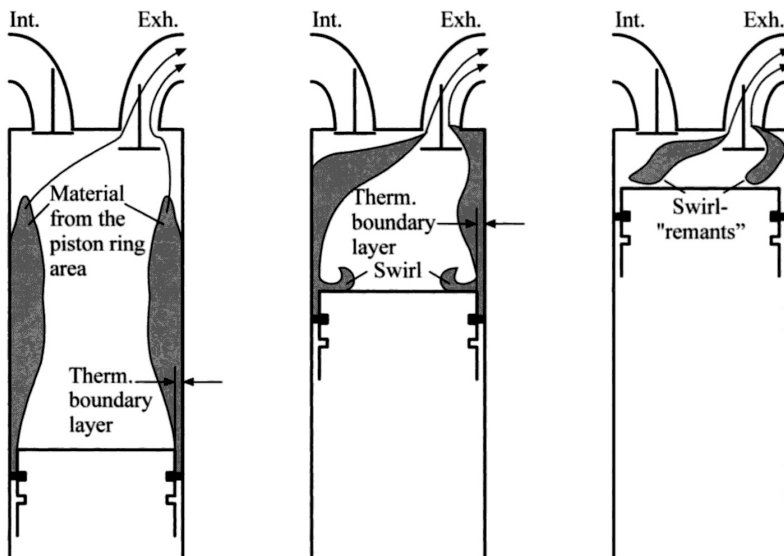
# A APPENDIX

## A.1 FSAE SCORE SYSTEM

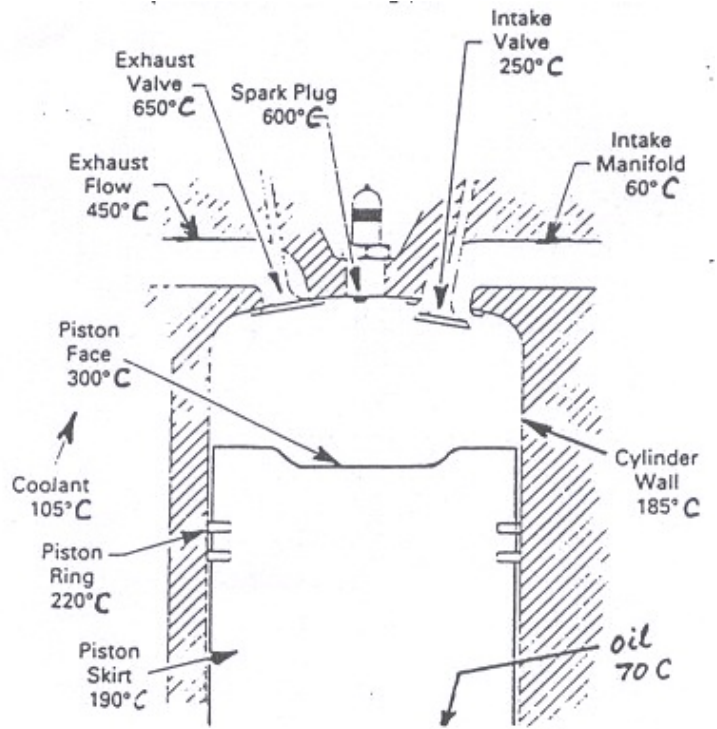
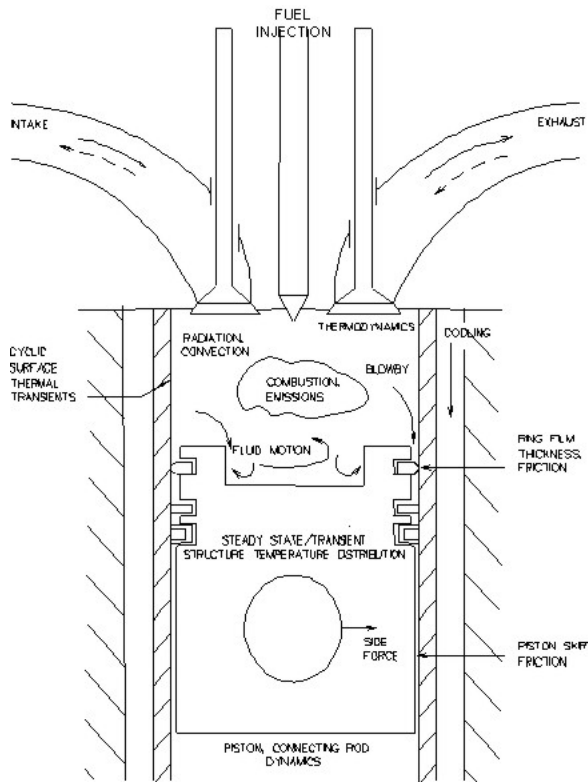
	Event	Max. Score (2008 rules)	Max. Score (2009-2011 rules)
Static Events	Presentation	75	75
	Cost and Manufacturing	100	100
	Design	150	150
Dynamic Events	Skidpan	50	50
	Acceleration	75	75
	Autocross	150	150
	Endurance	350	300
	Fuel Economy	50	100
	<b>Total</b>	<b>1000</b>	<b>1000</b>

Maximum points awarded for each event for the old and new rules. (FSAE Rules 2008-2011).

## A.2 CHARGE MOTION IN CYLINDER & REFERENCE OF HEAT TRANSFER



Charge motion in the combustion chamber "Swirl".



Schematic of IRIS individual engine cylinder capabilities<sup>9</sup> and typical temperature distribution in an IC engine operating at steady state [18].

<sup>9</sup>Ricardo Software, 2010. WAVE Knowledge Centre

## A.3 TECHNICAL DATA

### TECHNICAL DATA - ENGINE

201

Design	1-cylinder 4-stroke engine, water-cooled
Displacement	449.3 cm <sup>3</sup> (27.418 cu in)
Stroke	60.8 mm (2.394 in)
Bore	97 mm (3.82 in)
Compression ratio	12.5:1
Control	DOHC, four valves controlled via cam lever, drive via helical gear pair and tooth-wheel chain
Valve diameter, intake	40.4 mm (1.591 in)
Valve diameter, exhaust	31.7 mm (1.248 in)
Valve clearance, cold, intake	0.07... 0.13 mm (0.0028... 0.0051 in)
Valve clearance, cold, exhaust	0.12... 0.18 mm (0.0047... 0.0071 in)
Crankshaft bearing	2 cylinder roller bearing
Conrod bearing	Needle bearing
Piston pin bearing	Bronze bush
Pistons	Forged light alloy
Piston rings	1 compression ring, 1 oil scraper ring
Engine lubrication	Pressure circulation lubrication with 3 rotor pumps
Primary transmission	29:74
Clutch	Multidisc clutch in oil bath/hydraulically activated
Transmission ratio	
1st gear	16:34
2nd gear	19:31
3rd gear	20:26
4th gear	23:25
5th gear	26:24
Generator	12 V, 42 W
Ignition	Contactless controlled fully electronic ignition with digital ignition adjustment
Spark plug	NGK CR 9 EKB
Spark plug electrode gap	0.7 mm (0.028 in)
Cooling	Water cooling, permanent circulation of coolant by water pump
Starting aid	Electric starter

## A.4 MATERIAL SURFACE ROUGHNESS

Material	Surface Roughness [mm]
Aluminum (new)	0.001 - 0.002
Cast Iron (new)	0.25 - 0.8
Cast Iron (rusted)	1.5 - 2.5
Drawn Tubing	0.0015
Galvanized Metal	0.15
Glass	0.0001
Plastics	0.0015 - 0.007
Steel (new)	0.0015
Steel (rusted)	0.0015 - 4
Wrought Iron	0.046

## A.5 ENGINE GENERAL PANEL

Case #1: Engine General Panel

Geometry | Custom Geometry | Operating Parameters | Heat Transfer | Scavenge | Combustion | Conduction | Slaved Models

Configuration

No. of Cylinders: 1

Strokes per Cycle: 4

Engine Type: Spark Ignition

Bore: 97 mm

Stroke: 60.8 mm

Displacement: 0.449301 l

Connecting Rod Length: 107.4 mm

Wrist Pin Offset: 0.0 mm

Compression Ratio: 12.5

Clearance Height: 1 mm

Imposed Piston Motion:  AUTO

Printout Flag

In-Cylinder State: 0

Port Conditions: 0

Friction Correlation

ACF: 0.35 bar

BCF: 0.005

CCF: 400 Pa\*min/m

QCF: 0.2 Pa\*min<sup>2</sup>/m<sup>2</sup>

Firing Order and Relative TDC

Cylinder	TDC
1	0.0

Required for Swirl Prediction

Piston Bowl Depth: 0.0 mm

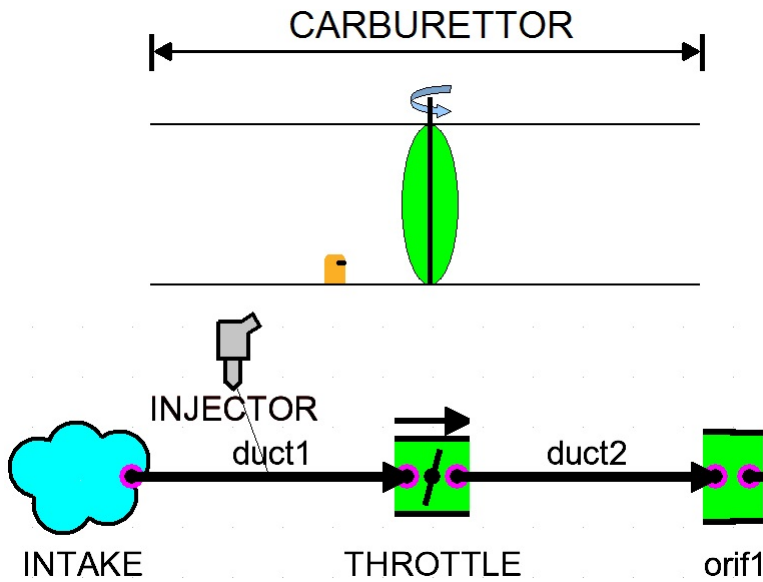
Piston Bowl Diameter: 0.0 mm

Piston Bowl Rim Diameter: 0.0 mm

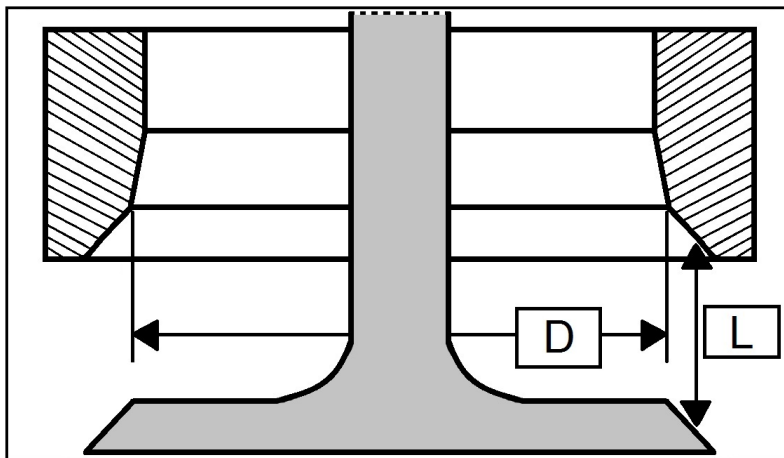
Piston Bowl Volume: 0.0 mm<sup>3</sup>

OK Apply Cancel Help

## A.6 SIMULATION OF THE CARBURETTOR



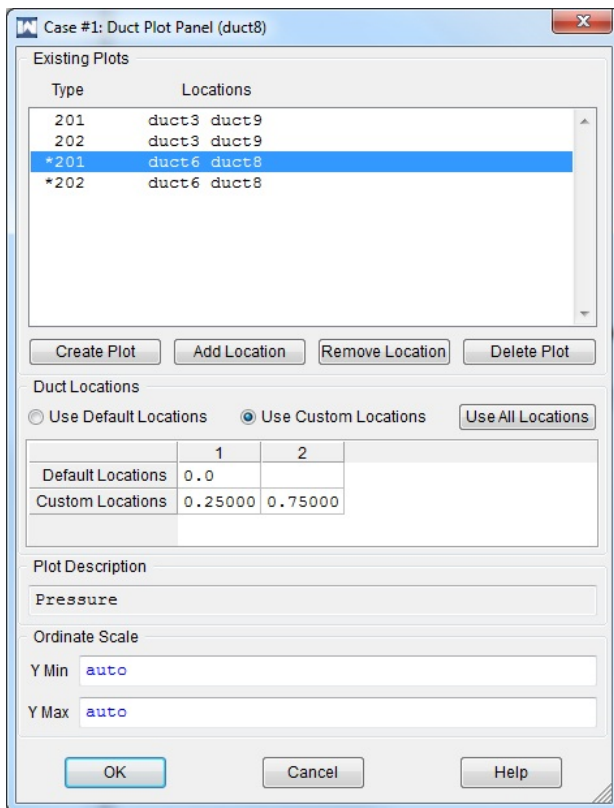
## A.7 MEASUREMENT TECHNIQS



Valve measurement representation where  $L$  = lift and  $D$  = diameter.



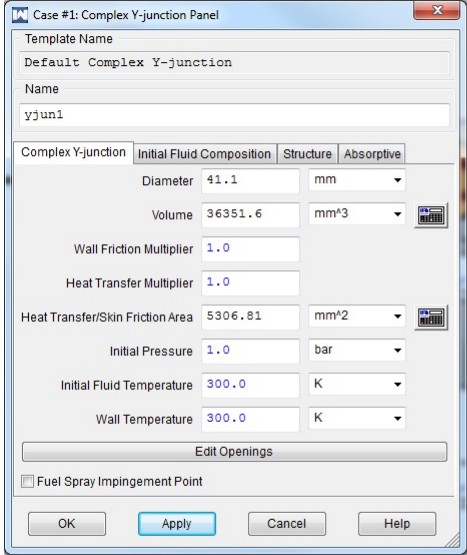
How to measure tappet clearance.



Duct plot panel showing connection of data.



## A.8 COMPLEX Y-JUNCTIONS



Case #1: Complex Y-junction Panel

Template Name: Default Complex Y-junction

Name: yjun1

Complex Y-junction | Initial Fluid Composition | Structure | Absorptive

Diameter: 41.1 mm

Volume: 36351.6 mm<sup>3</sup>

Wall Friction Multiplier: 1.0

Heat Transfer Multiplier: 1.0

Heat Transfer/Skin Friction Area: 5306.81 mm<sup>2</sup>

Initial Pressure: 1.0 bar

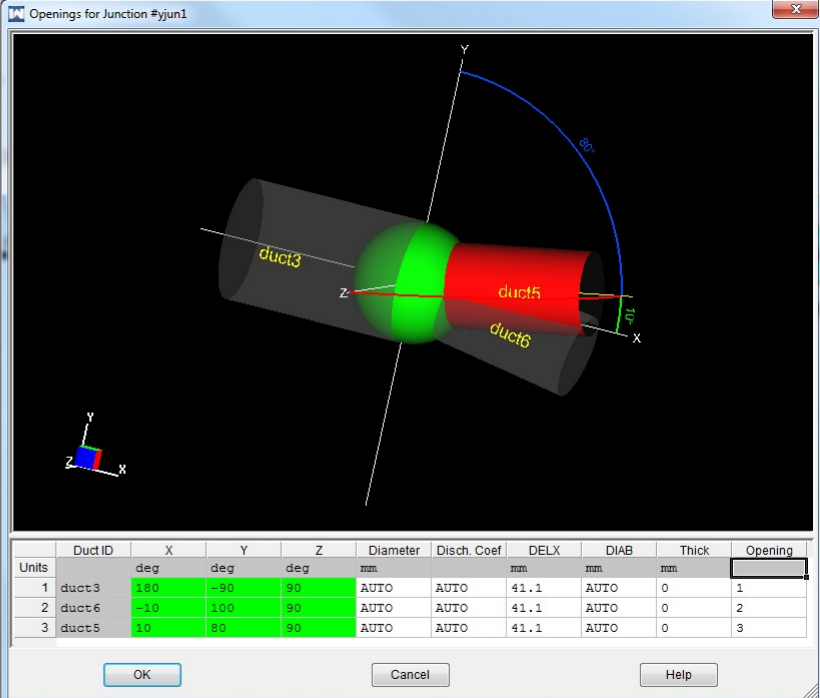
Initial Fluid Temperature: 300.0 K

Wall Temperature: 300.0 K

Edit Openings

Fuel Spray Impingement Point

OK Apply Cancel Help



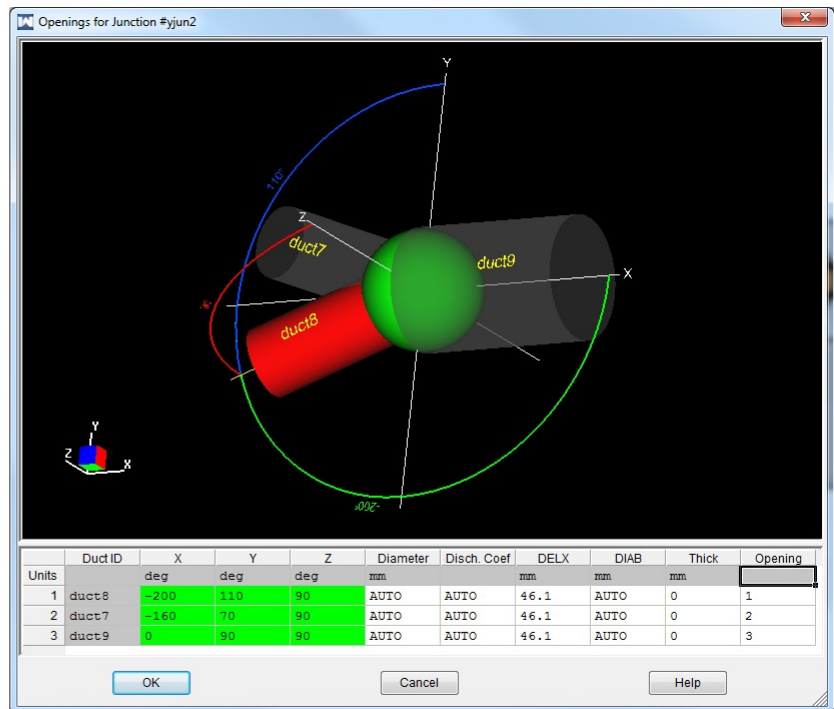
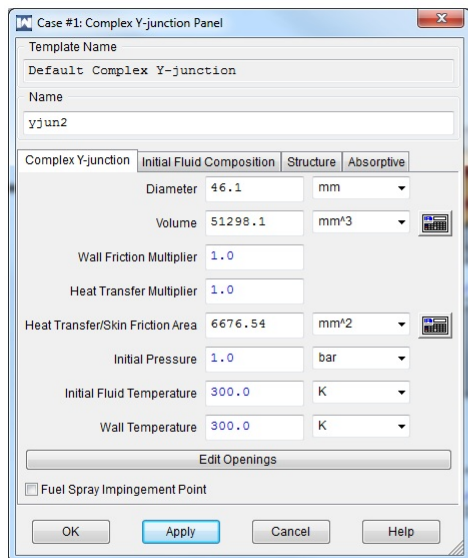
Openings for Junction #yjun1

3D visualization of a Y-junction with ducts labeled duct3, duct5, and duct6. A sphere is shown at the junction. A coordinate system (X, Y, Z) is visible.

Units	Duct ID	X deg	Y deg	Z deg	Diameter mm	Disch. Coef	DELX mm	DIAB mm	Thick mm	Opening
1	duct3	180	-90	90	AUTO	AUTO	41.1	AUTO	0	1
2	duct6	-10	100	90	AUTO	AUTO	41.1	AUTO	0	2
3	duct5	10	80	90	AUTO	AUTO	41.1	AUTO	0	3

OK Cancel Help

A visual representation of how the single intake canal splits into two in the intake port. The sphere in the middle represents the volume occupied by the Y-junction, while the connected ducts are scaled in size relative to the size of the sphere, based on the duct diameters. This feature represents the complex Y-junction 1.



A visual representation of how the two canals from the exhaust valves merge into one in the exhaust port. The sphere in the middle represents the volume occupied by the Y-junction, while the connected ducts are scaled in size relative to the size of the sphere, based on the duct diameters. This feature represents the complex Y-junction 2.

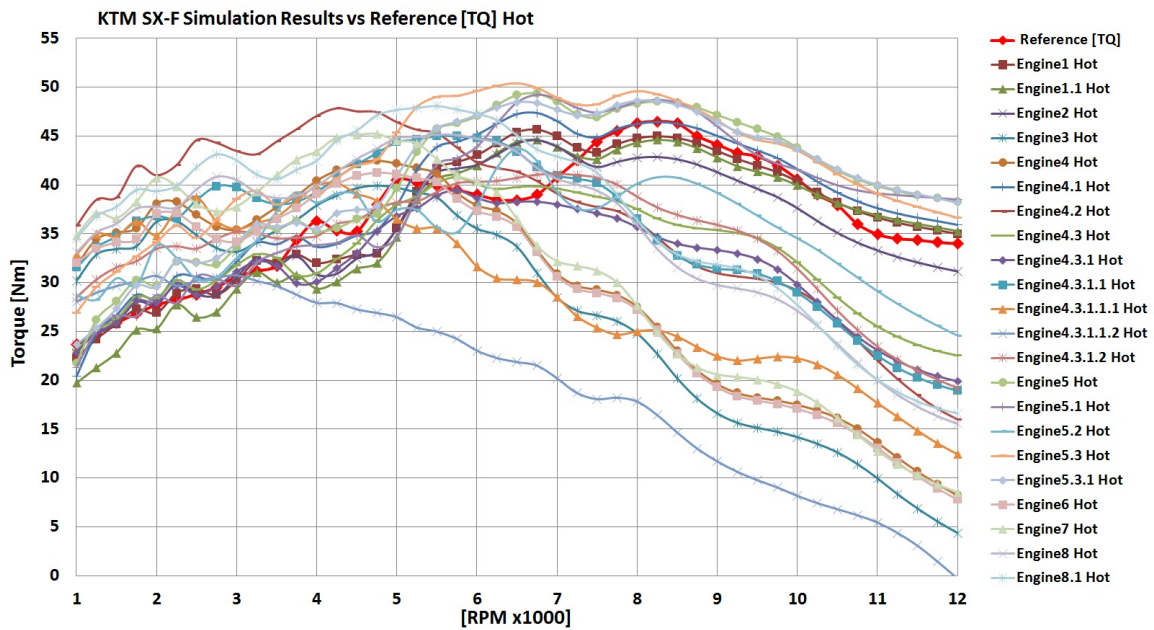
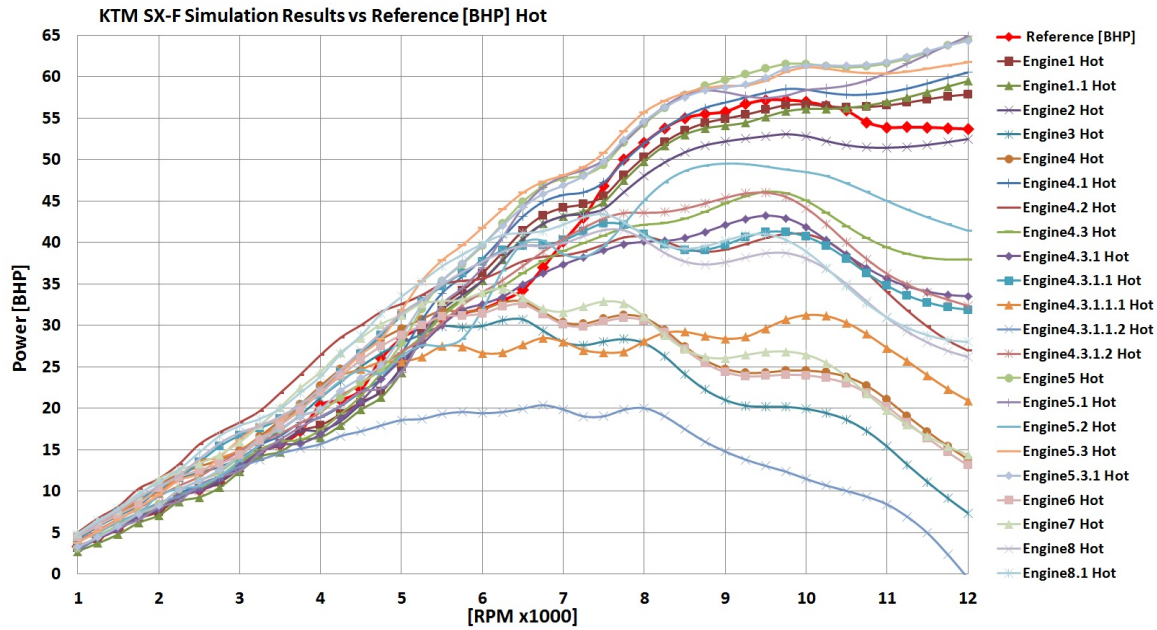
All of the tubes connected to the junctions can be set anywhere in the three dimensions, although all of these are in a single plane. Wave only takes the relative position between the tubes into consideration.

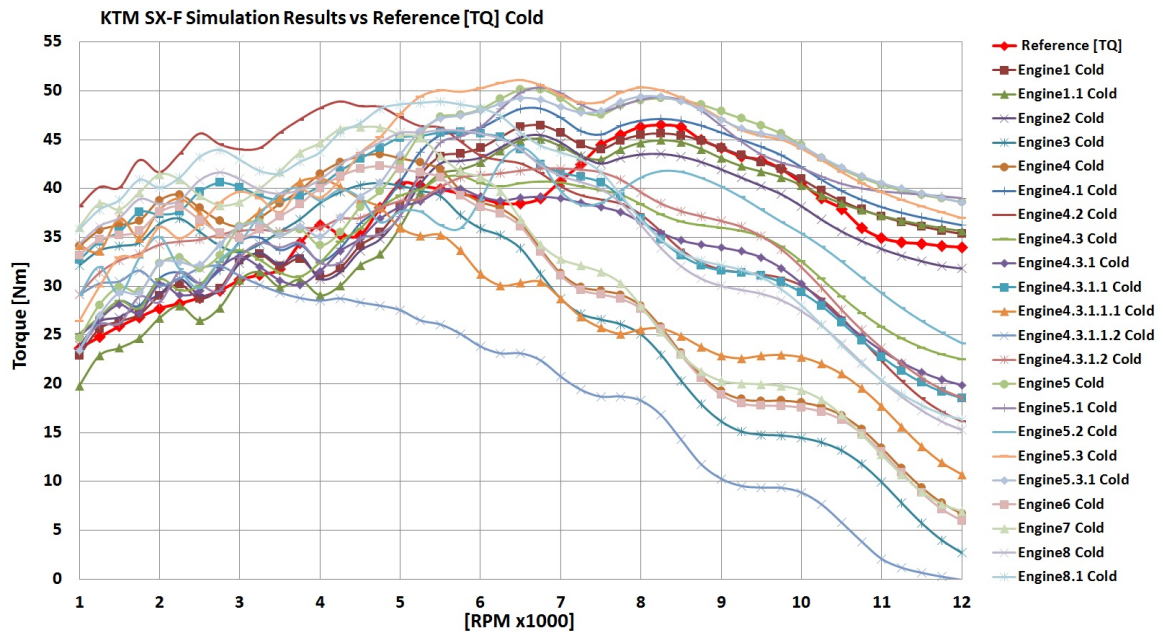
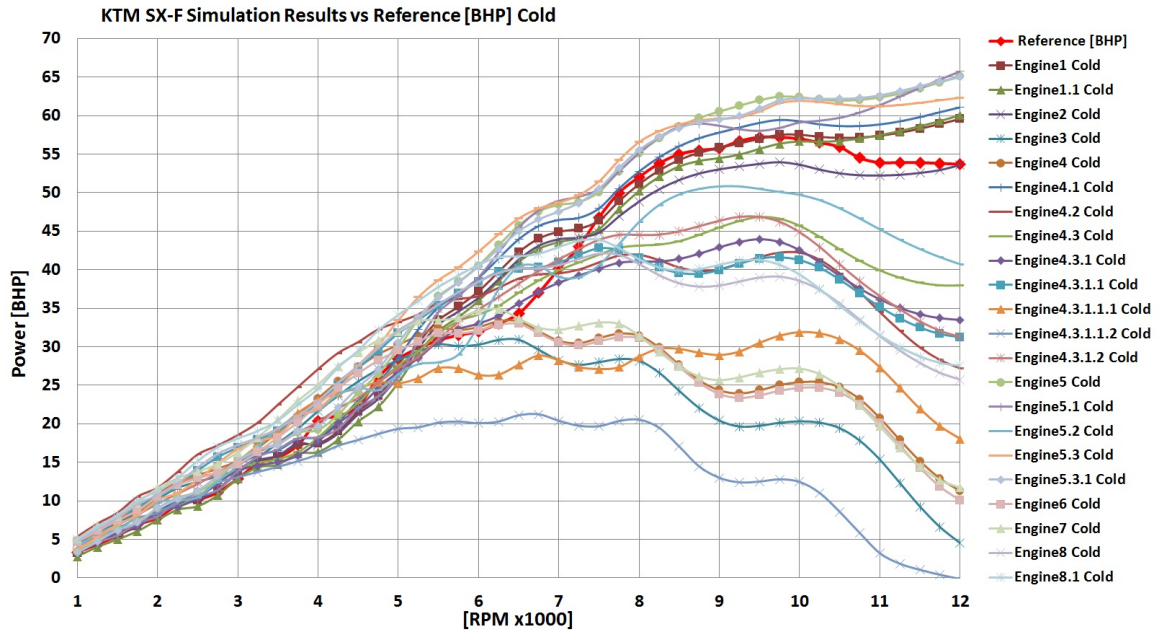
## A.9 RPM RELATED CONSTANTS

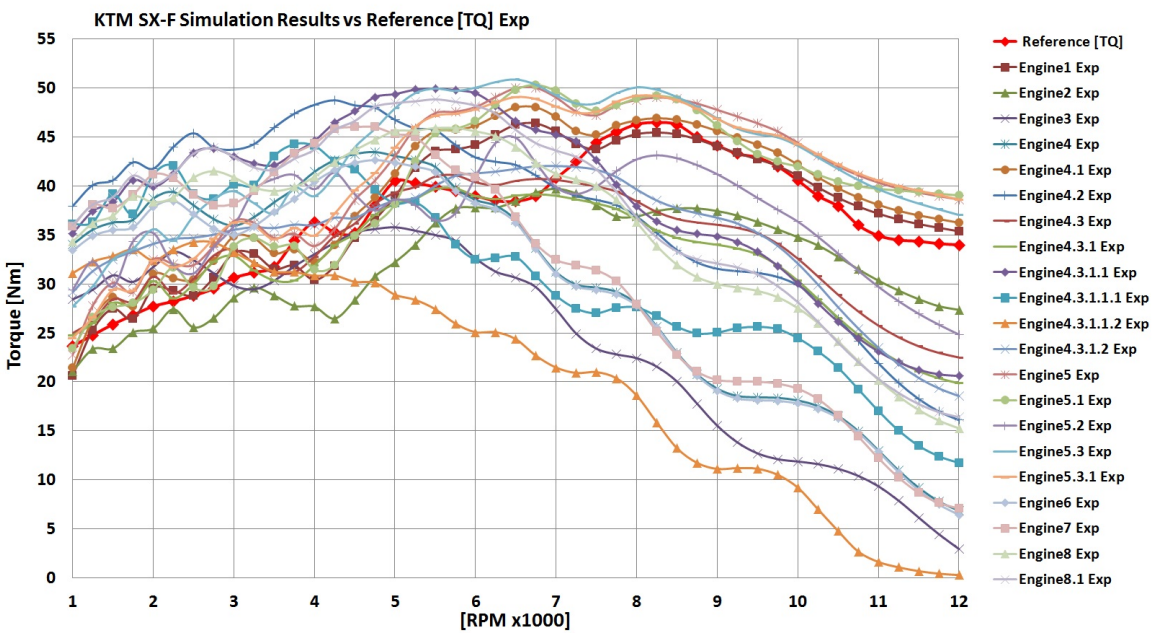
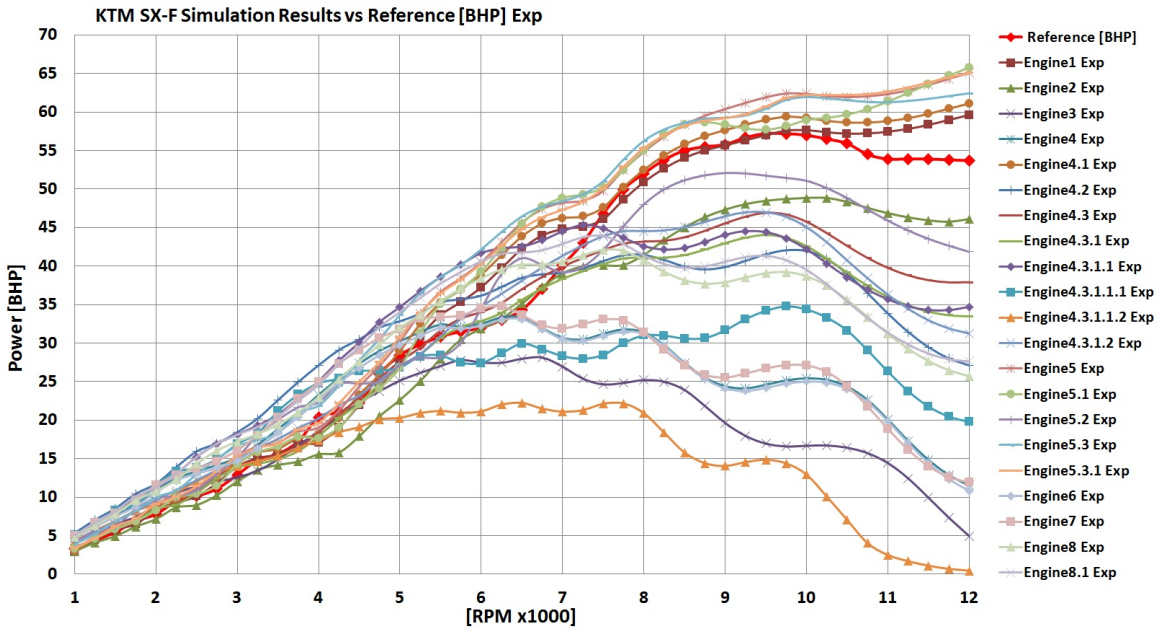
A_F		14.70	14.70	14.70	14.70	14.70	14.70	14.70	14.70	14.70	14.70	14.70	14.70	14.70	14.70	14.70
BDUR	deg	28.00	28.25	28.50	28.75	29.00	29.13	29.25	29.38	29.50	29.63	29.75	29.88	31.00	31.25	31.50
CA50	deg	9.00	9.00	9.00	9.00	9.00	9.00	9.00	9.00	9.00	8.88	8.75	8.63	8.50	8.50	8.50
EV_TEMP	K	365.00	365.25	365.50	365.75	366.00	367.00	368.00	369.00	370.00	371.25	372.50	373.75	375.00	375.50	376.00
HEAD_TEMP	K	550.00	557.50	565.00	572.50	580.00	583.75	587.50	591.25	595.00	601.25	607.50	613.75	620.00	622.50	625.00
IV_TEMP	K	312.00	313.00	314.00	315.00	316.00	316.50	317.00	317.50	318.00	318.50	319.00	319.50	320.00	320.00	320.00
LINER_TEMP	K	540.00	547.50	555.00	562.50	570.00	572.50	575.00	577.50	580.00	583.75	587.50	591.35	595.00	596.25	597.50
PISTON_TEMP	K	500.00	507.50	515.00	522.50	530.00	535.00	540.00	545.00	550.00	557.50	565.00	572.50	580.00	584.45	589.50
SPEED	rpm	1000.00	1250.00	1500.00	1750.00	2000.00	2250.00	2500.00	2750.00	3000.00	3250.00	3500.00	3750.00	4000.00	4250.00	4500.00
THROTTLE_ANGLE	deg	90.00	90.00	90.00	90.00	90.00	90.00	90.00	90.00	90.00	90.00	90.00	90.00	90.00	90.00	90.00
A_F		14.70	14.70	14.70	14.70	14.70	14.70	14.70	14.70	14.70	14.70	14.70	14.70	14.70	14.70	14.70
BDUR	deg	31.75	32.00	31.75	31.50	31.25	31.00	31.25	31.50	31.75	32.00	32.25	32.50	32.75	33.00	33.11
CA50	deg	8.50	8.50	8.38	8.25	8.13	8.00	7.88	7.75	7.63	7.50	7.50	7.50	7.50	7.50	7.40
EV_TEMP	K	376.50	377.00	377.75	378.50	379.25	380.00	381.00	381.50	382.00	383.00	384.25	385.50	386.75	388.00	387.68
HEAD_TEMP	K	627.50	630.00	631.25	632.50	633.75	635.00	636.00	637.00	638.00	639.00	641.25	643.50	645.75	648.00	662.14
IV_TEMP	K	320.00	320.00	320.00	320.00	320.00	320.00	320.50	321.00	321.50	322.00	322.75	323.50	324.25	325.00	325.48
LINER_TEMP	K	598.75	600.00	603.75	607.50	611.25	615.00	616.75	618.50	620.25	622.00	623.50	625.00	626.50	628.00	634.15
PISTON_TEMP	K	594.25	599.00	601.00	603.00	604.50	606.00	606.38	606.75	607.13	607.50	607.88	608.25	608.63	609.00	611.70
SPEED	rpm	4750.00	5000.00	5250.00	5500.00	5750.00	6000.00	6250.00	6500.00	6750.00	7000.00	7250.00	7500.00	7750.00	8000.00	8250.00
THROTTLE_ANGLE	deg	90.00	90.00	90.00	90.00	90.00	90.00	90.00	90.00	90.00	90.00	90.00	90.00	90.00	90.00	90.00
A_F		14.70	14.70	14.70	14.70	14.70	14.70	14.70	14.70	14.70	14.70	14.70	14.70	14.70	14.70	14.70
BDUR	deg	33.27	33.44	33.60	33.76	33.93	34.09	34.25	34.42	34.58	34.74	34.91	35.07	35.23	35.40	35.56
CA50	deg	7.34	7.28	7.22	7.15	7.09	7.03	6.97	6.91	6.84	6.78	6.72	6.66	6.59	6.53	6.47
EV_TEMP	K	388.57	389.46	390.35	391.24	392.13	393.01	393.90	394.79	395.68	396.57	397.45	398.34	399.23	400.12	401.01
HEAD_TEMP	K	665.38	668.63	671.87	675.12	678.36	681.60	684.85	688.09	691.33	694.58	697.82	701.07	704.31	707.55	710.80
IV_TEMP	K	326.13	326.78	327.43	328.08	328.73	329.38	330.02	330.67	331.32	331.97	332.62	333.27	333.92	334.57	335.21
LINER_TEMP	K	636.64	639.13	641.62	644.11	646.60	649.09	651.57	654.06	656.55	659.04	661.53	664.02	666.51	669.00	671.48
PISTON_TEMP	K	613.58	615.46	617.35	619.23	621.11	622.99	624.87	626.75	628.64	630.52	632.40	634.28	636.16	638.05	639.93
SPEED	rpm	8500.00	8750.00	9000.00	9250.00	9500.00	9750.00	10000.00	10250.00	10500.00	10750.00	11000.00	11250.00	11500.00	11750.00	12000.00
THROTTLE_ANGLE	deg	90.00	90.00	90.00	90.00	90.00	90.00	90.00	90.00	90.00	90.00	90.00	90.00	90.00	90.00	90.00

## A.10 RESULTS

### A.10.1 COMPARISON OF BHP AND TQ SIMULATION RESULTS VS REFERENCE







### A.10.2 TESTRUN SETTINGS FOR THE PROTOTYPE ENGINE

<i>AirFilter</i>	<i>N</i>
<i>Intake pressure [bar]</i>	0.986923
<i>IntakeTemperature[K]</i>	300
<i>Duct1LeftDiameter[mm]</i>	43.6
<i>Duct1RightDiameter[mm]</i>	42.85
<i>Duct1DiscretizationLength[mm]</i>	20
<i>Duct1OverallLength[mm]</i>	41.7
<i>Duct1RoughnessHeight[μm]</i>	1.5
<i>Duct1BendAngle[deg]</i>	0
<i>Duct1WallFrictionMultiplier</i>	1
<i>Duct1WallHeattransferMultiplier</i>	1
<i>Duct1Fluidpressure[bar]</i>	1
<i>Duct1Temperature[K]</i>	300
<i>Duct1WallTemperature[K]</i>	300
<i>Throttleangle[deg]</i>	90
<i>ThrottleBoreDiameter[mm]</i>	42.85
<i>ThrottleShaftDiameter[mm]</i>	3
<i>Restrictor[mm]</i>	<i>N</i>
<i>RunnerToPlenumLeangth[mm]</i>	<i>N</i>
<i>RunnerToPlenumLeftDiameter[mm]</i>	<i>N</i>
<i>RunnerToPlenumRightDiameter[mm]</i>	<i>N</i>
<i>PlenumVolume[mm<sup>3</sup>]</i>	<i>N</i>
<i>Injectorposition(distansfromleftendofduct2)[mm]</i>	1
<i>Injectorsprayspreadangle[deg]</i>	40
<i>InjectorNozzleDiameter[mm]</i>	0.2
<i>FuelMixtureTemperature[K]</i>	300
<i>Duct2LeftDiameter[mm]</i>	42.85
<i>Duct2RightDiameter[mm]</i>	42.1
<i>Duct2DiscretizationLength[mm]</i>	20
<i>Duct2OverallLength[mm]</i>	40
<i>Duct2RoughnessHeight[μm]</i>	1.5
<i>Duct2BendAngle[deg]</i>	0
<i>Duct2WallFrictionMultiplier</i>	1
<i>Duct2WallHeattransferMultiplier</i>	1
<i>Duct2Fluidpressure[bar]</i>	0.986923
<i>Duct2Temperature[K]</i>	300

<i>Duct2WallTemperature</i> [K]	300
<i>Injectortype</i>	<i>Proportional</i>
<i>IntakeRunnerLength</i>	<i>N</i>
<i>Duct3LeftDiameter</i> [mm]	41.1
<i>Duct3RightDiameter</i> [mm]	41.1
<i>Duct3DiscretizationLength</i> [mm]	20
<i>Duct3OverallLength</i> [mm]	48.1
<i>Duct3RoughnessHeight</i> [ $\mu$ m]	1.5
<i>Duct3BendAngle</i> [deg]	0
<i>Duct3WallFrictionMultiplier</i>	1
<i>Duct3WallHeattransferMultiplier</i>	1
<i>Duct3Fluidpressure</i> [bar]	0.986923
<i>Duct3Temperature</i> [K]	300
<i>Duct3WallTemperature</i> [K]	300
<i>Y – Junction1Diameter</i> [mm]	41.1
<i>Y – Junction1Volume</i> [mm <sup>3</sup> ]	36351.6
<i>Y – Junction1WallFrictionMultiplier</i>	1
<i>Y – Junction1HeatTransferMultiplier</i>	1
<i>Y – Junction1InitialPressure</i> [bar]	1
<i>Y – Junction1InitialFluidTemperature</i>	320
<i>Y – Junction1WallTemperature</i> [K]	350
<i>Connectedduct3AngleInX – directiontoY – Junction1</i> [deg]	180
<i>Connectedduct3AngleInY – directiontoY – Junction1</i> [deg]	-90
<i>Connectedduct3AngleInZ – directiontoY – Junction1</i> [deg]	90
<i>Connectedduct4AngleInX – directiontoY – Junction1</i> [deg]	10
<i>Connectedduct4AngleInY – directiontoY – Junction1</i> [deg]	80
<i>Connectedduct4AngleInZ – directiontoY – Junction1</i> [deg]	90
<i>Connectedduct5AngleInX – directiontoY – Junction1</i> [deg]	-10
<i>Connectedduct5AngleInY – directiontoY – Junction1</i> [deg]	100
<i>Connectedduct5AngleInZ – directiontoY – Junction1</i> [deg]	90
<i>Connectedduct3DELXtoY – Junction1</i> [deg]	41.1
<i>Connectedduct4DELXtoY – Junction1</i> [deg]	41.1
<i>Connectedduct5DELXtoY – Junction1</i> [deg]	41.1
<i>Duct4and5LeftDiameter</i> [mm]	28.4
<i>Duct4and5RightDiameter</i> [mm]	40.4
<i>Duct4and5DiscretizationLength</i> [mm]	20
<i>Duct4and5OverallLength</i> [mm]	70.2
<i>Duct4and5RoughnessHeight</i> [ $\mu$ m]	1.5



<i>Duct4and5BendAngle</i> [deg]	0
<i>Duct4and5WallFrictionMultiplier</i>	1
<i>Duct4and5WallHeattransferMultiplier</i>	1
<i>Duct4and5Fluidpressure</i> [bar]	0.986923
<i>Duct4and5Temperature</i> [K]	330
<i>Duct4and5WallTemperature</i> [K]	400
<i>CompressionRatio</i>	12.5 : 1
<i>CylinderheadClearanceHeight</i> [mm]	1
<i>ReferencePressure</i> [bar]	1
<i>ReferenceTemperature</i> [K]	298
<i>EngineFrictionCorrelationACF</i> [ $\mu$ ]	0.35
<i>EngineFrictionCorrelationBCF</i> [ $\mu$ ]	0.005
<i>EngineFrictionCorrelationCCF</i> [ $\mu$ ]	400
<i>EngineFrictionCorrelationQCF</i> [ $\mu$ ]	0.2
<i>IntakeValveAnchorsCycle</i> [deg]	0
<i>IntakeValveDurationMultiplier</i>	1
<i>1IntakeValveLash</i> [mm]	0.3
<i>IntakeAngleType</i>	<i>Cam</i>
<i>IntakeValveAnchorsProfile</i> [deg]	0
<i>IntakeValveLiftMultiplier</i>	1
<i>IntakeValveRockerRatio</i>	1
<i>IntakeValveReferenceDiameter</i> [mm]	40.4
<i>IntakeValveHeatTransferDiameter</i> [mm]	40.4
<i>IntakeValveFlowCoefficientProfile</i>	<i>CFTYP</i>
<i>IntakeValveSwirlCoefficientProfile</i>	<i>N</i>
<i>ExhaustValveAnchorsCycle</i> [deg]	0
<i>ExhaustValveDurationMultiplier</i>	1
<i>ExhaustValveLash</i> [mm]	0.19
<i>ExhaustAngleType</i>	<i>Cam</i>
<i>ExhaustValveAnchorsProfile</i> [deg]	0
<i>ExhaustValveLiftMultiplier</i>	1
<i>ExhaustValveRockerRatio</i>	1
<i>ExhaustValveReferenceDiameter</i> [mm]	31.7
<i>ExhaustValveHeatTransferDiameter</i> [mm]	31.7
<i>ExhaustValveFlowCoefficientProfile</i>	<i>CFTYP</i>
<i>ExhaustValveSwirlCoefficientProfile</i>	<i>N</i>
<i>Duct6and7LeftDiameter</i> [mm]	31.7
<i>Duct6and7RightDiameter</i> [mm]	24.68

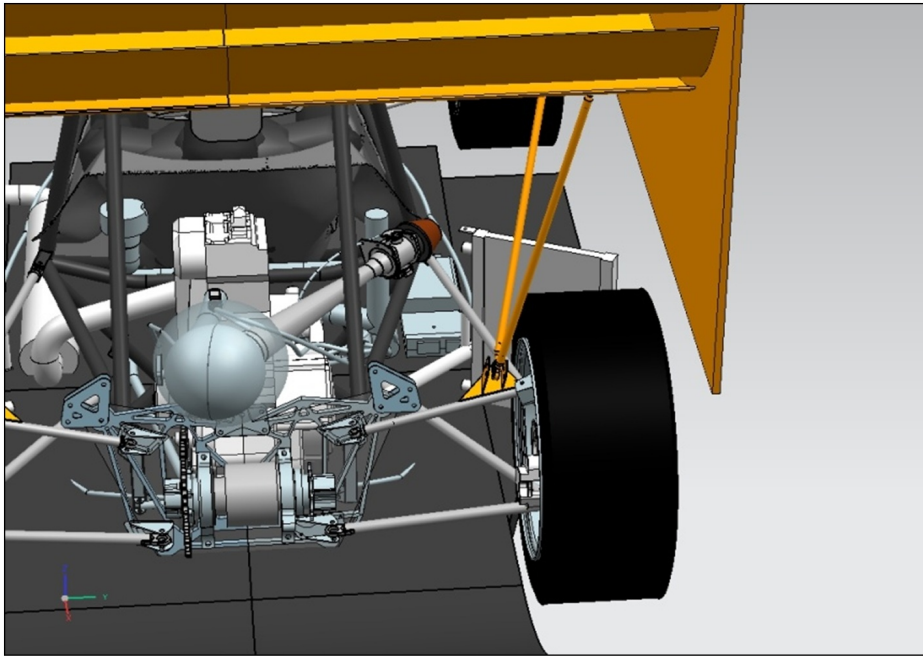
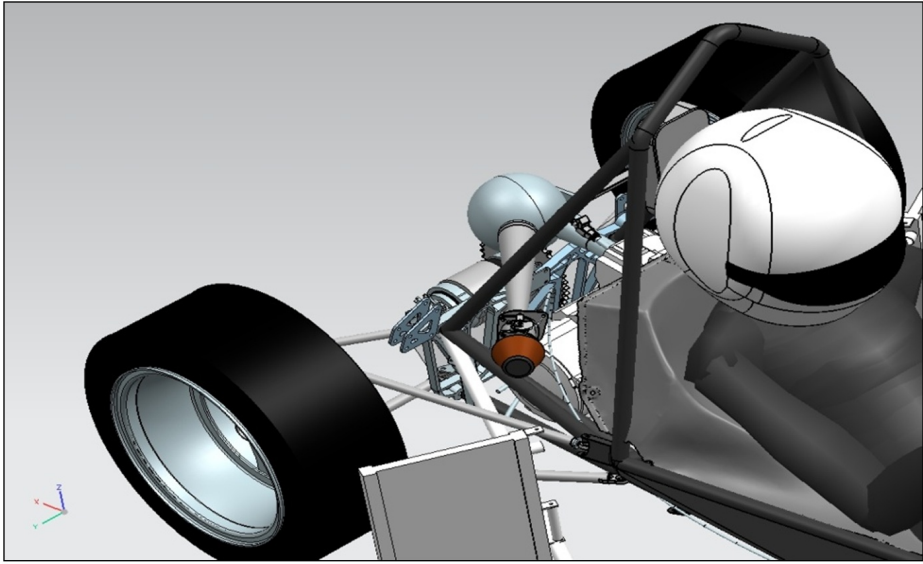
<i>Duct6and7DiscretizationLength</i> [mm]	20
<i>Duct6and7OverallLength</i> [mm]	33.8
<i>Duct6and7RoughnessHeight</i> [ $\mu$ m]	1.5
<i>Duct6and7BendAngle</i> [deg]	0
<i>Duct6and7WallFrictionMultiplier</i>	1
<i>Duct6and7WallHeattransferMultiplier</i>	1
<i>Duct6and7Fluidpressure</i> [bar]	1.03627
<i>Duct6and7Temperature</i> [K]	1000
<i>Duct6and7WallTemperature</i> [K]	500
<i>Y – Junction2Diameter</i> [mm]	46.1
<i>Y – Junction2Volume</i> [mm <sup>3</sup> ]	51298.1
<i>Y – Junction2WallFrictionMultiplier</i>	1
<i>Y – Junction2HeatTransferMultiplier</i>	1
<i>Y – Junction2InitialPressure</i> [bar]	1.05
<i>Y – Junction2InitialFluidTemperature</i>	900
<i>Y – Junction2WallTemperature</i> [K]	400
<i>Connectedduct6AngleInX – directiontoY – Junction1</i> [deg]	-160
<i>Connectedduct6AngleInY – directiontoY – Junction1</i> [deg]	70
<i>Connectedduct6AngleInZ – directiontoY – Junction1</i> [deg]	90
<i>Connectedduct7AngleInX – directiontoY – Junction1</i> [deg]	-200
<i>Connectedduct7AngleInY – directiontoY – Junction1</i> [deg]	110
<i>Connectedduct7AngleInZ – directiontoY – Junction1</i> [deg]	90
<i>Connectedduct8AngleInX – directiontoY – Junction1</i> [deg]	0
<i>Connectedduct8AngleInY – directiontoY – Junction1</i> [deg]	90
<i>Connectedduct8AngleInZ – directiontoY – Junction1</i> [deg]	90
<i>Connectedduct6DELXtoY – Junction1</i> [deg]	46.1
<i>Connectedduct7DELXtoY – Junction1</i> [deg]	46.1
<i>Connectedduct8DELXtoY – Junction1</i> [deg]	46.1
<i>Duct8LeftDiameter</i> [mm]	41.8
<i>Duct8RightDiameter</i> [mm]	41.8
<i>Duct8DiscretizationLength</i> [mm]	15
<i>Duct8OverallLength</i> [mm]	29
<i>Duct8RoughnessHeight</i> [ $\mu$ m]	1.5
<i>Duct8BendAngle</i> [deg]	0
<i>Duct8WallFrictionMultiplier</i>	1
<i>Duct8WallHeattransferMultiplier</i>	1
<i>Duct8Fluidpressure</i> [bar]	1.03627
<i>Duct8Temperature</i> [K]	950
<i>Duct8WallTemperature</i> [K]	550

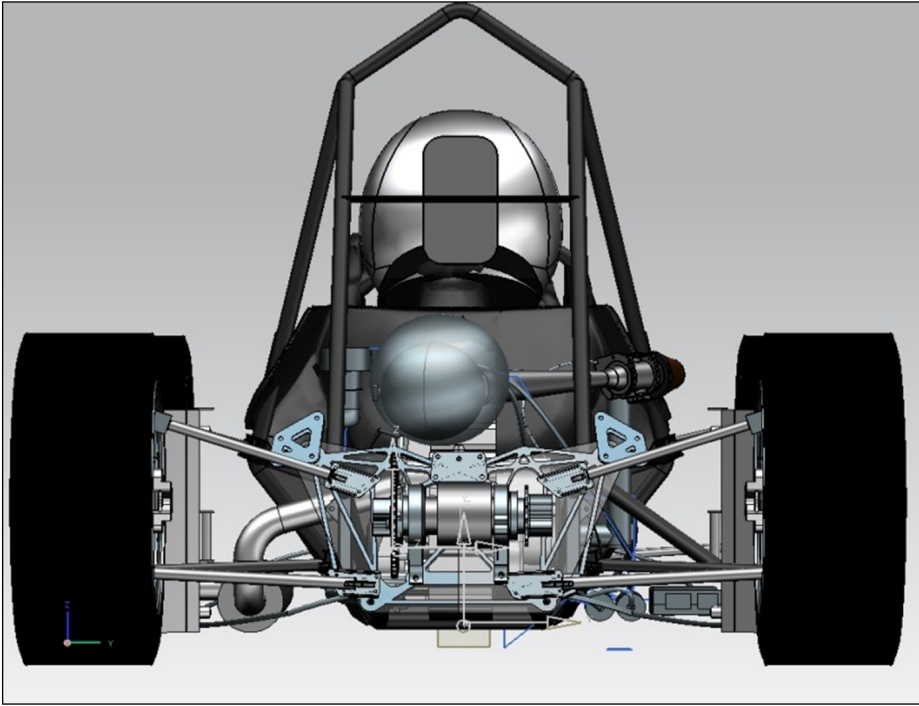
<i>Duct9LeftDiameter</i> [mm]	45
<i>Duct9RightDiameter</i> [mm]	45
<i>Duct9DiscretizationLength</i> [mm]	150
<i>Duct9OverallLength</i> [mm]	310
<i>Duct9RoughnessHeight</i> [ $\mu$ m]	1.5
<i>Duct9BendAngle</i> [deg]	0
<i>Duct9WallFrictionMultiplier</i>	1
<i>Duct9WallHeattransferMultiplier</i>	1
<i>Duct9Fluidpressure</i> [bar]	1.03627
<i>Duct9Temperature</i> [K]	900
<i>Duct9WallTemperature</i> [K]	700
<i>MufflerModel</i>	<i>N</i>
<i>Exhaustpressure</i> [bar]	1
<i>ExhaustTemperature</i> [K]	600

### A.10.3 INTAKE

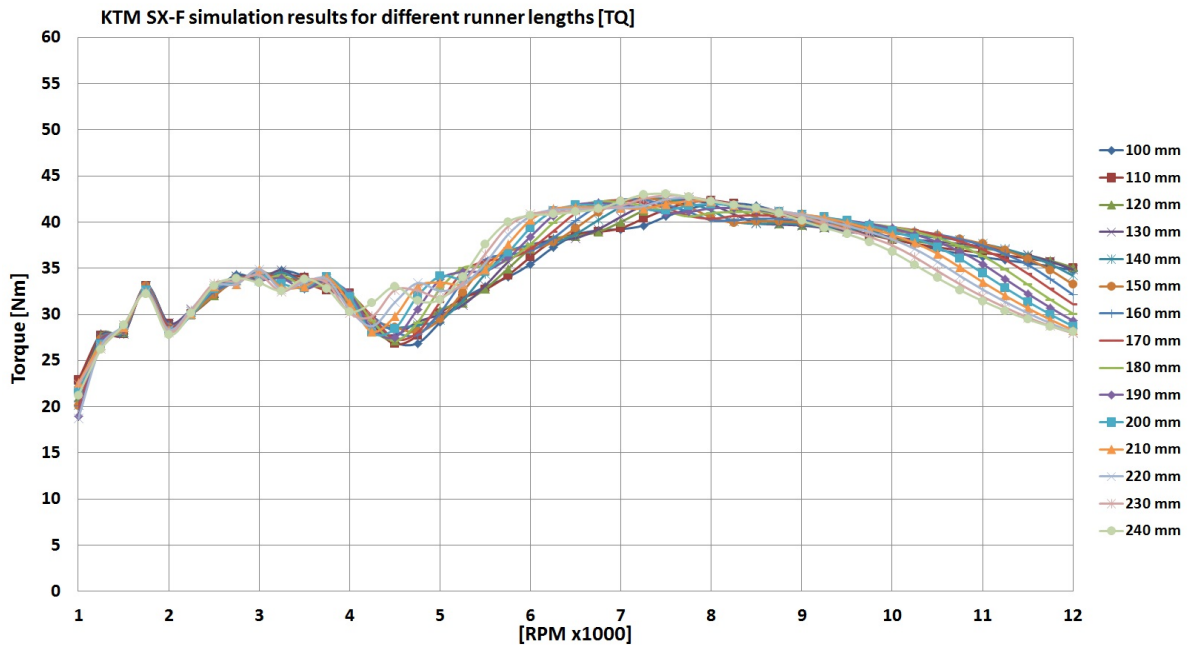
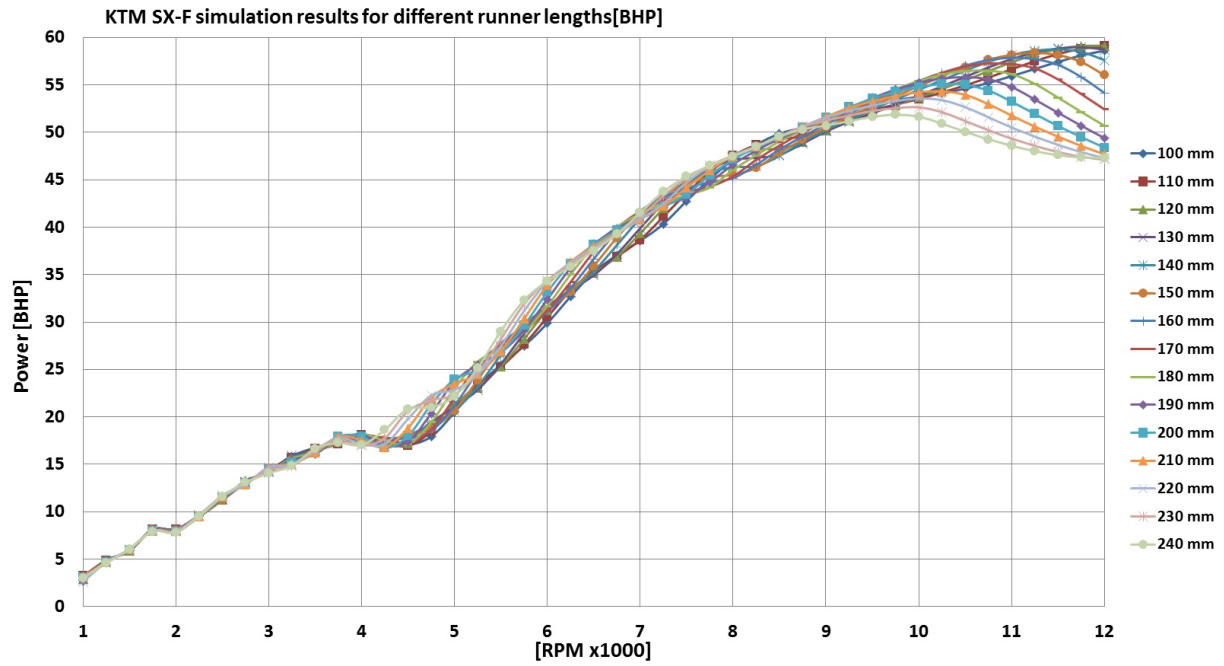
Geometry for new components.

<i>Throttle diameter</i> [mm]	34
<i>Throttle length</i> [mm]	60
<i>Restrictor left diameter</i> [mm]	34
<i>Restrictor right diameter</i> [mm]	19.93
<i>Diffuser length</i> [mm]	300
<i>Diffuser left diameter</i> [mm]	19.93
<i>Diffuser right diameter</i> [mm]	50
<i>Diffuser to plenum angle in X – direction</i> [deg]	30
<i>Diffuser to plenum angle in Y – direction</i> [deg]	120
<i>Diffuser to plenum angle in Z – direction</i> [deg]	90
<i>Bell mouth</i>	0 – 1
<i>Plenum volume</i> [l]	1.767 – 4.948
<i>Runner to plenum angle in X – direction</i> [deg]	30
<i>Runner to plenum angle in Y – direction</i> [deg]	60
<i>Runner to plenum angle in Z – direction</i> [deg]	90
<i>Injector distance from port</i> [mm]	60
<i>Injector angle</i> [deg]	20
<i>Injector nozzle diameter</i> [mm]	0.2
<i>Runner length</i> [mm]	100 – 240
<i>Runner left diameter</i> [mm]	40
<i>Runner right diameter</i> [mm]	40





### A.10.4 ALL SIMULATION RUNNER LENGTHS



## A.10.5 ALL SIMULATION PLENUM VOLUMES

